NASA/TM—2002—211613

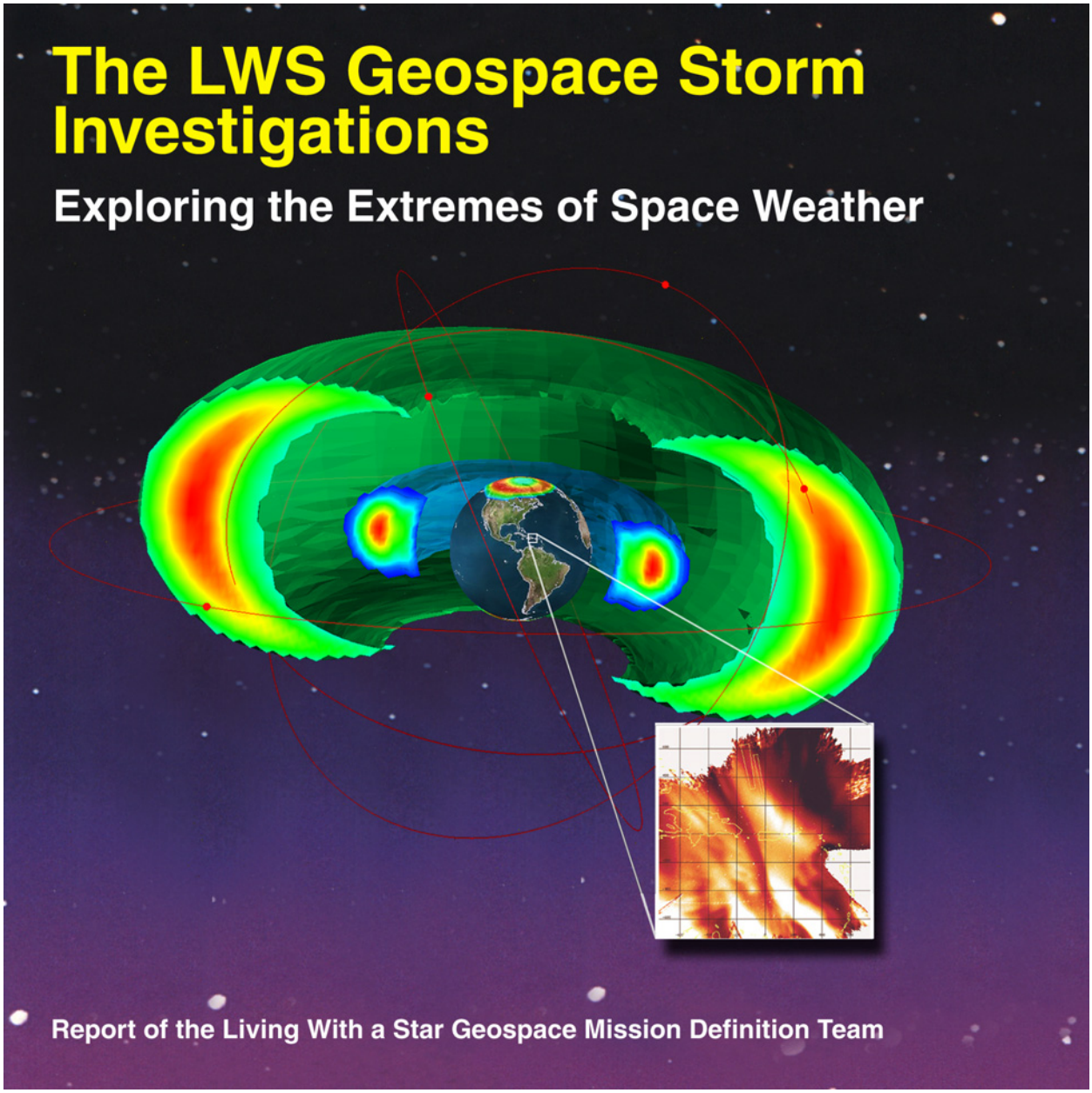

September 2002

The NASA STI Program Office … in Profile

Since its founding, NASA has been dedicated to the advancement of aeronautics and space science. The NASA Scientific and Technical Information (STI) Program Office plays a key part in helping NASA maintain this important role.

The NASA STI Program Office is operated by Langley Research Center, the lead center for NASA's scientific and technical information. The NASA STI Program Office provides access to the NASA STI Database, the largest collection of aeronautical and space science STI in the world. The Program Office is also NASA's institutional mechanism for disseminating the results of its research and development activities. These results are published by NASA in the NASA STI Report Series, which includes the following report types:

- TECHNICAL PUBLICATION. Reports of completed research or a major significant phase of research that present the results of NASA programs and include extensive data or theoretical analysis. Includes compilations of significant scientific and technical data and information deemed to be of continuing reference value. NASA's counterpart of peer-reviewed formal professional papers but has less stringent limitations on manuscript length and extent of graphic presentations.
- TECHNICAL MEMORANDUM. Scientific and technical findings that are preliminary or of specialized interest, e.g., quick release reports, working papers, and bibliographies that contain minimal annotation. Does not contain extensive analysis.
- CONTRACTOR REPORT. Scientific and technical findings by NASA-sponsored contractors and grantees.
- CONFERENCE PUBLICATION. Collected papers from scientific and technical -conferences, symposia, seminars, or other meetings sponsored or cosponsored by NASA.
- SPECIAL PUBLICATION. Scientific, technical, or historical information from NASA programs, projects, and mission, often concerned with subjects having substantial public interest.
- TECHNICAL TRANSLATION. English-language translations of foreign scientific and technical material pertinent to NASA's mission.

Specialized services that complement the STI Program Office's diverse offerings include creating custom thesauri, building customized databases, organizing and publishing research results . . . even providing videos.

For more information about the NASA STI Program Office, see the following:

- Access the NASA STI Program Home Page at http://www.sti.nasa.gov/STI-homepage.html
- E-mail your question via the Internet to help@sti.nasa.gov
- Fax your question to the NASA Access Help Desk at (301) 621-0134
- Telephone the NASA Access Help Desk at (301) 621-0390
- Write to:
  NASA Access Help Desk
  NASA Center for AeroSpace Information
  7121 Standard Drive
  Hanover, MD 21076-1320

NASA/TM—2002—211613

The LWS Geospace Storm Investigations: Exploring the Extremes of Space Weather

Report of the Living With a Star Geospace Mission Definition Team

September 2002

ACKNOWLEDGMENTS

Acknowledgements of highest regard are given by the Geospace Mission Definition team to the support teams from Goddard Space Flight Center and the Johns Hopkins University Applied Physics Laboratory in the areas of science, engineering, and program management. Expert mission experience is evident in the complete and realistic report in hand. The science team was lead by Robert Hoffman with members Barry Mauk, Barbara Giles, Nicola Fox, Dean Pesnell, Tom Sotirelis, and Frank Morgan. The engineering support was led by Laurence Frank with team members Andrew Lewin, Surjit Badesha, Chris Hersman, and Ron Mueller. The Project Management Team was lead by Robert LeBair with guidance and support from Gil Colon, Kenneth Potocki, John Robinson, Mary DiJoseph, Peter Bedini, Madhulika Guhathakurta, Jim Spann, Lawrence Zanetti, Arthur Poland and ex officio members Richard Fisher and George Withbroe.

Many thanks for the expert presentations on matters of critical importance to Living With a Star (LWS) Geospace concerns given by John Foster, Robert McCoy, Fred Herrero, Francois LeFeuvre, Peter Engleman , and Willian Denig. The team recognizes the leadership of chair Glenn Mason and the guidance put in place by the LWS Science Architecture Team, which defined the overall Sun-Earth system goals of the LWS Program. System science and goals are a challenging aspect of the LWS Program as a whole as well as to the individual pieces such as the Geospace Mission. This report is the Geospace integration of the Earth's radiation community and the ionospheric-thermospheric community, to date quite distinct disciplines. The trail blazing challenge to this core team and to the subsequent formal Geospace Mission Definition Team was to integrate these two Geospace science disciplines, a paradigm that could well lead to science integration for the entire Sun-Earth Connection (SEC) system

Available from:

NASA Center for AeroSpace Information
7121 Standard Drive
Hanover, MD 21076-1320
Price Code: A17

National Technical Information Service
5285 Port Royal Road
Springfield, VA 22161
Price Code: A10

Geospace Mission Definition Team

Chair
P. M. Kintner
School of Electrical and Computer Engineering
Cornell University
Ithaca, New York

Geospace Missions Manager
R. S. Lebair
NASA Goddard Space Flight Center
Greenbelt, Maryland

Geospace Missions Study Scientist
R. A. Hoffman
NASA Goddard Space Flight Center
Greenbelt, Maryland

Team Members
S. Basu
Air Force Research Laboratory
Hanscomb AFB, Massachusetts

J. F. Fennell
The Aerospace Corporation
El Segundo, California

T. J. Fuller-Rowell
NOAA Space Environment Center
Boulder, Colorado

G. A. Germany
University of Alabama in Huntsville
Huntsville, Alabama

G. P. Ginet
Air Force Research Laboratory
Hanscomb AFB, Massachusetts

M. J. Golightly
Lyndon B. Johnson Space Center
Houston, Texas

R. A. Heelis
W. B. Hanson Center
University of Texas at Dallas
Dallas, Texas

M. K. Hudson
Dartmouth College
Department of Physics and Astronomy
Hanover, New Hampshire

R. R. Meier
Naval Research Laboratory
Washington, D.C.

D. G. Mitchell
Applied Physics Laboratory
Johns Hopkins Road
Laurel, Maryland

R. F. Pfaff, Jr.
NASA Goddard Space Flight Center
Greenbelt, Maryland

G. D. Reeves
Los Alamos National Laboratory
Los Alamos, New Mexico

R. M. Robinson
National Science Foundation
Arlington, Virginia

R. W. Schunk
Center Atmospheric and Space Sciences
Utah State University
Logan, Utah

H. J. Singer
NOAA Space Environment Center
Boulder, Colorado

J. J. Sojka
Center Atmospheric and Space Sciences
Utah State University
Logan, Utah

R. M. Thorne
Department of Atmospheric Science
UCLA
Los Angeles, California

R. A. Wolf
Department of Physics and Astronomy
Rice University
Houston, Texas

J. R. Wygant
School of Physics and Astronomy
University of Minnesota
Minneapolis, Minnesota

Technical Writing Consultant
W. S. Lewis
Southwest Research Institute
San Antonio, Texas

(BLANK)

CONTENTS

Appendices

1. Traceability Matrix
2. Feasibility Studies
3. Selected References
4. Acronymns and Abbreviations

(BLANK)

EXECUTIVE SUMMARY

The space that surrounds the Earth—geospace—is neither empty nor quiescent. It is populated by electrically charged particles, whose motions are controlled by the Earth's magnetic field and driven by energy extracted from the solar wind, the Sun's supersonically expanding atmosphere. Although their densities are vanishingly low, far lower in fact than the density of the most perfect laboratory vacuum, these populations of charged particles (or plasmas) form a medium in which storm-like disturbances occur, disturbances that drive powerful electrical currents into the Earth's upper atmosphere and accelerate charged particles to extremely high energies.

Such disturbances, which are triggered by storms on the Sun, are known as geomagnetic storms and represent an extreme form of what has come to be known as "space weather." Like the more familiar weather on Earth, space weather can be mild, moderate, or severe. And like severe weather on Earth, the severe weather in space can adversely affect human activities. Indeed, as society becomes increasingly dependent on space-based technologies, our vulnerability to space weather becomes more obvious, and the need to understand it and mitigate its effects becomes more urgent. ***The Living With a Star (LWS) Geospace Program, which is described in this report, has been designed to make significant advances in meeting this need.***

Two geospace regions are of particular importance for our efforts to understand space weather and therefore form the focus of the LWS Geospace Program: the ***radiation belts*** and the ***ionosphere***. Both regions can be strongly disturbed during magnetic storms. And disturbances in both regions can interfere with the functioning of important military and commercial communications and navigation technologies. Storm-time ionospheric disturbances can cause range errors of tens of meters in the Global Positioning System (GPS) navigation systems currently in use by the Federal Aviation Administration and can disrupt high-frequency radio communications and military radar systems. Geomagnetic storms can "pump up" the radiation belts, producing increased fluxes of energetic electrons that can damage satellite electronics and can also represent a potential health hazard to astronauts on the International Space Station.

We have learned much during the last half century about these two key regions of geospace. We know their average configurations, the general character of their response to changing solar wind inputs, and the basic physics of some of the important processes that operate in them. But we have not yet established the connections between specific mechanisms and the phenomenology of the regions, nor have we achieved a predictive understanding of their behavior. The LWS Geospace Program has therefore been developed as a program of "targeted" basic research aimed at advancing our understanding of radiation belt dynamics and ionospheric variability. ***Specifically, the Program's objectives are (a) to characterize and understand the acceleration, global distribution, and variability of the radiation belt electrons and ions that produce the harsh environment for spacecraft and humans; and (b) to characterize and understand mid-latitude ionospheric variability and the irregularities that affect communications, navigation, and radar systems.*** An integral element of the Geospace Program is the development of models that will incorporate the improved physical understanding of these two regions that will lead to improved real-time specification of the space environment (nowcasting) and prediction of potentially hazardous space weather conditions (forecasting).

The Geospace Program flight elements consist of two investigations, a Radiation Belt Baseline Investigation and an Ionosphere-Thermosphere

(I-T) Baseline Investigation, which are designed to yield a robust understanding of radiation belt dynamics and mid-latitude ionospheric variability. The Radiation Belt Baseline Investigation comprises two spacecraft—"storm probes"—in a near-equatorial elliptical orbit (apogee of 5.5 R_E) and an energetic neutral atom imager in a high-latitude orbit. The Radiation Belt Storm Probes will make in situ measurements of relativistic electrons, electric and magnetic fields, wave fields, ring current particles, and radiation belt ions; the imager will provide information on the global distribution and dynamics of the ring current ion population. The I-T Baseline Investigation consists of two identical storm probes in circular, 60°-inclination low-Earth orbits with ascending nodes separated by 10° to 20° in longitude and a mid-latitude imager on a non-LWS spacecraft in geosynchronous orbit. The I-T Storm Probes will make in situ measurements of plasma density, drifts, irregularities, neutral density and winds, as well as currents, wave fields, and precipitating particles. The I-T mid-latitude imager will measure the O/N_2 ratio and N_e^2, providing a global context for the in situ measurements. Critically important for the Geospace Program's objective of understanding ionospheric variability is the ability to characterize the response of the I-T system to variations in solar extreme-ultraviolet (EUV) irradiance and to distinguish this response from variations in the state of the I-T system caused by the input of energy from the magnetosphere during geomagnetic storms. It is expected that this essential capability will be provided by an EUV spectral flux monitor on the LWS Solar Dynamics Observatory (SDO), which is to be launched in 2007.

The Ionosphere-Thermosphere Baseline Investigation and the Radiation Belt Baseline Investigation are scheduled to begin in 2008 and 2009, respectively. With nominal lifetimes of 3 and 2 years, respectively, the two investigations will take place concurrently for a portion of their operational lifetimes, which will permit important correlative studies of the coupling between the inner magnetosphere and the ionosphere-thermosphere system. In addition, this schedule provides the necessary overlap between the I-T Investigation and the SDO mission.

In addition to the Baseline Investigations, the Geospace Mission Definition Team identified three further investigation categories: Augmentations, Core Investigations, and Network-level Investigations. Augmentations are additions to the Baseline in situ measurement capabilities of the Radiation Belt and I-T Storm Probes that would significantly enhance their science return. The Core Investigations are a subset of the Baseline Investigations and are designed to achieve significant progress toward the Geospace Program objectives while remaining consistent with prescribed budget guidelines. They are the Baseline Investigations without the energetic neutral atom imaging capability and with simplification of the four in situ payloads. The Network-level Investigations would permit an expanded Geospace Program that would study the geospace environment as a complex, coupled system. Included in this category of investigations are high-latitude auroral imaging, an inner belt and slot investigation, measurement of radiation belt source populations at geostationary orbit, and increased local time and solar cycle coverage by the Storm Probes.

The LWS Geospace Program will lead to major advances in our understanding of—and ability to predict—space weather. But with increasing knowledge and understanding, new questions will doubtless emerge—questions to be addressed in the coming decades as *homo technologicus* continues to cope with the challenge of living with a star.

CHAPTER 1.
INTRODUCTION

1.1. Living with a Star: The Domain of Geospace

Life on Earth depends on energy released in thermonuclear reactions in the core of a middle-aged, G-class main-sequence star—the Sun—and transferred to the Earth by electromagnetic radiation. Solar radiation at visible and near-infrared wavelengths is processed and redistributed through complex interactions with the Earth's atmosphere, land masses, and oceans to maintain a relatively comfortable global average temperature of 15°C. Visible light from the Sun provides the energy used by green plants to convert carbon dioxide and water into carbohydrates and oxygen. The absorption of solar ultraviolet radiation by molecular oxygen in the stratosphere initiates the chemistry that leads to the formation of the ozone layer, itself an absorber of ultraviolet radiation and a critical part of the atmosphere's protective shield against the energetic short-wavelength radiation that could harm Earth's biosphere.

Energy is transferred from the Sun to the Earth by other means as well—by the supersonic outflow of magnetized, ionized gas from the Sun known as the solar wind and by energetic solar particles accelerated at shock waves driven by coronal mass ejections (CMEs) (**Figure 1**). Like the other planets, Earth is immersed in the solar wind flow, within which the geomagnetic field forms a cavity known as the magnetosphere. The magnetosphere contains highly tenuous plasmas that are organized in distinct particle populations with different energies and densities. The dynamical behavior of these particles—their flows and motions within the magnetosphere—is driven largely by energy extracted from the solar wind through the interaction of the geomagnetic field with the interplanetary magnetic field (IMF), the portion of the Sun's magnetic field that is entrained in the solar wind flow. The interface between the magnetosphere and the solar wind defines the outer boundary of the geospace domain. The inner boundary is the ionosphere, which is formed by the ionization and heating of the neutral gases of the upper atmosphere by solar extreme ultraviolet (EUV) radiation.

Storms on the Sun produce storms in the magnetosphere. Severe geomagnetic storms occur episodically and are triggered by the passage of major solar wind disturbances driven by CMEs. Such strong storms are most common around solar maximum, when CMEs are most frequent; however, CMEs and severe magnetic storms can occur at almost any phase of the solar cycle. During the declining phase of the solar cycle, many magnetic storms recur at the solar rotation period of 27 days. These recurrent storms tend to be weaker than the strongest episodic storms and are triggered by the passage of corotating interaction regions on the leading edges of high-speed streams from coronal holes.

Among the effects of geomagnetic storms are changes in the energetic populations of trapped particles that form the radiation belts. Such changes may involve either enhancements or decreases in the fluxes of energetic particles, particularly in the outer electron belt. In addition, temporary new belts can be created during storms, sometimes within minutes of the storm's onset. Solar energetic protons, accelerated at CME-driven shocks, can provide the "seed" population for new proton belts. Although it was once thought that the behavior of the radiation belts was well-understood, observations over the last decade or so have given rise to new and fundamental questions about the physical processes involved in the enhancement and decay of the belts and in the formation of new ones.

The majority of our satellites operate in regions where they can be exposed to intense fluxes

of extremely energetic radiation belt particles (**Figure 2**). In addition, the orbit of the International Space Station brings it into a latitude range where the exposure of astronauts to relativistic radiation belt electrons is a serious concern. Characterizing the dynamical behavior of the radiation belts and understanding the underlying physics are thus not merely matters of "disinterested" basic research. Rather, ***understanding the radiation belt environment and its variability has extremely important practical applications in the areas of spacecraft operations, spacecraft and spacecraft system design, and mission planning and astronaut safety***.

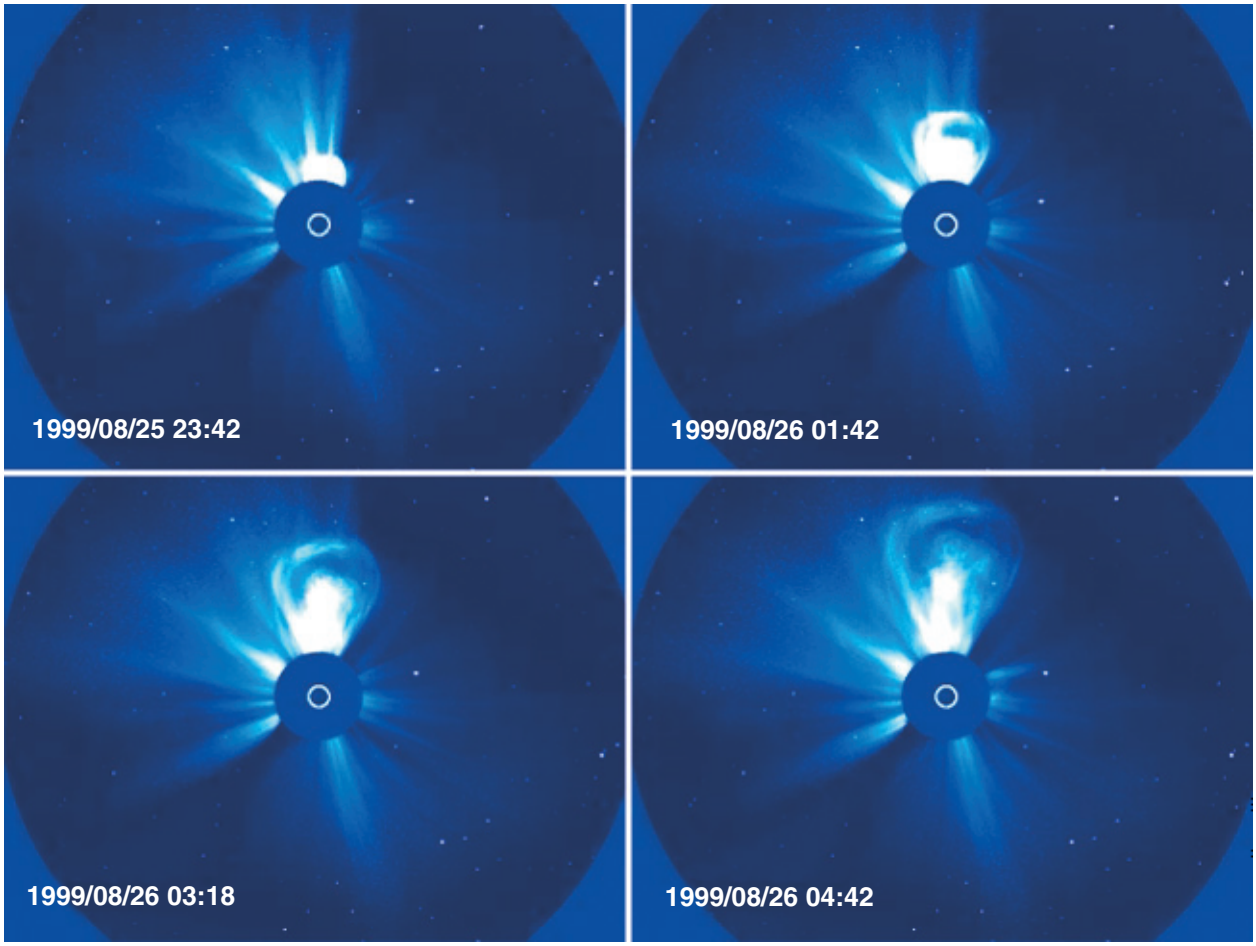

Figure 1. Series of images from the LASCO telescope on the Solar and Heliospheric Observatory (SOHO) showing the development of a coronal mass ejection (CME). CMEs are powerful eruptions of plasma and magnetic fields from the Sun that can propel 10^{+15} g of coronal plasma into interplanetary space at speeds of over 1000 km s^{-1}. CMEs occur most often around the peak of the 11-year solar activity cycle. As they pass through the interplanetary medium, fast CMEs drive shock waves at which the acceleration of charged particles to extremely high energies occurs. Fast CMEs and the CME-driven shocks that encounter the terrestrial magnetosphere cause disturbances in the Earth's space environment known as geomagnetic storms. The shock-accelerated particles are responsible for solar energetic particle events, which can occur in association with magnetic storms and can provide a seed population for the formation of new proton belts in the inner magnetosphere. SOHO is a joint project of the European Space Agency and NASA. (Figure courtesy LASCO team.)

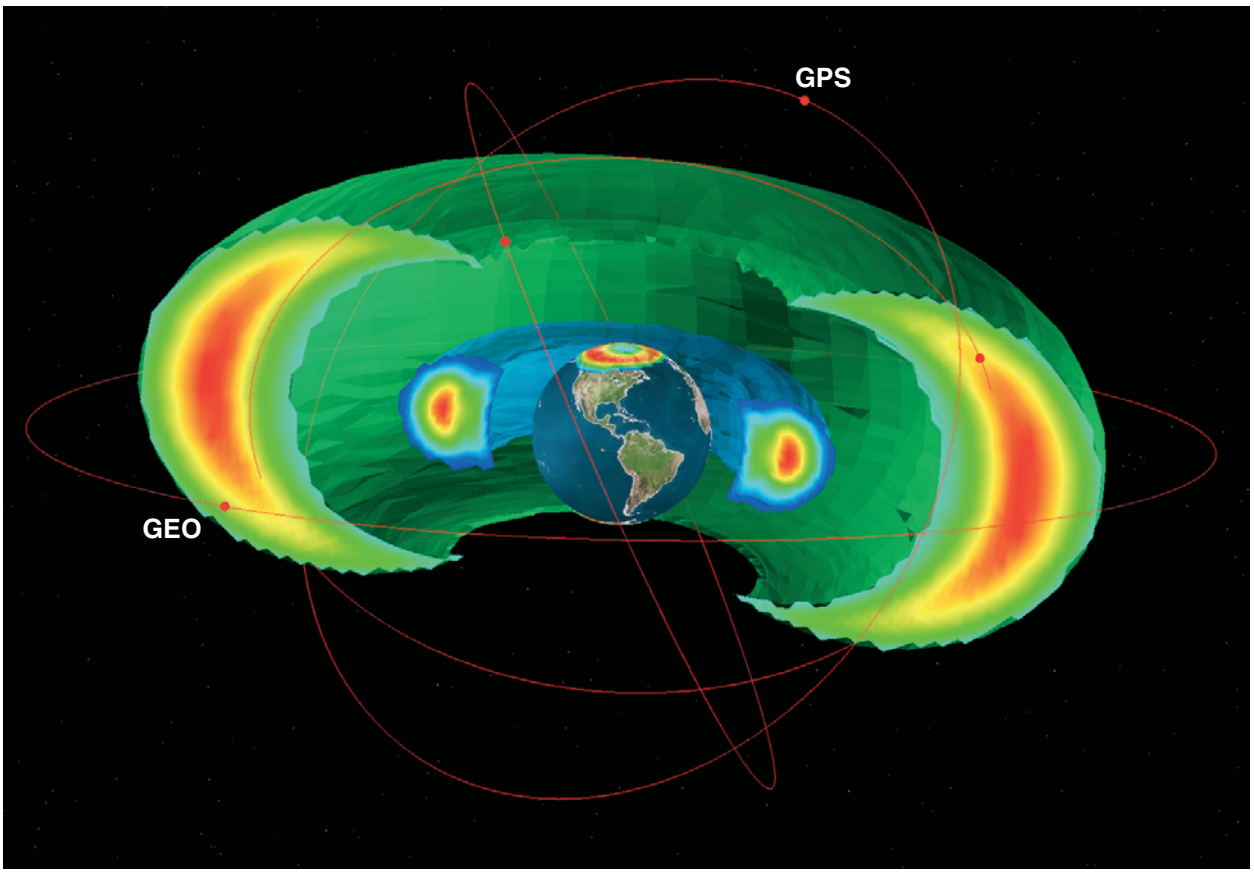

02-0600R-2

Figure 2. Model-generated image showing the two main radiation belts, the outer electron belt and the inner proton belt. The model, developed at the Air Force Research Laboratory, uses data acquired by the CRRES satellite during the period 1990-1991 to generate the radiation belt particle distributions. Shown here are calculated 1.6 MeV electron fluxes and 9.7 MeV proton fluxes. Also shown are representative orbits for three GPS and one geosynchronous spacecraft. (Figure courtesy R. V. Hilmer, Air Force Research Laboratory)

The magnetosphere is strongly coupled to the Earth's upper atmosphere by electric fields and currents that transfer energy into the ionosphere and thermosphere, energy that has been extracted from the solar wind and processed and redistributed by the magnetosphere. This coupling profoundly influences the structure, dynamics, and chemistry of the ionosphere-thermosphere system, the "ground state" of which is determined by the flux of solar EUV radiation, the dominant global energy source for the ionosphere and thermosphere. The state of the ionosphere-thermosphere system thus varies in response to changes both in EUV irradiance and in the energy received from the magnetosphere, with the latter causing the more extreme variability in the state of the system.

The most familiar and often highly dramatic manifestation of magnetospheric energy input into the upper atmosphere is the aurora, which is most often seen at high latitudes but which, during extremely intense magnetic storms, can be observed in the northern hemisphere as far south as Texas. While auroras have been observed and recorded for centuries, other effects of solar disturbances and magnetic storms on the upper atmosphere remained virtually unknown until the era of telecommunications began and the link between disruptions in communications (telegraph, telephone, and finally radio) and geomagnetic activity gradually became clear. These effects include both large-scale changes in ionospheric density during solar maximum and during geomagnetic storms

(density increases during the growth and main phases of a storm; density depletions during the recovery phase) and smaller-scale irregularities. Such variations in the state of the ionosphere interfere both with radio transmissions that are reflected off the ionosphere, such as high-frequency (HF) communications and over-the-horizon radar, and with the trans-ionospheric propagation of radio signals, such as those used by the Global Positioning System (GPS). GPS has become a critically important navigational asset for both the military and the transportation industry, and its vulnerability to ionospheric disturbances is a matter of serious concern.

Ironically, GPS-based systems are, and will continue to be, most heavily used in the middle latitudes—in precisely the latitude range where our knowledge of ionospheric variability is the most deficient (**Figure 3**). ***Thus understanding the behavior of the mid-latitude ionosphere, particularly during geomagnetic storms when variability is most extreme, is a research goal of considerable practical importance for a society that depends increasingly on systems such as GPS for both military and commercial activities.***

The radiation belts and the ionosphere-thermosphere system are thus environments (a) that profoundly affect the operation of critical technological systems, (b) in which extremes of space weather occur, and (c) whose behavior is not well characterized or understood. NASA's Living with a Star (LWS) Program has therefore selected these two geospace regions as the

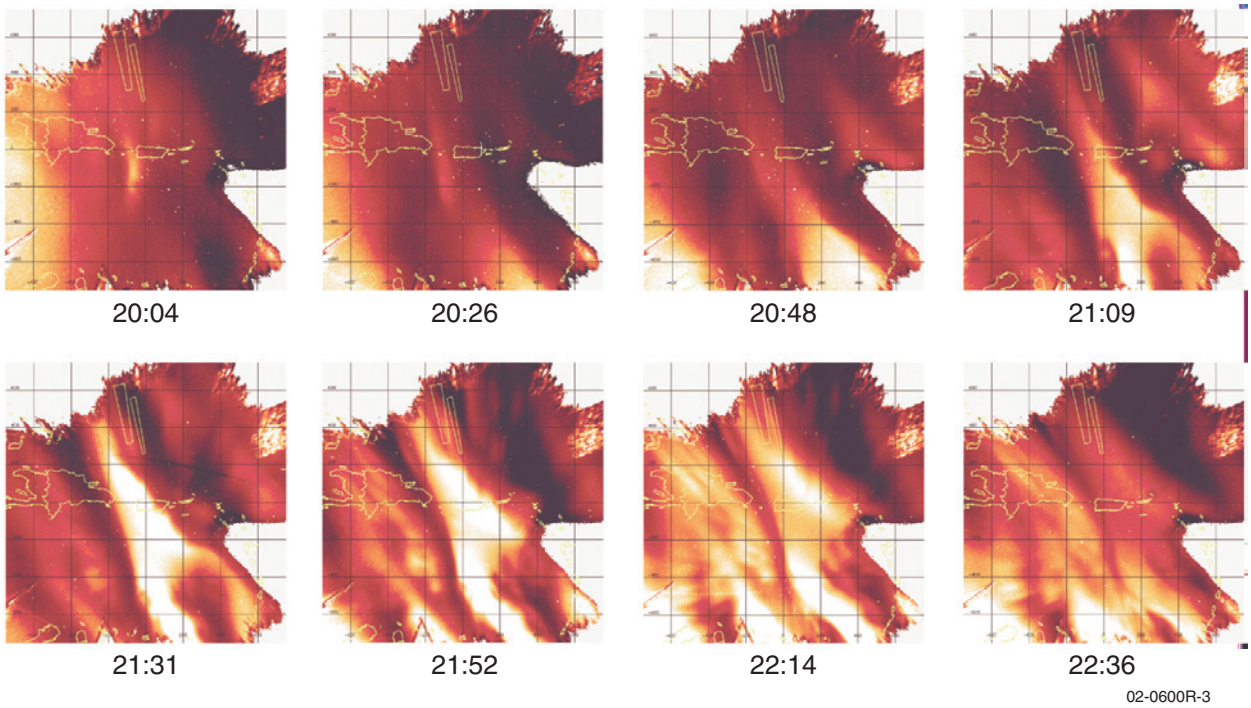

Figure 3. 630-nm airglow images taken with a fish eye camera, then mapped over the Caribbean. The camera was located at the NAIC Arecibo Observatory, Puerto Rico and the times refer to local time on February 17, 1998. The light areas represent regions of increased electron density equivalent to noon-time values; the dark areas are regions of severe electron density depletions. The eight panels show structures moving from southeast to northwest in a generally poleward direction. These events are seen in combination with magnetic storms and occur promptly with the geomagnetic activity, suggesting a link with the inner magnetosphere. The large electron densities, total electron content, and the large gradients associated with the depletions are a concern for GPS systems that employ differential corrections such as the Wide Area Augmentation System (WAAS). (Figure courtesy of J. Makela, Cornell University)

focus of two investigations, the Radiation Belt Investigation and the Ionosphere-Thermosphere Investigation. Both investigations are planned to coincide with the next solar maximum (2010), when the Earth's space environment will be most disturbed. The chapters that follow describe the scientific background to both investigations, the specific questions that each will address, the role of modeling in the LWS Geospace Program, the measurements needed and the investigation approaches to be employed, and the coordination of the Geospace Investigations with other research initiatives. The remainder of this introduction is devoted to a discussion of the place of the Geospace Investigations within the broader context of the Living with a Star Program and of the process followed by the Geospace Mission Definition Team in developing the Geospace Program.

1.2. Origins of the LWS Geospace Program

For decades the Geospace science community has promoted the importance of solar influences on magnetosphere and ionosphere plasma dynamics and the consequences of those influences on Earth- and space-based technological systems. In 2000, the United States Congress listened and awarded NASA's Space Science Enterprise with a new initiative, Living with a Star, whose goal is "to better study solar variability and understand its effects on humanity." Congress further stated that "[t]his initiative will fundamentally change the emphasis of the Sun-Earth Connections theme by having dual objectives, one studying solar-terrestrial physics to understand basic natural processes (current program) and the other stressing investigations into how solar variability affects humans and technology."

The Sun-Earth Connections (SEC) theme eagerly stepped up to this challenge and began an accelerated activity to define a Living With a Star Program. This report is the culmination of that effort within the Geospace component of LWS and defines a compelling program that will ***provide understanding of those geospace phenomena that most affect life and society.***

The program goal and objectives were initially articulated by the Sun-Earth Connection Advisory Subcommittee (SECAS); these are given in **Table 1**. The Program goal clearly emphasizes ***the uniqueness of the Program: that societal consequences are a requirement for assessing the relevance of Sun-Earth connected phenomena to the Program.*** SECAS, through NASA headquarters, then established a LWS Science Architecture Team (SAT) to examine the program requirements and architecture from an overall systems point of view. The SAT adopted the view that the role of observations was to provide the understanding of physical processes so that theory and models could be developed to enable fundamental improvements in environment specifications, nowcasting, and predictions. The SAT then identified sets of scientific problem areas associated with specific societal impacts with a view of defining the evolution of scientific knowledge and modeling that would be required for meaningful LWS contributions.

During the summer of 2001, SECAS and the LWS SAT called for the formation of a Geospace Mission Definition Team (GMDT) charged with identifying the science issues that would most lead to progress in meeting the LWS goals pertaining to geospace. These issues, derived from the LWS objectives and the problem areas developed by the SAT, were to be identified through a convolution of the best possible science having societal needs with the potential for significant progress. The Team was composed of scientists representing both the research and space operations user communities.

The guidance for the GMDT provided by the LWS SAT was necessarily at a system level appropriate for the overall LWS Program, not

Table 1. LWS goals and objectives as articulated by SECAS.

LWS Goal
Develop the scientific understanding necessary to enable the United States to address those aspects of the connected Sun-Earth system that directly affect life and society
LWS Objectives
• Identify and understand variable sources of mass and energy coming from our Star that cause changes in our environment with ***societal*** consequences, including the habitability of Earth, use of technology, and the exploration of space.
• Identify and understand the reactions of geospace regions whose variability has ***societal*** consequences (impacts).
• Quantitatively connect and model variations in the energy sources and reactions to enable an ultimate U.S. forecasting capability on multiple time scales.
• Extend our knowledge and understanding gained in this program to explore extreme solar-terrestrial environments and implications for life and habitability beyond Earth.

geospace in particular. It was left to the GMDT to develop a process for deriving geospace unique science objectives, their priorities, and the strategy for developing a geospace implementation plan.

The approach adopted by the GMDT was different from that usually employed in OSS discipline proposals and mission definition documents, which starts with "curiosity driven" science goals and objectives. Instead, the approach was designed to keep intact a traceability from the societal impacts through the science objectives, approach, techniques, missions, measurements and theory to the required specification, nowcasting, and forecasting goals of LWS.

1.3. Development and Prioritization of Geospace General Objectives

The GMDT derived seven geospace general science objectives by interpreting the problem areas listed in Tables 4 and 5 of the SAT report as applied to Geospace. The objectives are shown in the right column of **Table 2**. Since the SAT tables emphasize the portion of the geospace system most closely tied to societal impacts, the geospace objectives identify those science areas necessary to effectively understand those aspects of the Sun-Earth connected system that most affect society. The objectives include emphasis on energetic particle populations because of their impact on our technology-based society. There are fundamental and unresolved scientific questions about the transport, acceleration and loss of these particles. There is also emphasis on how the Sun's variable radiation changes the composition, ionization state, chemistry, and dynamics of the ionosphere and thermosphere. Superimposed on this is concern over the more extreme variability from magnetospheric energy sources. This variability affects societal systems employing trans-ionospheric signal propagation, HF radio propagation, and systems sensitive to drag on spacecraft and debris that orbit the Earth.

Also shown in **Table 2** are the six most important Space Weather Effects identified by the SAT. Because the general objectives were derived from the problem areas grouped under societal impacts in the SAT report, the Space Weather Effects closely map to the general objectives, as shown by the lettered tabs attached to the objectives. Note that multiple space weather effects on the left map to multiple general science objectives on the right.

Table 2. Geospace science general objectives derived by the GMDT from the space weather effects and the societal impacts of solar terrestrial physics identified by the LWS Science Architecture Team (SAT).

LWS/Space Weather Effect				LWS/Geospace General Objective:
Satellite Systems	The capability to monitor and predict energetic electron and ion exposure is needed for diagnosis of satellite anomalies and consideration during spacecraft design. (LWS program goal ranking 4)	A	A, C	**Priority 1:** Understand the acceleration, global distribution, and variability of energetic electrons and ions in the inner magnetosphere**.** SAT report: WG1-5 and 6, WG2-4
Nav/Com/ Rad Systems	The spatial distribution of electron density in the ionosphere is the key environmental parameter impacting NavComRad systems. (LWS program goal ranking 3)	B	B, E	**Priority 2A:** Determine the effects of long- and short-term variability of the Sun on the global-scale behavior of the ionospheric electron density. SAT report: WG1-1, WG2-1
Human Flight	The capability to monitor and predict energetic electron and ion exposure is needed to ensure the safety of astronauts in Earth orbit and of flight crews of high-altitude aircraft. (LWS program goal ranking 2)	C	B	**Priority 2B:** Determine the solar and geospace causes of small-scale ionospheric density irregularities in the 100 to 1000 km altitude range. SAT report: WG1-2, WG2-2
Satellite Drag	Neutral density is the key environmental parameter determining satellite drag. (LWS program goal ranking 5)	D	C, D	**Priority 3A:** Determine the effects of solar and geospace variability on the atmosphere enabling an improved specification of the neutral density in the thermosphere. SAT report: WG1-3, WG2-3
Ground Systems	Enhanced ionospheric currents during geomagnetic storms induce currents in ground-level conductors. (LWS program goal ranking 6)	E	B, D, E	**Priority 3B:** Understand how solar variability and the geospace response determine the distribution of electric currents that connect the magnetosphere to the ionosphere. SAT report: WG1-4, WG2-5
Global Climate Change	The effect of solar variability on ozone distribution and on near-surface temperature change must be characterized. (LWS program goal ranking 1)	F	A, B, C, F	**Priority 4:** Determine the quantitative relationship between very energetic electron and ion fluxes in the interplanetary medium and their fluxes at low altitude, particularly the geomagnetic cutoffs. SAT report: WG1-9, WG2-6
			F	**Priority 5:** Quantify the geospace drivers that potentially affect ozone and climate. SAT report: WG2-8

The GMDT carefully evaluated the priorities of the space weather effects and the general objectives from two perspectives, an assessment of the impact and importance of each on life and society, and also a judgment as to the likelihood that significant progress on understanding each effect could be made with LWS sponsored observation platforms, given the scope and time frame for the planned activities (years 2002-2012). The importance of each societal effect is shown as a LWS Program goal ranking, in parenthesis below each Space Weather effect. The top to bottom positioning indicates the degree to which the LWS/Geospace Program can contribute to our understanding of the various space weather effects. The convolution of importance to society and the promise of advancing scientific understanding yielded the prioritization of the general science objectives shown to the right in the table. Note that there are two objectives with equal priority 2 and two with equal priority 3. While Global Climate Change is considered most important to life and society, observationally, the most immediate scientific

progress can be made in the areas of Satellite Systems and Navigation/Communications. It was the judgment of the Team that near term progress on understanding Global Climate Change can best be made through investments in modeling and data mining.

The conclusion from this exercise is that the optimal Geospace Program should focus on the radiation belts and the variability of the global ionospheric electron density and its irregularities (General Objectives 1, 2A and 2B). Since understanding the ionosphere requires understanding the thermosphere, priority objective 3A will be simultaneously addressed. Lower priority objectives would be addressed where data from the LWS/Geospace observations are applicable, through the acquisition of data from other programs, and by theory and modeling. The completion of these highest priority objectives will yield the best possible science having societal impacts within the LWS/Geospace budgetary realities.

1.4. Priority Science Focus and Investigations

The GMDT recognized that the general objectives were very broad, so a set of specific objectives were developed for the higher-priority objectives (**Table 3**). Here we summarize the specific science objectives receiving the highest priorities and on which the Team focused.

The Team recognized the importance of the radiation belts for satellite health and satellite design as well as recognized that our understanding of the variability in radiation belt fluxes, especially during storm times and even over a solar cycle, is poor (General Objective 1). This conclusion led to three specific science questions:

- Which physical processes produce radiation belt enhancements? (Specific Objectives 1.1, 1.2b, 1.3a, 1.3b)
- What are the dominant mechanisms for relativistic electron loss? (Specific Objectives 1.2a, 1.2b, 1.3b)
- How does the ring current affect radiation belt dynamics? (Specific Objective 1.3c, 1.4a)

In concert with the approach of the SAT the Team also placed high priority on the development and validation of physics based assimilation and specification models (Specific Objectives 1.2c, 1.4b)

The Team recognized the significance of ionospheric variability on navigation, communications, and radar as well as recognized that ionospheric behavior during geomagnetic storms is not understood or even sufficiently characterized for LWS needs, especially at mid-latitudes (General Objectives 2A and 2B). This conclusion led to four scientific questions:

- What is the contribution of solar EUV to ionospheric variability? (Specific Objective 2A.1a)
- How does the middle- and low-latitude I-T system respond to geomagnetic storms (positive storm phases)? (Specific Objective 2A.1b)
- How do negative ionospheric storms develop, evolve, and recover? (Specific Objectives 2A.1b, 2A.2)
- How are ionospheric irregularities produced, especially at mid-latitudes? (Specific Objective 2B.1)

The general objective focusing on thermospheric density variability, satellite drag, and orbital prediction fell into the third priority (General Objective 3A). Nonetheless the Team noted that some of the specific objectives for this general objective overlapped with the investigations of ionospheric variability and will be studied simultaneously. These specific objectives are:

Table 3. Specific objectives for the highest-priority geospace investigations derived from the general objectives. Groups of specific objectives are prioritized within each general objective.

LWS/Geospace General Objective:	Specific Objectives:
Priority 1: Understand the acceleration, global distribution, and variability of energetic electrons and ions in the inner magnetosphere. SAT report: WG1-5 and 6, WG2-4	**Priority 1:** **1.1***:* Differentiate among competing processes affecting the acceleration and transport of outer radiation belt electrons.
	Priority 2: **1.2a***:* Differentiate among competing processes affecting precipitation and loss of outer radiation belt electrons. **1.2b***:* Understand the creation and decay of new electron radiation belts. **1.2c***:* Develop and validate physics-based data assimilation and specification models of outer radiation belt electrons.
	Priority 3: **1.3a***:* Understand the role of "seed" or source populations for relativistic electron events. **1.3b***:* Quantify the relative contribution of adiabatic and nonadiabatic processes on energetic electrons. **1.3c***:* Understand the effects of the ring current and other storm phenomena on radiation belt electrons and ions.
	Priority 4: **1.4a***:* Understand how and why the ring current and associated phenomena vary during storms. **1.4b**: Develop and validate physics-based and specification models of inner belt protons for solar cycle time scales.
Priority 2A: Determine the effects of long- and short-term variability of the Sun on the global-scale behavior of the ionospheric electron density. SAT report: WG1-1, WG2-1	**Priority 1:** **2A.1a***:* Quantify the relationship between the magnitude and variability of the solar spectral irradiance and the global electron density. **2A.1b**: Quantify the effects of geomagnetic storms on the electron density.
	Priority 2: **2A.2***:* Quantify how the interaction between the neutral atmosphere and the ionosphere affects the distribution of ionospheric plasma.
	Priority 3: **2A.3***:* Discover the origin and nature of propagating disturbances in the ionosphere.
Priority 2B: Determine the solar and geospace causes of small-scale ionospheric density irregularities in the 100 to 1000 km altitude range. SAT report: WG1-2, WG2-2	**Priority 1:** **2B.1***:* Characterize and understand the origin and evolution of newly-discovered storm-time mid-latitude ionospheric irregularities.
	Priority 2: **2B.2a***:* Understand the conditions leading to the formation of equatorial spread-F irregularities, and their location, magnitude and spatial and temporal evolution. **2B.2b**: Understand the conditions leading to the formation of polar patches and their high-latitude irregularities.
	Priority 3: **2B.3***:* Enable prediction of the onset, location, and development of E-region irregularities.
Priority 3A: Determine the effects of solar and geospace variability on the atmosphere enabling an improved specification of the neutral density in the thermosphere. SAT report: WG1-3, WG2-3	**Priority 1:** **3A.1a***:* Determine the variability in the neutral atmosphere attributable to the solar EUV spectral irradiance. **3A.1b**: Determine the variability in the neutral atmosphere attributable to magnetospheric inputs.
	Priority 2: **3A.2***:* Determine the variability in the neutral atmosphere attributable to internal processes.
	Priority 3: **3A.3***:* Determine the variability in the neutral atmosphere attributable to atmospheric waves from below.

- What is the variability of the thermosphere attributable to solar EUV spectral irradiance? (Specific Objective 3A.1a)
- What is the variability of the thermosphere attributable to magnetospheric coupling? (Specific Objective 3A.1b)

Because of the global nature of these objectives the Team recognized the need for further development of dynamic modeling of the coupled ionosphere, thermosphere, and magnetosphere system.

1.5. Development of the Program Plan

The GMDT found that the construction of a traceability matrix to be a useful tool in performing its task of developing a program plan and tracking the logic of the plan from the general science objectives through the specific objectives, the approaches required to fulfill the objectives, the techniques of obtaining necessary measurements both from Geospace Investigations and other programs, and finally the types of measurements themselves. The matrix also demonstrates the closure through modeling. **Appendix 1** shows the traceability matrix for the higher-priority science objectives.

Based on an analysis of the matrix, the GMDT defined a Geospace Program with four categories of investigations (see Chapter IV). **Baseline** science investigations are designed to lead to a robust understanding of the priority phenomena and processes. Possible **Augmentations** to the Baseline investigations consist of enhancements of the in situ measurement capabilities of the radiation belt and I-T spacecraft that will significantly enhance the science return of the two investigations. The **Core** investigations, a subset of the Baseline investigations, are those investigations that are consistent with a prescribed resource envelope and that allow significant progress to be made toward accomplishing the priority science objectives. Finally, **Network-level** investigations are those that enable expanded understanding of the geospace environment as a coupled system.

The LWS Geospace Program is thus a family of science investigations that focus on the compelling science questions that will advance our ability to specify, understand, and predict the societal impact of disturbances in the connected Sun-Earth system. The measurement and modeling investigations are synergistically related to each other and to the other elements of the Living with a Star Program. This LWS Geospace Program plan will solidify the connections between the frontiers of science as embodied in NASA space missions and the knowledge-base required to understand solar effects on those systems in which we have an ever-increasing investment.

CHAPTER 2.
SCIENTIFIC OBJECTIVES OF THE LWS GEOSPACE PROGRAM

2.1 Investigating the Geospace System

The LWS Geospace Program focuses on the following scientific objectives: (a) understanding the dynamics of the radiation belts; (b) understanding the variability in the ionosphere-thermosphere system; and (c) understanding the causes of ionospheric density irregularities. As discussed in the preceding chapter, in evaluating the seven general objectives derived from the space weather effects defined by the Science Architecture Team (SAT), the Geospace Mission Definition Team (GMDT) identified these three objectives as (a) the ones that are of particular importance for improving our ability to mitigate the effects of space weather on important technological systems and (b) the ones toward which the LWS Geospace Program can make the most significant progress.

To achieve each of these broadly defined objectives, we must answer a number of specific questions relating to the complex physics that underlies the behavior of the two regions of geospace that are the focus of this component of the LWS Program. True to the intent of the LWS Program, the science questions that the Geospace Program addresses concern physical processes and phenomena that must be characterized and understood in order to enable society to predict disturbances in the Earth's space environment and to protect against the deleterious effects of space weather. At the same time, however, successfully answering some or all of these questions will represent a substantial advance in our understanding of certain important basic physical processes, such as particle acceleration or the development of irregularities in a plasma medium.

This chapter is organized in two sections, corresponding to the two regions of geospace that the Geospace Program will study, the radiation belts and the ionosphere-thermosphere system. Each section is, in turn, structured in terms of the specific science questions[1] that must be addressed in order to accomplish the Geospace science objectives. The scientific background of the questions is briefly discussed, key outstanding issues and problems are identified, and the measurements needed to resolve the questions are indicated. Underscoring the character of the Geospace Program as "targeted" basic research, each section concludes with a discussion of the effects of the radiation belt environment and the ionospheric-thermospheric disturbances on spacecraft and communications and navigation systems.

Although the radiation belt and ionosphere-thermosphere objectives are treated separately in this chapter, it must be emphasized that the inner magnetosphere and the ionosphere-thermosphere are strongly coupled electromagnetically.[2] Thus full understanding of the behavior of both regions requires that they be studied as an integrated system whose components are linked and modified through complex feedback mechanisms operating on a variety of temporal and spatial scales. The Geospace Program offers an ideal opportu-

[1] The relation of the science questions to the specific objectives derived through the traceability process and listed in Chapter 1, **Table 3**, is indicated through parenthetical references in the text and section headings.

[2] Spatial gradients in the pressure distribution of ring current particles cause the inner magnetosphere to behave as a generator of electric currents. Some of these currents close through the highly non-linear ionosphere, where electric fields drive the currents through the variable and structured ionospheric loads. These electric fields map out into the inner magnetosphere, where they, in turn, influence particle transport, affecting the pressure distributions. The process begins anew with the now modified pressure distributions. Complicating this picture is the modification of the properties of the ionosphere-thermosphere system (e.g., conductivity)—and thus of the electric fields—by both the precipitation of energetic particles from the magnetosphere and the Joule heating that accompanies the electric currents.

nity for such a systems-oriented study of these key geospace regions; it is therefore important that the Radiation Belt and Ionosphere Thermosphere Investigations[3] overlap at least partially in time so that both are operating simultaneously during a portion of their lifetimes.

2.2 Understanding Radiation Belt Dynamics

The identification of the Earth's radiation belts was one of the first discoveries of the space age. Since that time many measurements of the radiation belts have been made and, as recently as 10 years ago, the radiation belts and the processes affecting them were considered to be relatively well-understood. A dramatic change in that perception can be traced to the March 1991 CRRES satellite observation of an entirely new belt of >5-MeV electrons and >20-MeV protons that was produced in a matter of minutes. Observations by geosynchronous satellites, by CRRES, SAMPEX, and POLAR (among others) have now shown that the radiation belts are spatially structured and highly dynamic, exhibiting variability on time scales of minutes, days, season, and solar cycle (**Figure 4**).

The dynamics of the radiation belts have received considerable attention in recent years because of their impact on our technology-based society and because of the fundamental and unresolved scientific questions about the transport, acceleration and loss of these particles. The renewed interest in the dynamics of the radiation belts arises in part because of new observations that have raised questions about standard textbook descriptions of the radiation belts and in part because of society's increasing reliance on

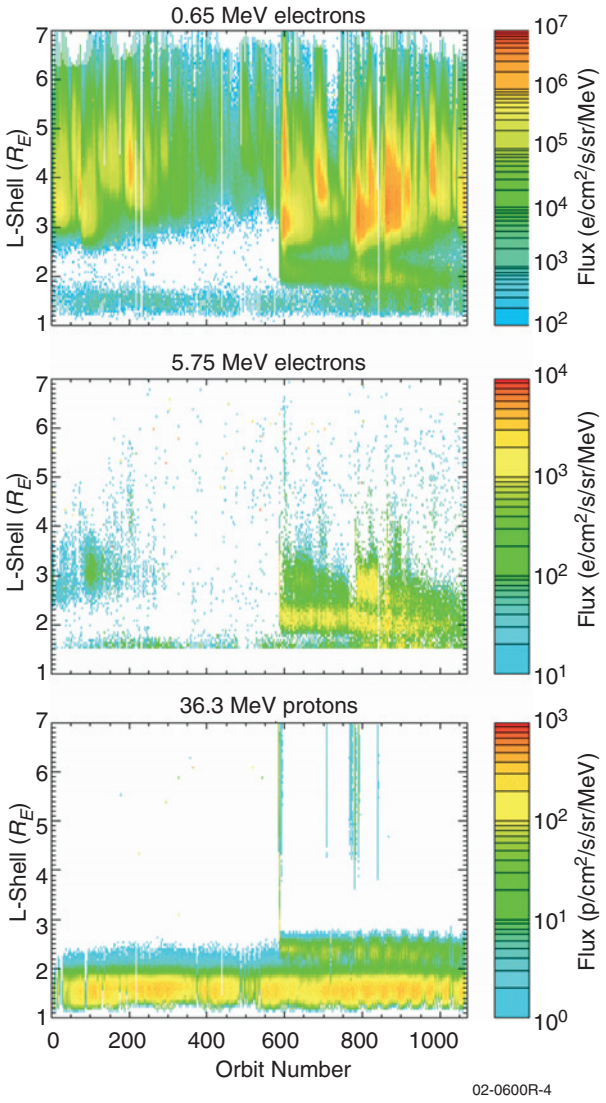

Figure 4. Dynamic radiation belt processes alter the structure of the outer zone electrons (top and middle panels) on time scales ranging from minutes to solar cycles. These panels show 0.65-MeV electrons, 5.75-MeV electrons, and 36.3-MeV protons as a function of L-shell and time for the entire CRRES mission. Individual flux enhancements are generally associated with geomagnetic storms but exhibit large variation in spatial, temporal, and spectral properties, and generally electrons are much more variable than protons. In March 1991, near the middle of this interval, a strong interplanetary shock produced an entirely new belt of electrons and protons near L = 2.5, which is normally the electron slot region. The Radiation Belt Storm Probe (RBSP) mission is designed to understand and model this dynamic behavior. (Figure courtesy G. Ginet, Air Force Research Laboratory)

[3]The discussion of specific science questions that follows is referenced to the Baseline Radiation Belt and Ionosphere-Thermosphere Investigations, both of which comprise in situ and remote sensing measurements of their respective regions of geospace. The Baseline Investigations—and their important subset, the Core Investigations—are defined and discussed in detail in Chapter 4.

space systems that must operate in this severe environment. The prediction and mitigation of these effects will only be possible when the causes of the flux changes are understood. In addition, developing this understanding will lead to fundamental discoveries about energetic particle acceleration, magnetospheric physics, and astrophysical processes.

The Baseline Radiation Belt Investigation will investigate the physics of radiation belt electrons and ions, but it emphasizes the understanding of the outer electron radiation belt because ***this region is the most dynamic part of the radiation belts, embodies the broadest range of physical processes, and has high practical relevance.*** (Objectives 1.1, 1.2a, 1.2b)

Because there is a strong association between enhanced geomagnetic activity and changes in the radiation belts, this report emphasizes the need for simultaneous study of the radiation belts and the storm-time ring current. As early as 1966, periodic increases in the trapped relativistic electron populations were shown to be related to increases in the solar wind kinetic energy density. In the 1970s, the well-known relationship between enhanced solar wind velocity and increases in relativistic electron fluxes was established. Subsequent predictive numerical models of relativistic electron fluxes have been based on the geomagnetic indices Kp and Dst. The close relationship between geomagnetic storms and changes in the radiation belts drives many of the requirements in this report. While that relationship is well established (**Figure 5**), it is by no means a simple one. It has recently been shown that geomagnetic storms can produce dramatic decreases in relativistic electron fluxes, as well as the more well-studied increases in fluxes (**Figure 6**). This emphasizes the need to understand loss processes as well as acceleration processes.

In a typical relativistic electron event, a flux dropout is observed during the main phase of the storm, followed by a buildup of relativistic electrons to flux levels significantly higher than before the storm. The flux dropout is at least partially due to an adiabatic response to the buildup of the storm-time ring current. However, if the entire response were adiabatic there would be no lasting changes in radiation belt fluxes. The fact that non-adiabatic acceleration processes, loss processes, and adiabatic processes all operate simultaneously adds a significant complication to the study of radiation belt dynamics.

To date, most studies have focused on the acceleration of radiation belt electrons and the dramatic increases in fluxes that accompany about half of all storms. Studies based on geosynchronous observations showed that the peak fluxes are typically observed 1 to 3 days after the storm main phase, in the middle of the ring current recovery phase. The delayed response was originally explained by Fujimoto and Nishida in terms of "recirculation" through several phases of betatron acceleration and pitch angle scattering. Recent, multi-spacecraft observations from the International Solar Terrestrial Physics (ISTP) Program revealed that this delay is primarily a characteristic of the outer edges of the radiation belts near geosynchronous orbit, while in the heart of the radiation belts the enhancement can occur in a matter of hours (Objective 1.2b). This rapid response is fast compared with a spacecraft orbital period (typically >12 hours), which explains why multiple spacecraft measurements were needed before these rapid dynamics could be observed.

Understanding acceleration, transport, and loss processes also requires more than measurements of local particle fluxes. It requires simultaneous multi-point measurements of phase space densities at fixed values of the three invariants of the particle motion. Time-dependent radial profiles of phase space densities must be obtained in order to differentiate among various physical mechanisms such as radial diffusion vs. local-

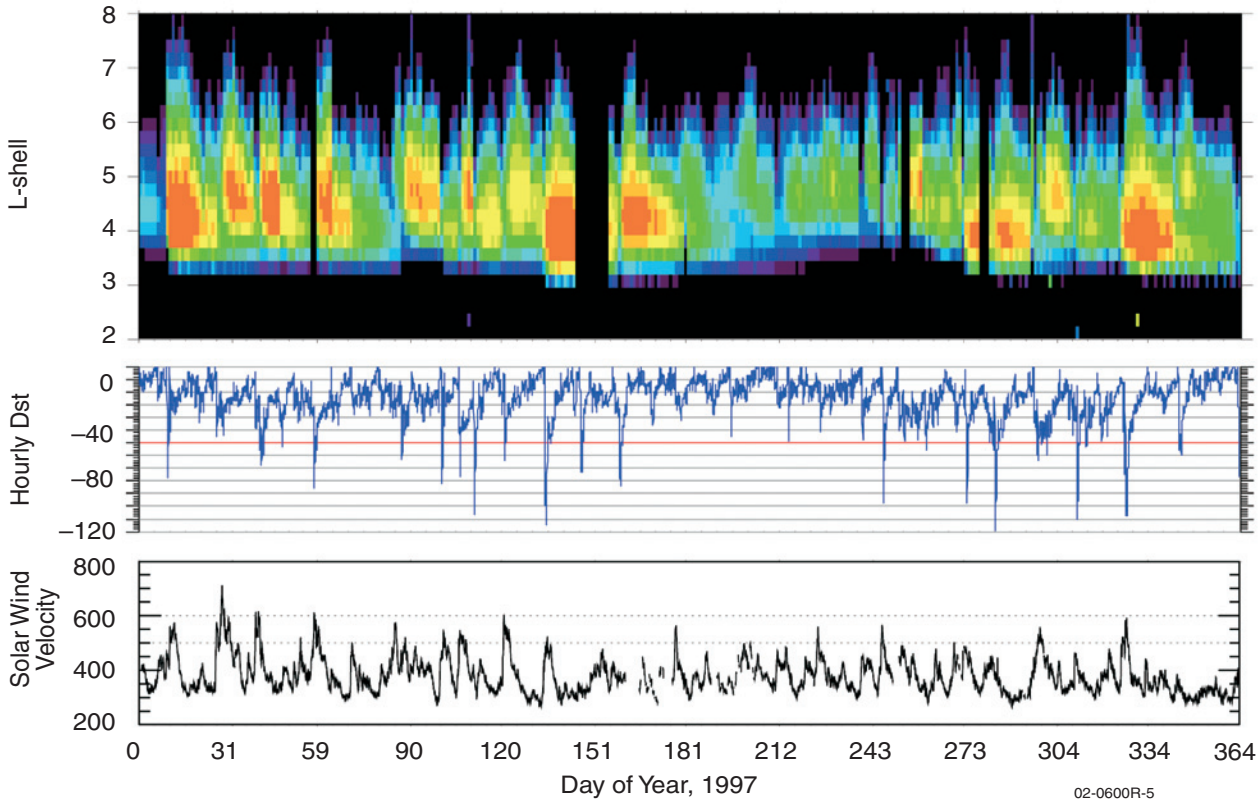

Figure 5. The variability of relativistic electron flux (top panel) observed on POLAR during several magnetic storms in 1997, showing the nearly 1-to-1 correlation in occurrence but not necessarily amplitude with Dst (middle) and solar wind velocity (bottom). Rapid flux dropouts occur during the main phase of each storm (as Dst is depressed), followed by enhancements during the first few days of the storm recovery phase. In the absence of magnetic activity associated with solar wind forcing, fluxes decay slowly over time at scales of a week. (Reeves et al., 2002)

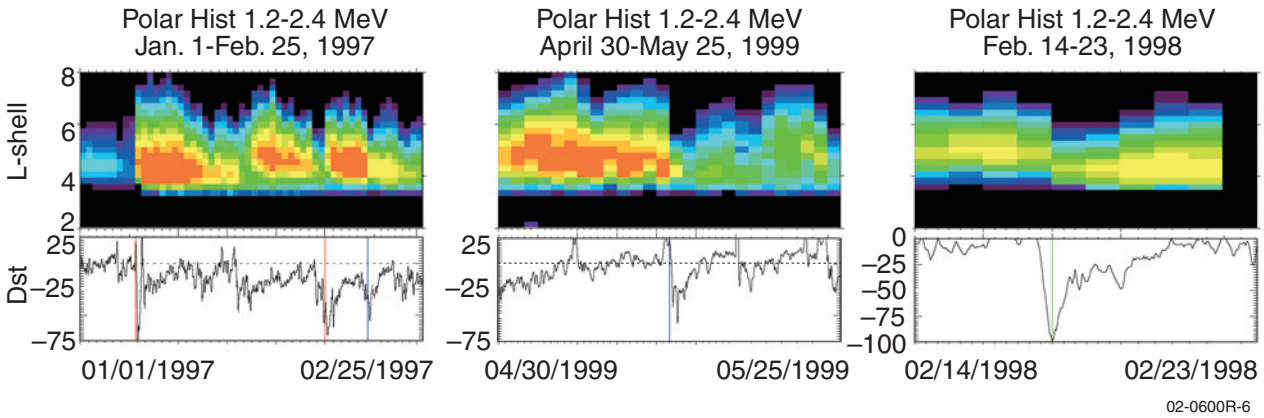

Figure 6. Examples of the widely different response of relativistic outer zone electrons (top) to magnetic storms as monitored by the Dst index (bottom). Flux levels after a storm can be enhanced (left), depressed (middle), or essentially unchanged (right) compared with conditions before the storm. This emphasizes the need to understand and quantify both acceleration and loss processes, which can occur simultaneously during the storm period. (Reeves et al., 2002)

ized acceleration. It is also necessary to measure both the source populations and the accelerated populations simultaneously. While individual spacecraft such as POLAR and CRRES have been able to provide measurements of local phase space density, other spacecraft such as GPS and GOES are severely limited by lack of magnetometers, energy resolution, or other factors. ***The Radiation Belt Investigation will provide the multi-point, time-dependent phase space density profiles that are needed to understand and model the physics of the radiation belts.***

Phase space density profiles are particularly important for understanding wave–particle mechanisms which are involved in all three aspects of dynamics: acceleration, transport, and losses. Wave–particle interactions can produce resonant acceleration (or loss) or can produce enhanced radial diffusion. Moreover different wave–particle interactions almost certainly operate simultaneously and with profound consequences. Direct measurement of these interactions will lead to a better understanding of the root physical processes and of the general mechanisms for the acceleration of charged particles to extremely high energy.

While physical understanding is the top priority of this mission, the mission cannot be considered a success without the development of a new generation of radiation belt models. That next generation of models (cf. Chapter 3) must be based on improved physical understanding of the processes involved and on the large number of measurements that have been made and will be made by both research and programmatic satellites. In order to enable a future space weather capability these models will need to be time-dependent and data-driven. But models must also be developed for sufficiently long time scales to enable reliable and cost-effective spacecraft design.

2.2.1 Which Physical Processes Produce Radiation Belt Enhancement Events?

The radiation belts are composed of energetic electrons and ions on closed or "trapped" drift trajectories in the inner magnetosphere. During radiation belt enhancements the fluxes of energetic particles (with energies from ~20 keV to >10 MeV) can increase by more than a factor of 1000 over time scales as short as a few minutes. In the case of electrons, these dramatic flux enhancements are the result of acceleration of a portion of the more numerous lower-energy particles to these very high energies. However, it is not yet known which mechanisms are responsible for this dramatic acceleration.

To determine which physical processes produce radiation belt enhancement events we need to answer the following questions:

- What processes are responsible for radial transport and acceleration?
- Do localized acceleration processes contribute significantly to radiation belt acceleration?
- How do we distinguish among competing or simultaneous acceleration and transport mechanisms?
- How do we predict and model the spatial, spectral, and temporal characteristics of radiation belt enhancements?

2.2.1.1 What processes are responsible for radial transport and acceleration? (Objective 1.1)

Energetic particles in the inner magnetosphere can be accelerated by two classes of processes, those that conserve the first adiabatic invariant ($p_\perp^2/2mB$) and those that do not. (Here $p_\perp$ is momentum, m is mass, and B is field strength.) To increase the energy of a particle while conserving its first adiabatic invariant, the particle

must also be transported to a region of higher magnetic field strength B. Therefore, in this class of processes, acceleration and transport are intimately linked. The majority of processes which have been proposed to account for radiation belt enhancements conserve the first adiabatic invariant and therefore involve some form of radial transport.

The first important process is direct energization by the electric fields associated with intense large-scale convection flows. During geomagnetic storms, when the convection electric field is strongest, $E \times B/B^2$ flows energize plasma sheet electrons up to energies of ~100 keV as they are transported into the inner magnetosphere.

The second process is driven by the explosive release of energy stored in the geomagnetic tail associated with substorms which are particularly intense during geomagnetic storms. Substorms create injection fronts of energized ions and electrons which propagate towards the Earth and which accelerate electrons and ions to energies up to several hundred keV to 1 MeV over periods of minutes. Changes in the large-scale and substorm-associated convection electric fields are necessary for transporting fresh plasma from the plasma sheet into the inner magnetosphere where radiation belt particles are magnetically trapped. At a minimum, this fresh material provides a source population for subsequent acceleration to relativistic energies. The delivery of this source, or "seed," population and subsequent acceleration to radiation belt energies needs to be understood (Objective 1.3a). Changes in the storm time electric field and delivery of H^+ and O^+ to the inner magnetosphere also produce the storm-time ring current, which is intimately coupled with radiation belt dynamics, as discussed below (Objective 1.4a).

A third process which can produce acceleration and transport of radiation belt electrons is interactions with ultra-low frequency (ULF) waves. ULF wave power in the inner magnetosphere is greatly enhanced during geomagnetic storms and is one of the key parameters that distinguish storms which produce radiation belt enhancements from those which do not. These ULF waves lead to enhanced rates of radial diffusion compared with classical diffusion resulting from impulsive changes in the convection electric field (Objectives 1.1, 1.3c).

For classical radial diffusion associated with impulsive electric fields, the impulse time is short and the decay time is long compared with the particle drift period, resulting in energy-independent diffusion rates. In contrast, radial diffusion by ULF waves is enhanced by distortion of particle drift paths in a compressed dipole which introduces acceleration by radial as well as azimuthal components of wave electric fields. Those fields are present continuously and act on a particle each drift period. Thus one would expect a higher rate of diffusion for more energetic particles which have shorter drift periods. The enhanced diffusion produced by ULF waves can therefore act very efficiently to accelerate radiation belt electrons.

The fourth mechanism involves prompt acceleration by interplanetary shocks. Shocks can induce intense compressional MHD wave fronts that surge through the inner magnetosphere and accelerate and transport electrons and ions to L-shells as low as 2 and energies as high as tens of MeV, creating transient new belts on time scales as short as minutes (**Figure 7**; cf. also **Figure 4**). Such events have been observed to produce the most intense and long-lived changes in the radiation belts currently known (Objectives 1.2b and 1.4b).

These processes are all important at various times and under various conditions. Other processes not yet investigated theoretically may also contribute to radiation belt acceleration and transport. ***A key goal of the Baseline Radiation Belt Investigation is to make a set of measurements sufficient to determine which processes,***

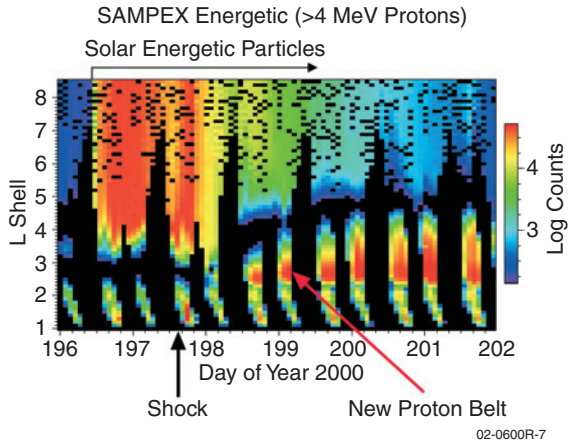

Figure 7. Energetic (>4 MeV) protons measured by SAMPEX during the 2000 Bastille Day magnetic storm. The figure shows both the solar energetic protons prior to the arrival of the shock that marked the onset of the storm and a newly trapped transient population that formed after the shock's arrival. (The periodic modulation seen in the figure are orbital effects associated with the location of the South Atlantic Anomaly relative to the plane of the SAMPEX orbit.) Solar energetic particles, accelerated by CME-driven interplanetary shocks, can penetrate into the inner magnetosphere to an equatorial geocentric distance of four Earth radii. Solar energetic protons (and heavier ions) can be trapped for days to months by the radial transport associated with the compression of the magnetopause by the shock, thereby creating new radiation belts, distinct from the stably trapped inner zone proton population. Since the proton gyroradii are comparable to the scale size of magnetic field gradients and curvature, they are easily lost to the atmosphere by abrupt changes in the magnetic field caused by subsequent geomagnetic storms. A significant change in the fluxes and outer boundary of trapped protons and introduction of new quasi-trapped populations can cause single event upsets to spacecraft electronics, while solar energetic particle events can directly affect manned space flight activities. (Figure courtesy of J. B. Blake, Aerospace Corporation)

singly or in combination, accelerate and transport electrons and ions most efficiently and under what conditions they do so.

2.2.1.2 Do localized acceleration processes contribute significantly to radiation belt acceleration? (Objective 1.1)

Some processes that may contribute significantly to radiation belt enhancements violate the first adiabatic invariant and can accelerate part of a lower-energy population to high energies through localized, stochastic processes. To violate the first invariant, the electric field acting on the particle must change on time scales comparable to or faster than a gyroperiod, which implies fluctuations in the very low frequency/extremely low frequency (VLF/ELF) range.

Radiation belt electrons encounter several different types of resonant waves during their drift orbit around the Earth. Interactions with low frequency whistler-mode hiss within the dayside plasmasphere and interactions with electromagnetic ion cyclotron (EMIC) waves near the duskside bulge of the plasmapause primarily cause pitch-angle scattering which tends to make the pitch-angle distributions more isotropic (as well as cause possible losses from precipitation). In contrast, resonant interactions with VLF "chorus" outside the plasmapause can lead to substantial energy diffusion, especially in regions of low plasma density where the wave phase speed is comparable to the resonant electron velocity. Stochastic acceleration, leading to a hardening of the high-energy tail population, can be maintained, as long as the pitch-angle distribution well away from the loss cone remains quasi-isotropic. Plasmaspheric hiss, EMIC waves, and VLF chorus are all enhanced during geomagnetic storms at the same time that strong convection electric fields transport plasmaspheric material associated with hiss toward the dayside magnetopause. (Objectives 1.1, 1.3c)

Stochastic processes are thought to be particularly important for electron acceleration in the radiation belts. To be effectively accelerated, electrons typically need to make multiple passes through energization-transport pitch-angle scattering. In one proposed scenario (**Figure 8**), energization by VLF chorus followed by pitch-angle isotropization by VLF hiss and EMIC waves could produce the necessary stochastic acceleration of radiation belt electrons.

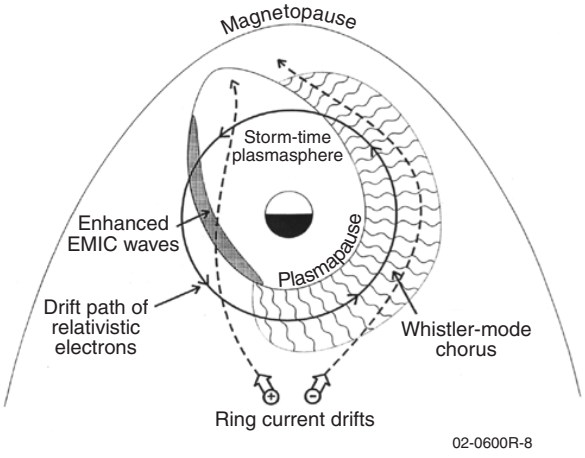

Figure 8. A schematic diagram of the equatorial magnetosphere illustrating the spatial regions for wave-particle interactions between relativistic electrons and various plasma waves. Relativistic electrons encounter a variety of plasma wave environments during their drift paths, which can produce diffusion, scattering, and acceleration. The details of the wave-particle interactions contribute to the dynamic behavior of the radiation belts. (Summers and Ma, 2000).

In contrast to the mechanism of inward radial diffusion, where particle acceleration is associated with the conservation of the first adiabatic invariant during transport into regions of increasing magnetic field, the signatures for local stochastic acceleration are:

- The development of localized peaks in the relativistic electron phase space density in the spatial region where interaction with VLF waves is important
- Hardening of the high-energy tail population (>300 keV) while lower energy electrons remain stably trapped at a flux level caused by the onset of wave instability
- Maintenance of quasi-isotropic pitch-angle distribution for the high-energy population, which is needed to maintain stochastic acceleration process
- The presence of enhanced VLF/ELF waves during the period of acceleration (for several days in storm recovery phase)

Therefore, with the measurements outlined in this report, the Baseline Radiation Belt Investigation should be able to determine when stochastic acceleration processes occur and how efficient they are in relation to other acceleration processes (Objective 1.1).

2.2.1.3 How do we distinguish among competing or simultaneous acceleration and transport mechanisms? (Objective 1.1)

During geomagnetic storms, when the radiation belts undergo the most dramatic changes, many mechanisms operate simultaneously, and the magnetosphere is highly distorted compared with typical conditions. Impulsive electric fields, convection electric fields, ULF wave power, VLF wave power, and energy input from the solar wind are all enhanced. Additionally, the storm-time ring current distorts the magnetic field, producing adiabatic changes (the "Dst effect") superimposed on other processes (Objective 1.3b). ***It is therefore very difficult to identify unambiguously one process or another as the causal mechanism for radiation belt enhancements. Fortunately, there are physical characteristics that make it possible to distinguish among various acceleration and transport mechanisms.***

Perhaps the most important of these characteristics is the radial gradient of phase space density for fixed adiabatic invariants. The second and third adiabatic invariants cannot be measured locally, although they can and need to be modeled (Objective 1.3c). The Baseline Radiation Belt Investigation has therefore been designed with two near-equatorial spacecraft. Equatorial measurements allow the assumption that the second invariant (the bounce invariant) is nearly zero and phase space density profiles at fixed values of the first invariant can be used.

As shown in **Figure 9**, three classes of processes can be readily distinguished by phase space density profiles. Large-scale (quasi-steady)

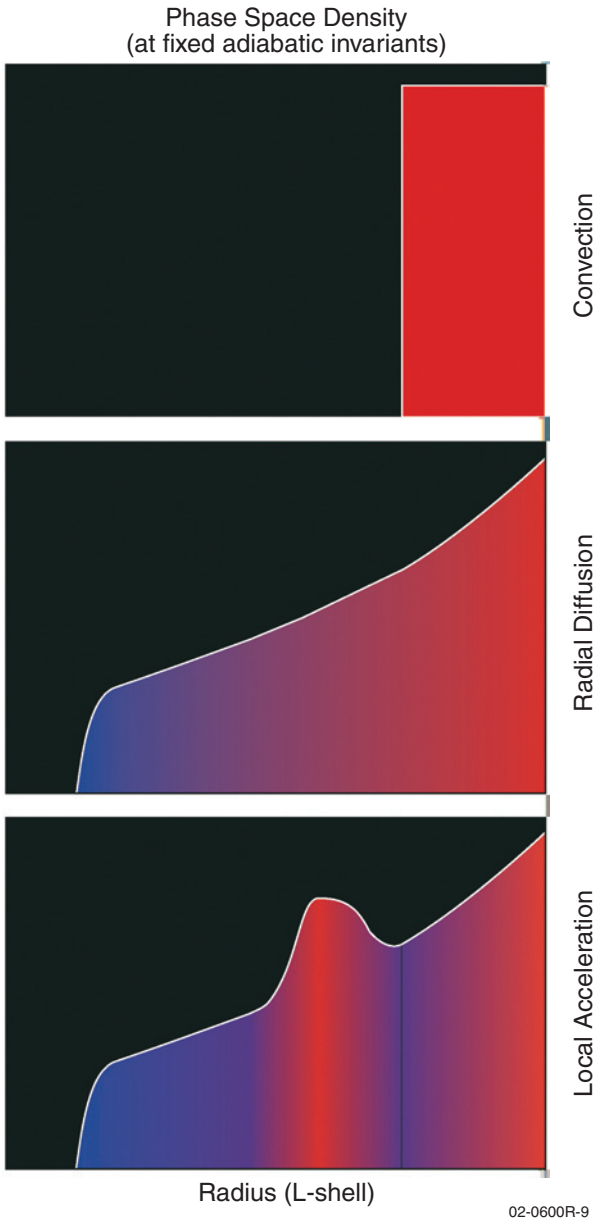

Figure 9. The radial variation of phase space density associated with three different transport and acceleration processes. These processes produce dramatically different radial profiles. The distributions are unlikely to be stable for longer than an orbital period; therefore, they can be differentiated only by measurements from more than one satellite. (Figure courtesy of G. D. Reeves, Los Alamos National Laboratory)

convection conserves the adiabatic invariants and produces flat phase space density radial profiles. Processes which accelerate particles through enhanced radial diffusion produce phase space densities that increase monotonically with radius. In contrast, stochastic acceleration process can produce local heating and resulting bumps or inflections in the phase space density profiles.

The equatorial pitch-angle distribution of radiation belt particles is also an important discriminator. Radial diffusion tends to enhance fluxes of 90° pitch-angle particles, producing pancake-like pitch-angle distributions. Stochastic wave–particle interactions rely on mechanisms that keep the particles outside the loss cone nearly isotropic.

The temporal evolution of events, on time scales of 1 hour or less, also distinguishes one process from another. The temporal evolution of spectral, spatial, and pitch-angle distributions all provide essential information. For example, ULF drift resonance is more effective at higher energies, so the spectrum and pitch-angle distribution should change more quickly at higher energies and at L-shells where the particles and waves are in resonance. Stochastic acceleration at, say, L ~ 4 enhances fluxes in that region first while diffusion from an external source enhances fluxes at high L first—yet those differences are only apparent in the very early phases of an event (**Figure 10**).

2.2.1.4 How do we predict and model the spatial, spectral, and temporal characteristics of radiation belt enhancements? (Objectives 1.2c, 1.4b)

While physical understanding of the processes that accelerate radiation belt particles is of paramount importance, our ability to answer some utilitarian questions reliably and accurately will be a good practical test of that understanding. Such questions are the following: For any given event, how intense will it be? How spectrally "hard" will it be? Where will the most intense fluxes be located? What are the solar wind conditions that produced it? How quickly will it develop and how long will it last?

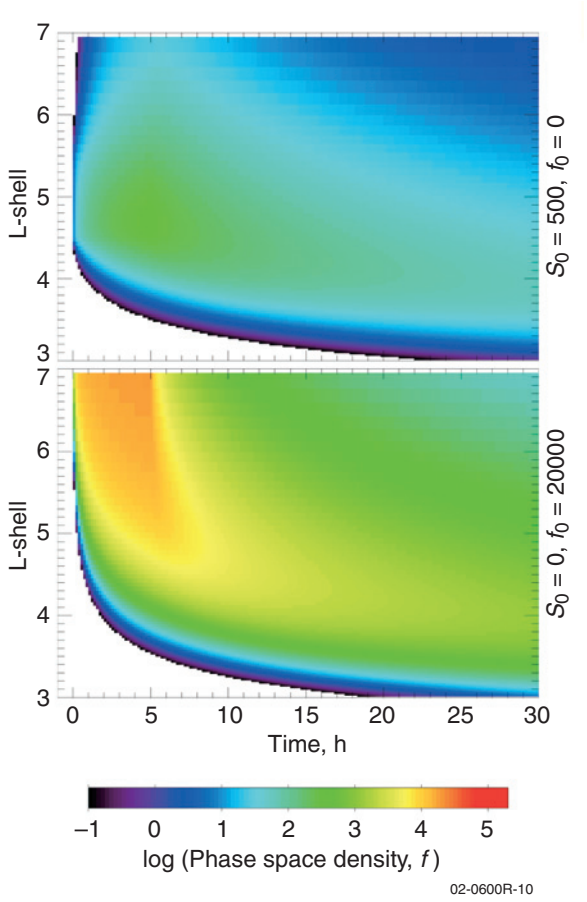

Figure 10. Model simulations of the spatial and temporal variability of phase space density associated with either local acceleration (top) or enhanced radial diffusion (bottom). Local acceleration leads to an early radial peak in phase space density for 4.5 > L > 5.0, which persists for over a day after the acceleration event. Enhanced radial diffusion initially produces a monotonic radial gradient in phase space density, but peaks may develop later due to losses from the system. (Selesnik and Blake, 2000)

Answers to these questions are challenging because each event has different spatial, spectral, and temporal characteristics (e.g., **Figure 5**). The intensity of the fluxes is not correlated with the radial extent of the enhancement, the location of the peak fluxes, or with the size of the geomagnetic storm (measured by Dst). Higher-time-resolution data (such as those available from geosynchronous satellites) further show that the rise time of an event, the time at which the event peaks, and the time it takes to decay also vary from event to event. It is also widely recognized that the intensity, spatial extent, and time profile within a given event are strongly dependent on the particular energy considered (**Figure 4**).

This is not to say that these characteristics are unpredictable. One of the interesting relationships is that the location (in L) of the peak fluxes at a given energy is strongly correlated with Dst (**Figure 11**). This phenomenon may be due to the fact that Dst strongly influences the location of the plasmapause, where waves certainly influence losses and may also influence acceleration. There have also been successful numerical predictions of, for example, fluxes of >2 MeV electrons at geosynchronous orbit based on internal magnetospheric parameters alone, as well as predictions based on solar wind parameters alone. While these predictions are reasonably accurate, the physical reasons for their successes are not well understood. ***The ability to accurately predict and model the spatial, spectral, and temporal characteristics of a given event based on a physical model is a goal that embodies both physical understanding and societal utility and therefore is one of the highest priorities of the Baseline Radiation Belt Investigation.***

Successful prediction and modeling may be possible based on magnetospheric observations

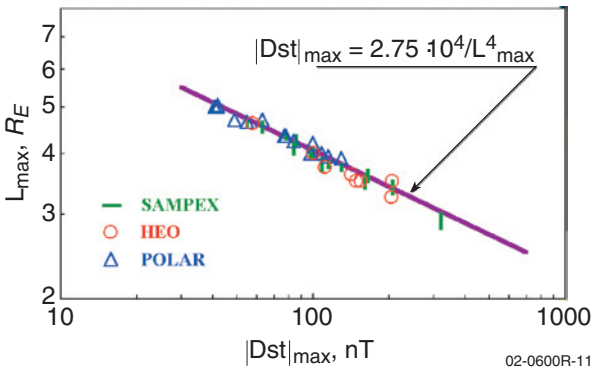

Figure 11. The location of the peak outer belt electron fluxes plotted against Dst, demonstrating a linear relationship. This is an example of a relationship that is clearly demonstrated but whose physical causes are not understood. (Tverskaya et al., 2001)

alone. Ultimately, however, we also need to understand the chain of causality that links solar activity to solar wind conditions to the magnetospheric processes that produce radiation belt enhancements. We do not currently know which conditions are either ***necessary*** or ***sufficient*** to produce radiation belt events.

We do know that many different types of solar wind drivers can produce radiation belt enhancements (**Figure 12**). These include high-speed solar wind streams, coronal mass ejections (CMEs), co-rotating interaction regions (CIRs), shocks, and other, more complicated solar wind structures. Likewise, we know that certain geophysical processes and conditions—such as enhanced wave activity and strong electric fields—are associated with these solar wind drivers.

The Baseline Radiation Belt Investigation will make the measurements necessary to develop a quantitative understanding of how various solar wind conditions activate the magnetospheric processes which accelerate and transport radiation belt electrons. ***A full understanding of the causal links between solar activity, solar wind conditions, magnetospheric processes, and radiation belt populations is necessary both for the development of long-term "climatological" models and for short-term space weather forecasting.***

2.2.1.5 Measurement objectives

In order to answer the questions and meet the objectives discussed above it is necessary to measure the source and accelerated particle populations with good energy and pitch angle coverage and to measure the electric and magnetic field fluctuations over a broad range of frequencies. A single well-instrumented spacecraft can measure the processes that produce accel-

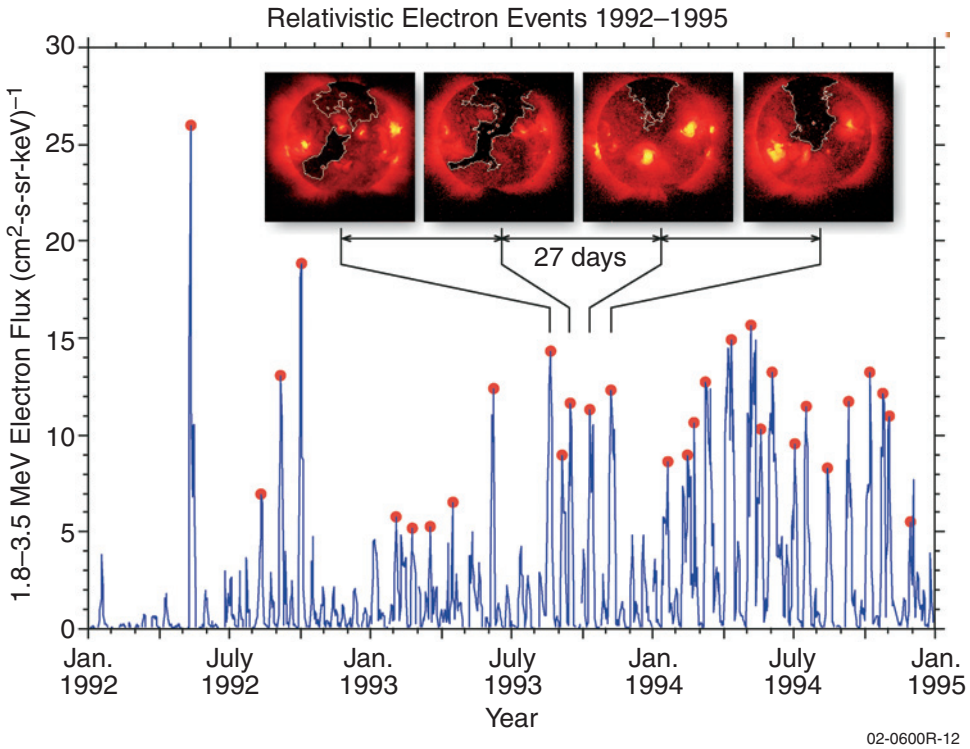

Figure 12. Relativistic electron enhancements driven by recurrent streams occurring during the declining phase and minimum of the solar cycle. Since CMEs produce relativistic electron events during the maximum period of the solar cycle, one can expect relativistic electron enhancements during all phases of the solar cycle in response to a variety of solar wind drivers. The most intense events are associated with high-speed streams from equatorial coronal holes such as those pictured here from Yohkoh. (Reeves, 1998)

eration and transport, but at least two spacecraft are required to actually ***measure*** the acceleration and transport—one in the region that the particles are transported ***from*** and one in the region that the particles are transported ***to***. An orbital configuration that produces a variety of radial separations of the spacecraft over the mission lifetime provides the greatest opportunity to understand these processes.

Therefore the Baseline Radiation Belt Investigation will:

- Simultaneously measure the radiation belt particle fluxes at a variety of radial separations over the course of the mission
- Measure near-equatorial pitch angle distributions and magnetic fields to determine multi-point phase space densities and radial phase space density profiles
- Measure the local convection electric field as well as electrostatic and electromagnetic waves which produce particle acceleration and transport
- Simultaneously measure the magnetic field and its variation at two points in the magnetosphere and develop statistical descriptions of the large-scale magnetic field dynamics
- Measure the ring current ion composition and intensity as inputs for global, storm-time magnetic field models
- Use the above measurements to develop self-consistent models of the magnetic field and radiation belt structure and dynamics as a function of the three adiabatic invariants

2.2.2 What Are the Dominant Mechanisms for Relativistic Electron Loss? (Objective 1.2a)

The radiation belts are maintained through the competing processes of acceleration from a lower-energy source population, radial diffusion, and loss through precipitation into the atmosphere or loss to the magnetopause. Electron loss becomes more pronounced during magnetically disturbed periods, and geomagnetic storms often produce a net loss of the relativistic electron population (**Figure 6**). These losses are permanent and are distinct from the temporary adiabatic dropouts associated with the "Dst effect." To be able to specify and predict changes in the radiation belt populations requires measurement and a quantitative understanding of the dominant loss processes.

2.2.2.1 What processes are responsible for electron loss?

Electrons can be lost from the radiation belts in two basic ways. They can either drift into the magnetopause or they can be scattered into the loss cone to be lost to the atmosphere through collisions. Magnetopause losses primarily affect the energetic electron population near the outer boundary of trapping and are most important under conditions of strong magnetopause compression. The process of "Magnetopause Shadowing" cannot account for losses at lower L-shells, near the region where peak fluxes are typically observed. Losses from the heart of the outer zone ($3 < L < 6$) are primarily associated with precipitation into the atmosphere, which can be directly measured on low-altitude spacecraft, or inferred from balloon observations of Bremsstrahlung X-rays. The precipitation is due to a combination of current sheet scattering, Coulomb scattering, or pitch-angle scattering during resonant interaction with various plasma waves. Scattering by enhanced plasma waves is thought to be a dominant process during magnetically disturbed conditions, but the relative effectiveness of such loss and its variability under different conditions are not sufficiently well understood to develop quantitative models. Precipitating high-energy electrons also penetrate to relatively low altitudes because of their high energy. There they can have important effects on magnetosphere-ionosphere coupling and, it has been postulated, may even influence climate through modulation of the global electrodynamic circuit.

Precipitation loss is caused by pitch-angle scattering in which either the first or second adiabatic invariant is violated. The rate of particle removal depends on the rate of pitch-angle scattering. Under weak pitch-angle diffusion the time scale for scattering is much longer than the particle bounce time, and a well-defined loss cone continues to be observed in the pitch-angle distributions. Under strong diffusion the pitch-angle distribution becomes nearly isotropic across the loss cone and the electron loss rate approaches an upper limit controlled only by the size of the loss cone and the particle bounce time.

The following questions are critical for a quantitative understanding of the role of electron loss:

- Can plasma wave scattering account for the temporal variability and global morphology of relativistic electron precipitation from the heart of the outer radiation belt?
- Which wave-particle scattering processes are most effective during different levels of geomagnetic activity?
- What is the contribution of magnetopause shadowing and current sheet scattering to relativistic electron loss during storms?
- What are the overall time scales for relativistic electron loss and how do these compare with the rate of radial diffusion?

Several distinct classes of plasma waves are able to interact with the relativistic electron population. The regions in the magnetosphere where such scattering occurs are illustrated in **Figure 8**. Both cyclotron and Landau resonant interactions contribute to the rate of scattering. With information on the power spectral density of the resonant waves, the local pitch-angle diffusion rates can be computed as a function of particle energy and pitch-angle. The average rate of precipitation loss requires averaging over the electron bounce and drift motions. The averaging requires detailed statistical models for the global distribution of wave and plasma properties for different levels of geomagnetic activity. Such models are currently unavailable, but they will be developed from measurements of the wave power spectral density made by the Radiation Belt Investigation. Among the plasma waves, which can produce significant scattering, are:

Plasmaspheric Hiss (300 Hz to 3 kHz). These are broadband whistler mode waves which are confined within the plasmasphere and produce weak pitch-angle diffusion with typical precipitation loss times comparable to a week. These waves, which persist under less disturbed conditions, may be responsible for the slow decay of relativistic electrons after a storm.

Electromagnetic Chorus (1 to 10 kHz). These discrete bursts of whistler-mode emissions are primarily observed outside the plasmapause over a broad region on the dawnside of the magnetosphere. These waves are generated by the injection of plasmasheet electrons during substorms and can produce microbursts of precipitation leading to average lifetimes comparable to a day during a storm. This loss will compete with any acceleration process during the recovery phase of a storm.

Electromagnetic Ion Cyclotron (EMIC) Waves (0.1 to 10 Hz). EMIC waves are generated by the injection of ring current ions and are primarily observed in the dusk-side plasmaspheric bulge. These intense waves can produce strong pitch-angle scattering of relativistic electrons in spatially localized regions where the drift paths intersect the plasmasphere and may play a major role in relativistic electron loss during the main and recovery phase of geomagnetic storms.

2.2.2.2 What are the average electron loss rates during storms?

Statistical models for the average scattering rate due to each class of plasma wave need to be developed (Section 3.2.1) to determine which wave-particle interactions are most important for

any specific storm. The associated precipitation removal can exceed the rate of inward radial diffusion in the inner magnetosphere (**Figure 13**), leading to a steep gradient in phase space density and a sharp inner edge of the stormtime outer zone population.

Coulomb scattering is most important for lower-energy particles and lower altitudes where collisions are more frequent. The degree of Coulomb scattering determines the size of both the bounce loss cone and the drift loss cone and is a strong function of the atmospheric scale height which is in turn a function of solar cycle. Coulomb scattering should not significantly affect the overall rate of loss of relativistic electrons, but its effect still needs to be evaluated. Current sheet scattering can cause a violation of the first adiabatic invariant when the radius of curvature of the magnetic field becomes comparable to the particle gyro-radius. Therefore this

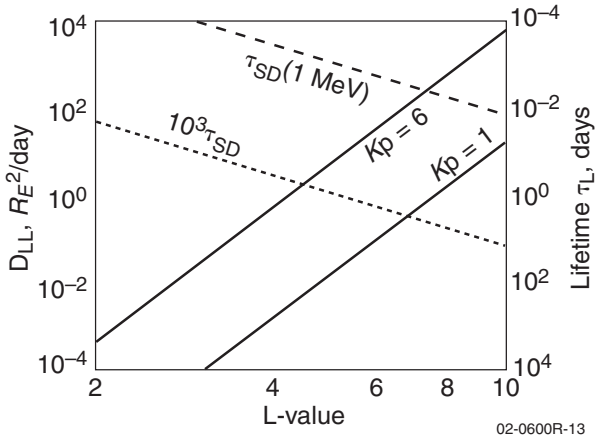

Figure 13. A comparison between the rates of radial diffusion (solid lines) for both storm-time (Kp = 6) and quiet (Kp = 1) conditions, with the rates of strong diffusion loss (dashed) for MeV electrons as a function of L shell. When averaged over the bounce and drift orbits, loss rates for relativistic electrons are probably between 0.1% ($\tau_{loss} = 10^3\ \tau_{SD}$) and 1% of the strong diffusion rate during a magnetic storm. Steep gradients occur in the relativistic electron phase space density when the rate of radial diffusion becomes slower than the rate of scattering loss in the inner magnetosphere (L < 5). (Note: τ is the time scale for radial transport and SD is the strong diffusion limit for electron loss.) (Brautigam and Albert, 2000)

mechanism tends to be more important at higher energies and at higher L-shells where the magnetic field can become sufficiently stretched. Distortion of the magnetic field due to the formation of the stormtime ring current (Section 2.2.3) can allow current sheet scattering to move to lower L during the main phase of storms. The field distortion will also cause electrons to drift outwards during the main phase of a storm, which can enhance the rate of magnetopause shadowing loss.

2.2.2.3 Measurement objectives

Because the rates of electron loss can be comparable to the rates of acceleration during certain phases of a storm, it is necessary to quantify the loss processes and include their effect in future predictive models. To accomplish this objective the LWS Radiation Belt Storm Probes must:

- Measure the energetic electron pitch-angle distribution near the loss cone and its variability during storms
- Measure the energetic electron precipitation flux on low altitude satellites (which can resolve the loss cone) and compare them with equatorial flux levels
- Measure the power spectral intensity of plasma waves which are responsible for pitch-angle scattering of energetic electrons

2.2.3 Ring Current Observations as Context for Radiation Belt Science (Objectives 1.3c, 1.4a)

Understanding the dynamics of the radiation belts is dependent on characterizing the ring current, its dynamics, and its modification of the global magnetospheric magnetic and electric fields. The Baseline Radiation Belt Investigation will directly address the following questions regarding the ring current and its influence on the radiation belts:

- What are the time history, locus, composition, and energy of ring current ions?
- What role does the ring current play in the storm-time wave phenomena affecting the acceleration, transport, and loss of radiation belt particles?
- What and how important are the ring current effects on the external electric and magnetic fields that cause transport and diffusion of radiation belt particles?

The storm-time ring current affects the radiation belts in three principal ways. First, the geomagnetic field defines the "coordinate system" that specifies the structure of the radiation belts and the motion of electrons. The diamagnetic effects associated with particle pressure of ring current ions (the principal carriers of ring current energy density) constitute a major perturbation of this coordinate system, affecting radiation belt particle drift paths. These magnetic field perturbations—and the associated changes in the radiation belts—evolve continuously throughout the main and recovery phases of geomagnetic storms as ring current plasma is injected, drifts, and is lost from the inner magnetosphere. Determination of the global ring current energy density and dynamics will provide the global current patterns needed for accurate modeling of the global magnetic field and thus of the coordinate system that governs the motion of the radiation belt particles.

A second simple, but profoundly important effect of the ring current on radiation belt dynamics is called the "Dst effect," after the magnetic index used to estimate ring-current strength. When injection of the ring-current particles inflates the magnetic field in the inner magnetosphere, a fast-drifting relativistic electron generally conserves its third invariant, which is the total magnetic flux inside its drift orbit. As the magnetic field decreases, the area inside the orbit increases, and the electrons move away from the Earth. The field decrease is accompanied by an eastward induction electric field, which de-energizes the electrons as they move outward. The net result is a major decrease, sometimes by more than an order of magnitude, in electron flux at a given location and energy. This process reverses during the recovery phase of the storm, when the field contracts and the electrons are drawn back into the inner magnetosphere. A significant challenge in our understanding and modeling of radiation belt fluxes is that the critical acceleration, transport, and loss processes appear to be strongest during storm main phases when the Dst effect is operating simultaneously.

Third, the storm-time ring current is a controlling factor in many of the processes known to affect radiation belt electrons, such as the wave spectrum and radial diffusion. Ring current ion distributions provide the free energy (sometimes with the requirement of plasmasphere overlap) for the wave growth that contributes to electron acceleration, transport, and loss. Detailed in situ measurements will determine the free energy available locally; however, because many interesting effects may take place at locations remote from the in situ measurements, global characterization of the free energy content is also desirable. The ring current is also both an indicator and a significant modifier of the global electric field strength and distribution, which are the critical parameters in quantifying the elements of the diffusion matrix.

In summary, the radiation belts are strongly influenced by the highly dynamic electric and magnetic fields associated with geomagnetic storms and the build-up of the storm-time ring current. Understanding this influence will depend on the ability to follow the dynamics of the ring current, and on using that information in physics-based assimilation models to derive the electric and magnetic fields. Together, localized in situ measurement and global imaging

of the ring current will provide the constraints needed to improve models of the storm-time magnetic and electric fields in the inner magnetosphere (**Figure 14**; cf. Section 3.2.3 in the following chapter).

To provide the contextual information needed for understanding the behavior of the radiation belts, the Baseline Radiation Belt Investigation should

- Measure in situ the composition of the ring current ions, both to understand their sources and to determine their energy density and pressure gradients
- Determine the global distribution of ring current ion composition, energy density, and pressure gradients

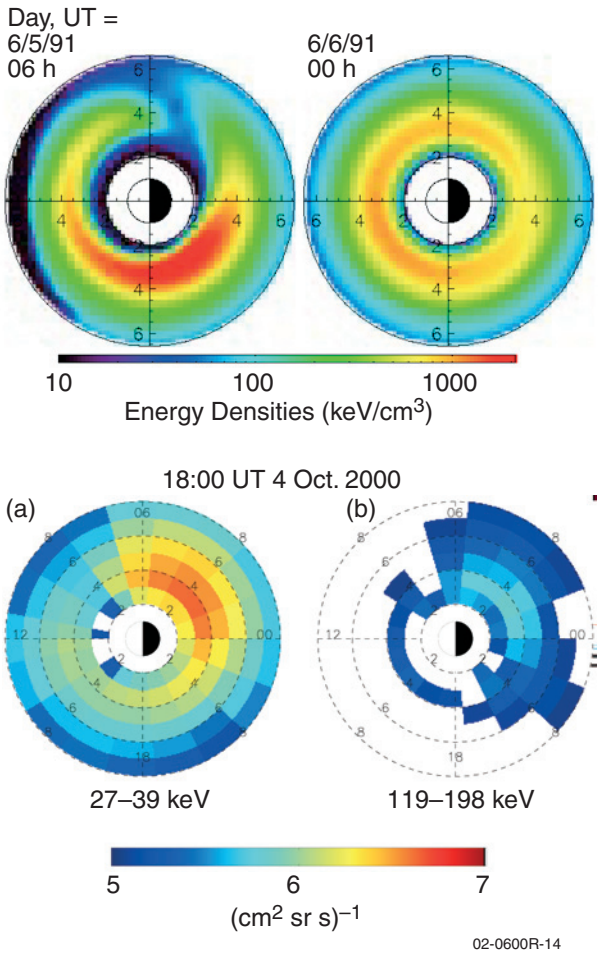

Figure 14. Comparisons between present-day physics-based models of the ring current populations (top row) and the populations derived by inverting energetic neutral atom (ENA) images (bottom row) reveal discrepancies. Dramatic and unanticipated azimuthal structure is revealed in the ENA-derived distributions, reflecting corresponding azimuthal structure in magnetospheric and ionospheric currents. The comparison shows the value of obtaining global information. (Top row from Kozyra et al., 2002; bottom row courtesy of IMAGE/HENA team)

The ring current not only affects the radiation belts but also plays a crucial role in the coupling of the inner magnetosphere to the ionosphere-thermosphere system (Objective 2A.1b). The asymmetric ring current is made continuous by field-aligned currents that close through the ionosphere, and the pressure gradients within the ring current map along geomagnetic field lines to create ionospheric electric fields. At high latitudes, the combination of currents and fields can lead to Joule heating. At middle and equatorial latitudes, the ring current may be responsible for penetrating electric fields. These fields create uplift of the equatorial ionosphere and drive ionospheric plasma poleward. These fields may also be responsible for the latitudinally confined flow of plasma to mid-latitudes seen in positive phase storms (see Section 2.3.2). ***Understanding the relation of the ring current to these ionospheric electric fields is key to understanding ionosphere-magnetosphere coupling during geomagnetic storms.*** To establish this relationship, ring current imaging can be used to

- Infer mid-latitude and penetrating storm-time electric fields from the global distribution of ring current pressure gradients

2.2.4 Space Weather Effects of the Radiation Belts

Since the dawn of the space age in 1957, there has been explosive growth in both the number of satellites operating in Earth's harsh space environment and in the variety of functions that

these satellites perform to support human activities and the nation's economy. We depend on satellites for purposes that range from military functions such as surveillance and communications, to commercial enterprises such as national and international banking transactions, to science and the exploration of Earth, the solar system, and the universe. Satellites are used for meteorology, land and ocean resource management, and to support countless new communication technologies such as pagers, satellite television, and the Internet. The uses of satellites reach deep into the fabric of our society. And just as land-based resources are vulnerable to hurricanes and tornadoes, our space assets are vulnerable to storms in the space environment. Moreover, with the occupancy of the International Space Station beginning in 2000, there is now a permanent presence of humans in space, and the effects of the space environment on the health and safety of astronauts must be taken in account in mission planning.

The Baseline Radiation Belt Investigation will measure components of the radiation belt environment that can cause such effects on satellites as surface charging, deep dielectric or bulk charging, single event upsets (SEU), total dose effects, and material degradation (**Figure 15**). Effects can range from simple upsets on satellites from which recovery is relatively easy to total mission failure. A major spacecraft insurance company recently estimated that over $500,000,000 in insurance claims, made during

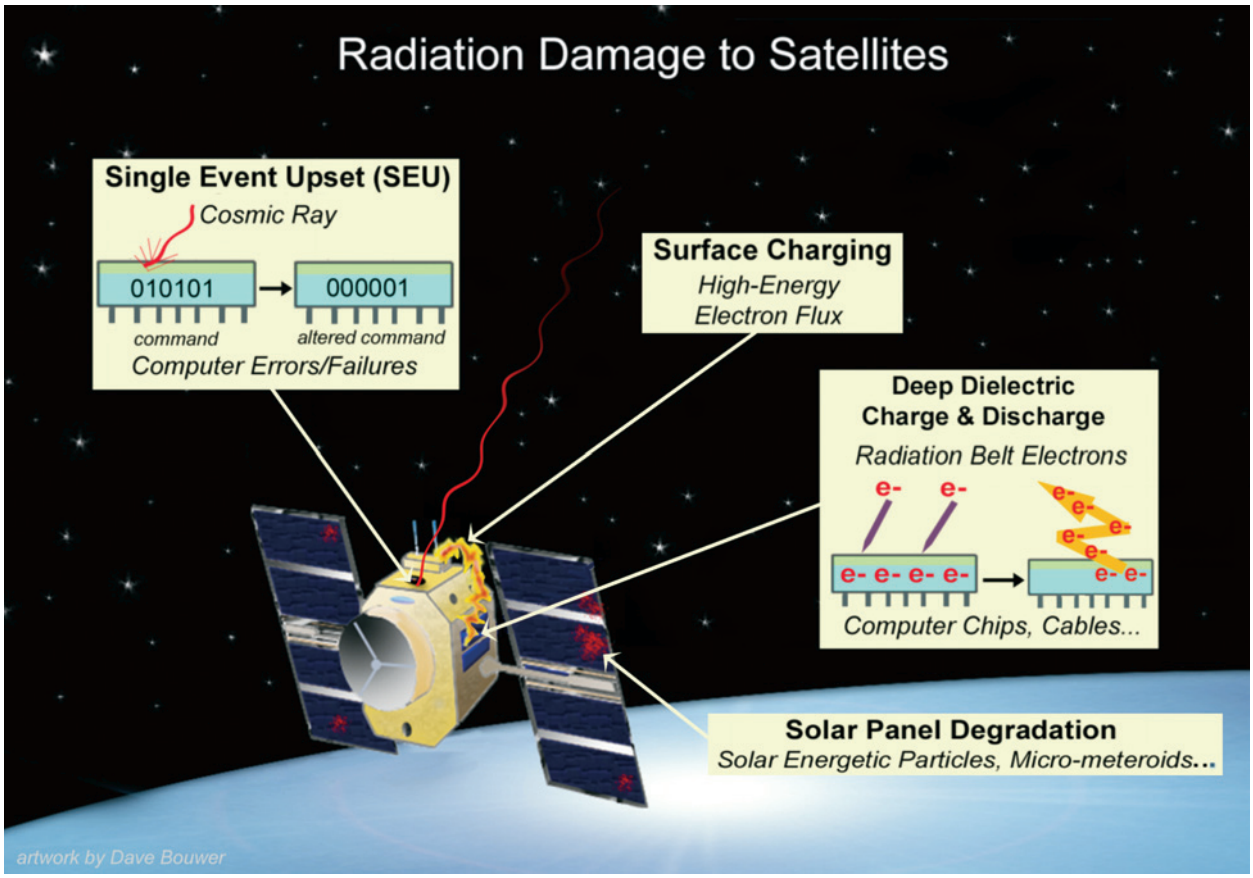

02-0600R-15

Figure 15. Satellite electronics can be harmed by energetic particle radiation from the galaxy, the Sun, and from particles accelerated in Earth's magnetosphere. The Radiation Belt Storm Probes will measure the energetic particles that are responsible for satellite effects. (Figure courtesy of H. Singer, T. Onsager and D. Bouwer, NOAA/SEC)

a four-year interval in the late 1990s, were caused or contributed to by space weather.

Surface charging and differential charging can damage electronic devices. Such charging is caused by electrons in the 1 to 100 keV range and occurs predominantly during geomagnetic storms and substorms. Numerous geosynchronous satellite anomalies have been attributed to surface charging, since anomalies often occur on Earth's dawnside at geosynchronous orbit in the path of these electrons.

Deep dielectric charging occurs when high fluxes of relativistic electrons, ranging in energy from several hundred keV to many MeV, penetrate spacecraft shielding and imbed themselves in spacecraft dielectrics such as coaxial cables or circuit boards. Discharges and subsequent damage appear to occur after long periods of high fluxes. These effects have been demonstrated in the laboratory, and spacecraft problems during increased fluxes of these high-energy electrons are evident. It is still not clear, however, which, if any of the spacecraft failures, can be ascribed specifically to radiation effects.

Single event upsets occur when high-energy protons or heavy ions (~>50 MeV) penetrate spacecraft shielding and interact with electronic logic, causing device tripping, component latch-up, or failure. Particle bombardment of memory devices can also change onboard software through physical damage or through deposition of charge, resulting in a "bit flip." SEUs are most frequent around solar maximum owing to the increase in the number of solar flares and CMEs.

Total dose effects are related to spacecraft aging from the continual exposure to the energetic particle environment. One example of **material degradation** experienced by spacecraft is the permanent damage to solar panels that results from the exposure to energetic protons, with energies of tens of MeV, during solar proton events. Such damage to the solar panels causes a loss in satellite power output, shortening satellite lifetimes or forcing less than optimal power management schemes.

Astronauts could be affected by the high-energy radiation that will be measured by the Baseline Radiation Belt Investigation, because the high-inclination orbit of the International Space Station makes it susceptible to solar proton events and exposes it to dangerous portions of the radiation belts.[4] Efforts to meet radiation dosages that are "as low as reasonably achievable" require monitoring and modeling of the radiation environment. In addition, aircraft that fly polar routes are affected by high-energy protons because the protons impact the ionosphere and interfere with HF communications. High-energy protons also pose a potential health hazard for aircraft crews and passengers and should be monitored.

The characterization and understanding of the radiation belt environment and dynamics that will result from the Baseline Radiation Belt Investigation will lead to practical benefits for technological systems and human activities. Radiation belt data will be incorporated into new models that will be used by spacecraft designers and manufacturers to build more robust satellites that are more resistant to, if not immune from, dangers in the space environment. Improved models, which calculate not just worst case or static averages but also the actual solar cycle radiation exposure during expected mission lifetimes, will provide spacecraft manufacturers with the knowledge needed to address issues such as satellite replacement strategies and materials usage. Understanding of the radiation belt environment acquired during the Radiation Belt Investigation will be used to develop new physics-based models that can be employed by the Space Weather Operations Centers in the

[4] Cf. National Research Council, *Radiation and the International Space Station: Recommendations to Reduce Risk*, National Academy Press, Washington D.C., 2000.

National Oceanic and Atmospheric Administration (NOAA) and the Department of Defense (DoD). Data will also be assimilated into models to improve their performance and to extend the characterization of the radiation environment from localized measurements to locations throughout geospace. A subset of the radiation belt data that is available in real time, or near real time, will be useful for situational awareness for space weather forecasters and spacecraft operators, while archived data will be used for resolving and understanding spacecraft anomalies that occur during the Radiation Belt Investigation. Finally, data from the Radiation Belt Investigation and improved radiation belt models will be used to help reduce the radiation risk to astronauts, for example, by adjusting scheduled space walks.

2.3 Ionospheric-Thermospheric Variability

Solar radiation constitutes the dominant global energy source in the ionosphere and thermosphere (I-T). As the Sun's ultraviolet radiation changes, so too do the composition, ionization state, chemistry, and dynamics of Earth's near-space environment. Superimposed on this global source is even more extreme variability in the thermosphere and ionosphere during times of geomagnetic storms. This variability affects systems employing trans-ionospheric signal propagation (communication and navigation) and HF radio propagation and can increase atmospheric drag on spacecraft and orbital debris.

Decades of effort have been expended in observing the ionosphere at both high latitudes and low latitudes where variability is common. At low latitudes considerable progress has been made, and new missions such as Communication/Navigation Outage Forecasting (C/NOFS) have been designed to address specific questions related to identifying the important influences that control the onset and evolution of plasma structure. We know that the high-latitude ionosphere responds rapidly to the variable solar wind. Distributed space-based and ground-based measurements are now being used to describe these variable inputs and the corresponding responses. Only recently, however, with the increased utilization of ground-based diagnostics, have we been sensitized to the frequent occurrence and dramatic impact of ionospheric structures at middle latitudes. Interestingly, these structures appear in a region of geospace where the ionosphere and thermosphere are coupled to the inner magnetosphere.

Storm time influences represent the strongest drivers of variability in this mid-latitude region. In order to describe these influences we must be able to consider the magnetospheric drivers and variations in the solar extreme ultraviolet (EUV) separately. The Baseline I-T Investigation therefore focuses on electrodynamic influences on the mid-latitude ionosphere-thermosphere system. During disturbed times, the electrodynamics of the region is strongly influenced by electric fields resulting from particle motions in the inner magnetosphere and from neutral wind perturbations produced by particle and Joule heating. Thus a strong connection exists between the phenomena being studied by the I-T and radiation belt Baseline Investigations. The causes and properties of mid-latitude ionospheric variability, especially during storm times, are neither well characterized nor well understood. Ground-based observations have organized mid-latitude storm time variability into two phases: the positive phase, which often occurs during the periods of decreasing Dst when ionospheric densities peak at 3 to 5 times their quiescent values, and the negative phase, which often occurs during storm recovery when ionospheric densities can be depleted by a factor of 3 to 5. ***Characterizing the spatial properties and understanding the sources of the dynamic behavior of the mid-latitude I-T system is a prime focus of the LWS/Geospace Program***.

Single-spacecraft data typically provide "line cuts" through the ionosphere and thermosphere, with varying altitude, latitude, longitude, and local time but with revisit times that are frequently much longer than storm-time evolution scales. Ground-based observations provide good temporal coverage but are restricted to small spatial scales. Advances in our understanding of the global state of the I-T system will therefore depend largely on data from multiple spacecraft that reduce the revisit times and on the integration of data sets with results from thermospheric general circulation models (TGCMs) that include most of the known physical, chemical, and dynamical processes internal to the upper atmosphere. However, important discrepancies in density, composition, and circulation exist between physics-based models and empirical models. And these modeled states of the atmosphere and ionosphere have not been validated on global scales. Underlying this lack of quantitative assessment are large uncertainties in our knowledge of the solar radiation deposited in the I-T region on time scales from minutes (flares) to decades (solar cycle); of the coupling of the magnetosphere and plasmasphere to the I-T system; of propagating waves from the lower atmosphere; and of the length scales associated with all these phenomena. ***Critically needed are new observations of the global I-T system that provide information with which to specify the system's behavior under various conditions of solar and geomagnetic activity on time scales that are shorter than an orbital period.***

Two classes of data are needed to satisfy the priority science objectives of the I-T Investigation. First, in situ measurements from multiple satellites flying through the I-T system are required to provide precise, detailed measurements of the ionosphere as a function of latitude and longitude. Additionally, major new capability can be brought to bear on space weather research through global imaging of high latitude storm-time drivers (via auroral imaging) and of the corresponding ionospheric response (via global imaging of ionospheric densities and neutral composition). ***Imaging not only establishes the global response of the I-T system to solar and geomagnetic forcing, but also provides context for the in situ measurements.*** Two-dimensional remote sensing and in situ measurements thus support and reinforce each other in a synergistic, cost-effective fashion. Imaging also tests large-scale predictions of TGCMs. Ultimately, both in situ and imaging data need to be assimilated into physics-based models to provide the essential steps toward the specification and prediction capability that is needed for space weather systems.

2.3.1 How Does the Ionosphere-Thermosphere System Vary in Response to Changing Fluxes of Solar Extreme Ultraviolet Radiation?

Solar EUV irradiance creates virtually the entire ionosphere and provides most of the thermospheric heating at high altitudes. Consequently, solar radiation establishes the basic state of the I-T system. EUV irradiance varies greatly on time scales ranging from minutes to decades and perhaps longer. ***In order to characterize, to assess, and ultimately to forecast space weather in the ionosphere and thermosphere, we must have a thorough understanding of the qualitative and quantitative relationship between the incident solar irradiance and the state of the I-T system.*** Presently, we do not have that understanding.

The principal uncertainties have been distilled into two key science questions dealing with the consistency between the EUV irradiance, the I-T system response, and their respective variations. These issues and their resolution by the I-T Investigation are discussed next.

2.3.1.1 Is solar EUV radiative forcing consistent with the I-T ground state temperature, composition, electron density, and dynamics? (Objectives 2A.1a, 2A.2, 3A.1a, 3A.2)

The most fundamental prerequisite for understanding a physical system and its variability is the demonstration of congruency among energy sources, sinks, and the state of that system. There are major difficulties not only with our knowledge of the magnitude and variability of the solar radiative energy input, but also with the agreement among models of the corresponding I-T state. For example, recent observations of solar EUV fluxes at wavelengths below 30 nm are discrepant by as much as a factor of 4 with the community standard empirical spectral irradiance model based on Atmosphere Explorer satellite data. Neither irradiance models nor measurements are yet able to specify the absolute magnitude of the EUV irradiance to better than a factor of 2 at many geoeffective wavelengths. Such discrepancies between observations and models in the fundamental energy input to the I-T system lead to enormous uncertainties in the determination of temperature, composition, electron density, and solar-forced dynamics that physical models predict. ***Knowledge of the global scale behavior of the I-T system and its internal consistency with solar energy input will establish the validity of our most basic understanding of the space weather of this region.***

So far, no simultaneous measurements of the solar spectral irradiance and the global-scale character of the atmospheric and ionospheric composition and dynamics have been made. As a result, only partial validation of first-principles models has been possible. However, even when global circulation models of atmospheric composition and temperature are "tuned" to the same solar (and geomagnetic) conditions as the community standard empirical (Mass Spectrometer and Incoherent Scatter, MSIS) neutral density model, important differences exist between the two. One example of these differences in the thermospheric composition and temperature under low geomagnetic activity conditions is shown in **Figure 16.** Systematic discrepancies between the two models exist throughout the atmosphere. The state of affairs is at least as bad for the ionosphere. **Figure 17** shows a comparison between the community standard International Reference Ionosphere empirical model and the SAMI2 physics-based model. Major discrepancies can be seen in both the horizontal and vertical structure of the electron density. It is unclear whether these discrepancies are the result of deficiencies in general circulation models, perhaps having to do with inadequate or missing physical processes, or are the results of improper solar and geomagnetic inputs or uncertainties in the observational database used to construct the empirical models. The new NASA Thermosphere, Ionosphere, Mesosphere Energetics and Dynamics (TIMED) satellite measurements of the EUV irradiance by the SEE

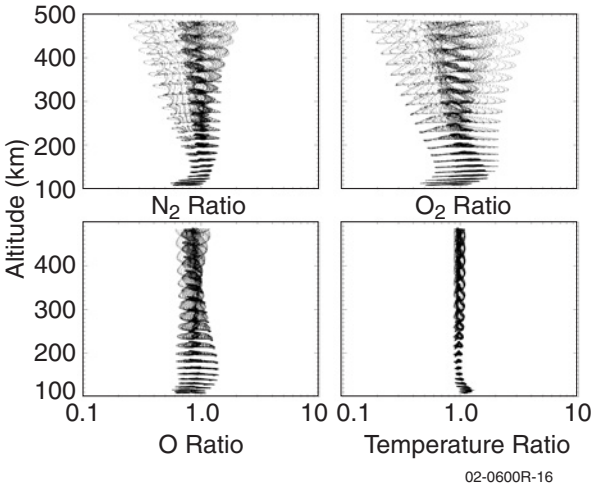

Figure 16. A comparison between the thermospheric–ionospheric general circulation first principles model and the Mass Spectrometer and Incoherent Scatter (MSIS) empirical model. The panels display ratios of the neutral species concentrations and temperature versus altitude for 1752 geographic locations for moderate solar activity conditions. Even though the models have been run for the same solar-geophysical conditions, very significant systematic differences can be seen over much of the upper atmosphere. (Meier et al., 2001)

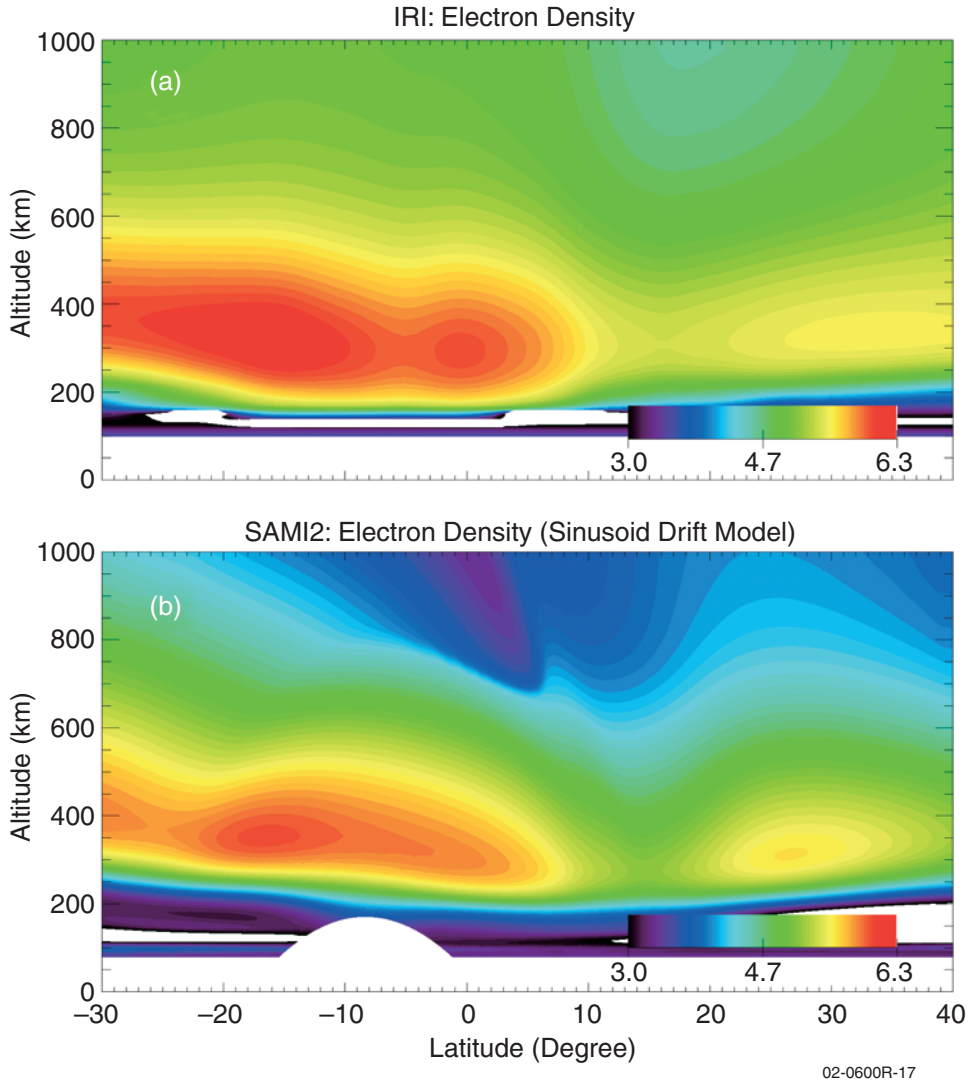

Figure 17. Major differences appear between the predictions of the ionospheric electron density by the International Reference Ionosphere (IRI) empirical model (upper panel) and the SAMI2 first principles model (lower panel). The locations of the Appleton Anomaly (peaks in the southern hemisphere) and the northern hemisphere enhancement near 30°N are significantly different in the two models. Striking disparities are evident in the high-altitude morphology. (Figure courtesy J. Huba)

instrument and measurements of the thermosphere and ionosphere by GUVI are beginning to redress this situation but lack the global scope, temporal cadence, and completeness of ionospheric parameter measurements to secure full understanding. Clearly, these issues require resolution before space weather assessment and forecasting can be carried out with any degree of confidence.

In order to answer the title science question, it is necessary to:

- Establish the internal consistency between the solar EUV and the atmospheric and ionospheric ground state predicted by first principle models and validated with in situ and global measurements
- Define quantitatively the relationship between the neutral composition and the electron density, both locally and globally

To accomplish these objectives, the Baseline I-T Investigation will provide simultaneous measurements of:

- Solar EUV spectral irradiance (from Solar Dynamics Observatory)
- I-T composition, temperature, and plasma (by in situ measurement)
- The O/N_2 ratio and nighttime electron density (via global I-T imaging)

2.3.1.2 How does the I-T system respond directly to changing solar radiation on all time scales? (Objectives 2A.1a, 2A.2, 3A.1a)

Portions of solar FUV and EUV spectral irradiance can vary by factors of 2 or more over the 11-year solar cycle; X-rays exhibit even more variability. As the solar irradiance increases, the I-T system responds directly. Temperature and neutral density both rise in concert, the electron density increases, and the ion and neutral composition change. In the example shown in **Figure 18,** the estimated solar cycle variation in the EUV sunlight causes the temperature at 500 km to vary by a factor of 2, the neutral density by a factor of 40, and the electron density by more than a factor of 10. Smaller changes occur on a 27-day cycle as solar active regions rotate to face the Earth. EUV variations on solar flare time scales (minutes or less) are also observed. **Figure 19** shows a prediction that the F-region ionosphere can change dramatically and non-uniformly in response to a major flare (Bastille Day, 14 July 2000). The EUV irradiance at many geoeffective wavelengths increased during the period of an hour by amounts comparable to their solar cycle amplitudes. Clearly, solar irradiance variations can produce complex I-T system weather on many time scales.

Our understanding of how the Sun forces the ionosphere and thermosphere to respond on these time scales hinges first on an accurate knowledge of solar variability. Predictions of

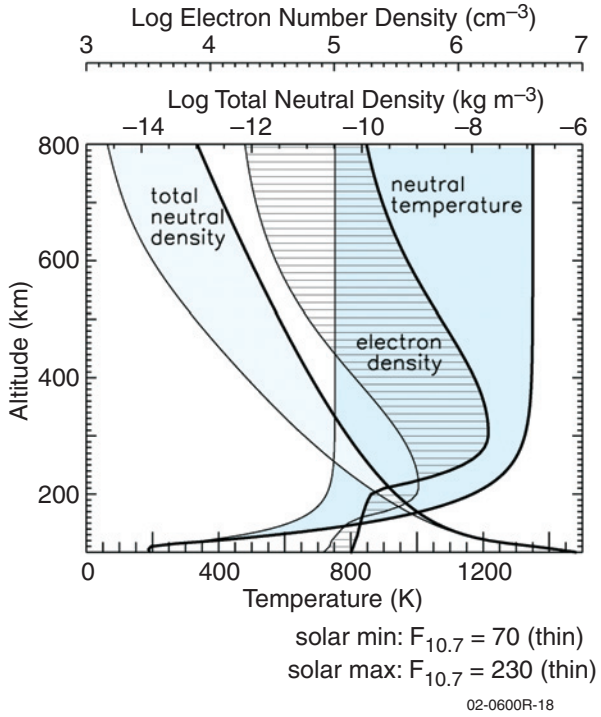

Figure 18. Temperatures and densities calculated using the MSIS and IRI empirical neutral and ionosphere models, respectively. Variability in far and extreme UV solar irradiance from low to high activity levels heats the upper atmosphere and increases the total neutral and electron densities, leading to variations of more than an order of magnitude. (Lean, 1997)

the solar cycle variation of the EUV spectral irradiance from physics-based and empirical models are widely discrepant. Important differences exist on 27-day rotational scales as well. Only a dedicated program to observe the solar spectral irradiance and the global I-T system concurrently can provide the information needed for a comprehensive understanding on the relevant time scales.

To understand how the ionosphere and thermosphere respond to solar forcing, the Baseline I-T investigation will obtain:

- EUV spectral fluxes and global thermospheric images to determine how the radiative forcing, the neutral atmosphere composition, and the electron density change in concert

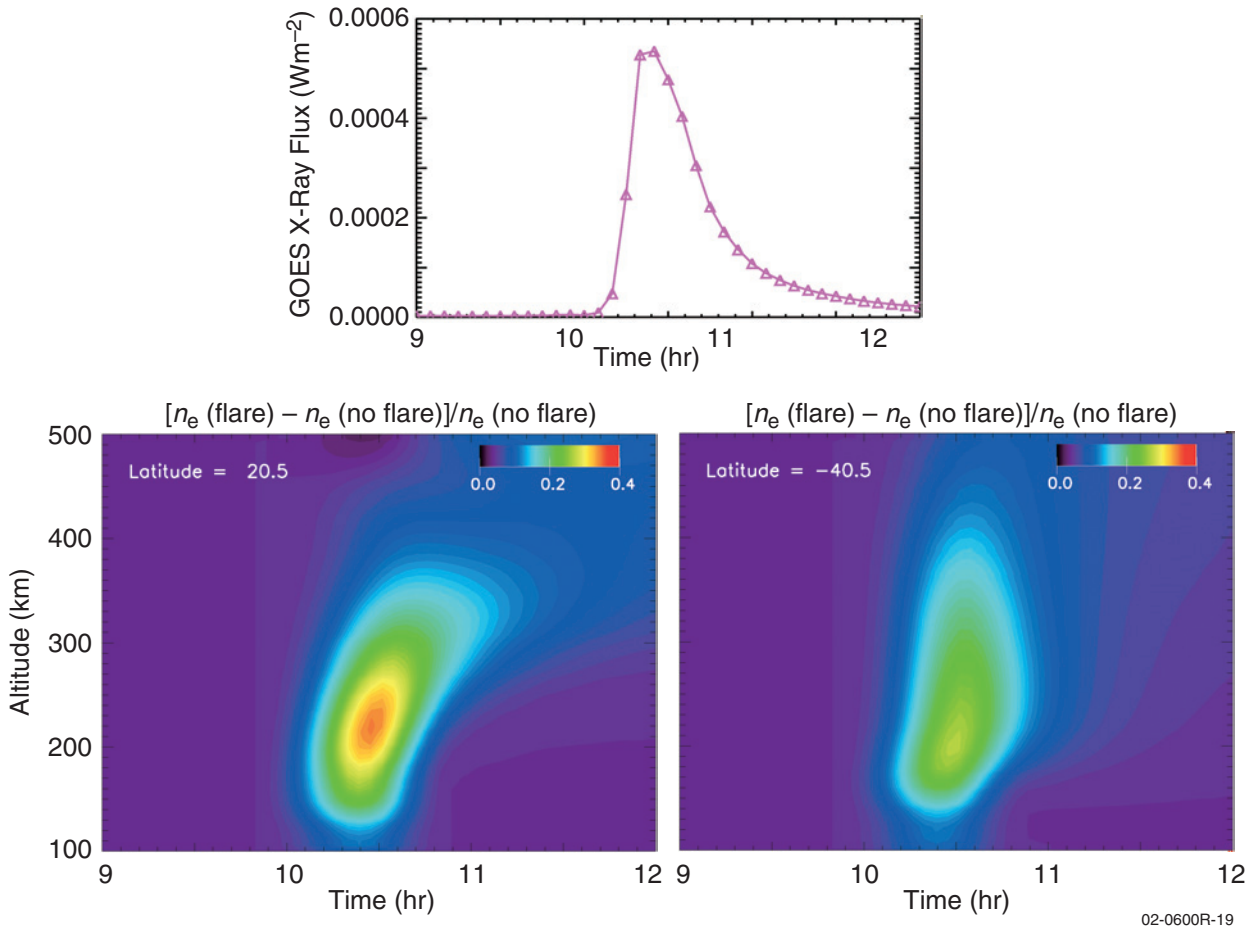

Figure 19. Ionospheric variability predicted by the SAMI2 model during the Bastille Day flare 14 July 2000. The upper panel shows the (0.1 – 0.8 nm) solar x-ray irradiance from GOES-8. The lower left panel shows the predicted change in electron density at 20°N magnetic latitude on the Greenwich magnetic meridian, compared with the quiescent ionosphere. The lower right panel shows the predicted change at 40°S magnetic latitude on the Greenwich magnetic meridian. The significant differences in both the magnitude and the shape of the production and recovery can be explained by neutral winds that have a net upward component in the north and a downward component in the south. (Figure courtesy J. Huba)

- EUV spectral fluxes and I-T in situ composition, electron density, winds, and temperature to establish how the state of the neutral atmosphere and ionosphere changes as the solar EUV varies on time scales from minutes to a solar cycle

2.3.2 How Does the Mid- and Low-Latitude Ionosphere-Thermosphere System Respond to Geomagnetic Storms? (Positive Phase Storms)

Positive-phase ionospheric storms are the first half of the typical mid-latitude ionospheric response to geomagnetic storms. First identified using ionograms, the positive phase is an increase in ionospheric density during the growth and main phase of a geomagnetic storm. The ionospheric densities may increase by 2 to 5 times their quiet-time values and may also rapidly decrease or fluctuate from the viewpoint of a ground-based observer. An example of a mid-latitude response to a geomagnetic storm is shown in **Figure 20**. The increases in ionospheric plasma density result from (a) horizontal and vertical transport of ionization, (b) field-aligned transport that raises the F-peak, and (c) changes in neutral composition, which increase or decrease the chemical loss rate. All these processes are modulated by magnetic activity.

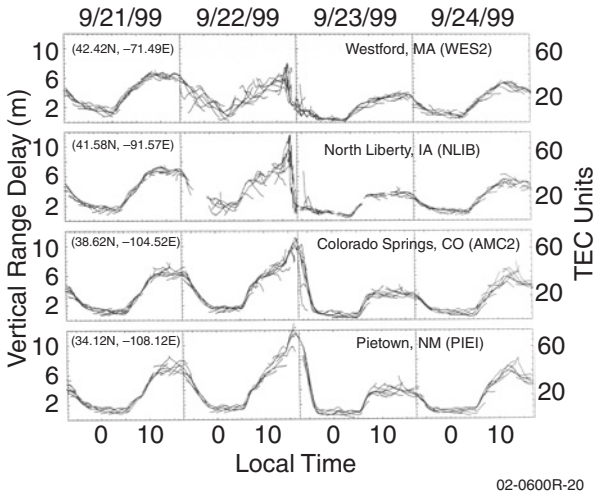

Figure 20. Range delays (from GPS satellites to receivers) recorded at four GPS stations distributed across the United States during the period September 21–24, 1999. The first and last days show the quiet-time ionosphere range delays. The second and third days show a typical mid-latitude ionospheric response to a geomagnetic storm. On the second day, during the positive phase, the range delay is larger and more variable. On the third day, during the negative phase, the range delay is smaller, corresponding to a depleted ionosphere. This figure demonstrates the fast time variations and spatial gradients in range delay that make the ionosphere problematic for GPS-dependent technology.

Our primary objectives are to

- Discover the relative importance of mechanisms responsible for positive storm signatures
- Discover the temporal and spatial scales that characterize the different mechanisms

The scientific issues relating to storm-enhanced densities can be summarized in two significant questions regarding unresolved processes.

2.3.2.1 What are the distributions and characteristics of positive phase ionospheric storms as a function of latitude and longitude? (Objectives 2A.2b, 3A.1b)

Figure 21 illustrates some key features of a positive-phase storm-time density enhancement in the ionosphere. During storm times, enhanced density regions appear in longitudinally confined regions at middle latitudes and subsequently extend poleward and toward the dayside. The longitudinally confined density regions are associated with extremely high total electron content, and the density gradients that mark the edges of the enhancements apparently seed irregularities. In the presence of extremely large total electron content, these irregularities produce significant radio scintillation (i.e., rapid fluctuation in signal power). In order to assess the effect of these density enhancements on trans-ionospheric radio propagation we must determine where such enhancements appear, the conditions under which they occur, and the factors that control their dynamics.

The enhanced density appears to be due initially to transport from lower latitudes. But the subsequent poleward transport is also influenced by the electrodynamic interaction between the magnetosphere and the plasmasphere. Our ability to distinguish between a longitudinally confined plasma source and a longitudinally confined electrodynamic configuration will mark a key advancement in our understanding. ***Characterization of the longitude distribution of temporally evolving electric fields and neutral winds, which are directly or indirectly driven by magnetospheric activity, is of fundamental importance to a proper nowcast and subsequent forecast of the state of the low- and mid-latitude ionosphere.***

A prompt penetration electric field followed by a delayed disturbance field is a well-documented response of the equatorial I-T system to geomagnetic storms. To date, however, observations of these fields are restricted to a single longitude region with a peculiar magnetic field orientation (eastern United States). Little is known of the longitude or latitude variations in the large-scale electric fields that evolve during a magnetic storm. Modeling studies suggest that, for a uniform increase in the magnetospheric potential, thermospheric disturbances propagate

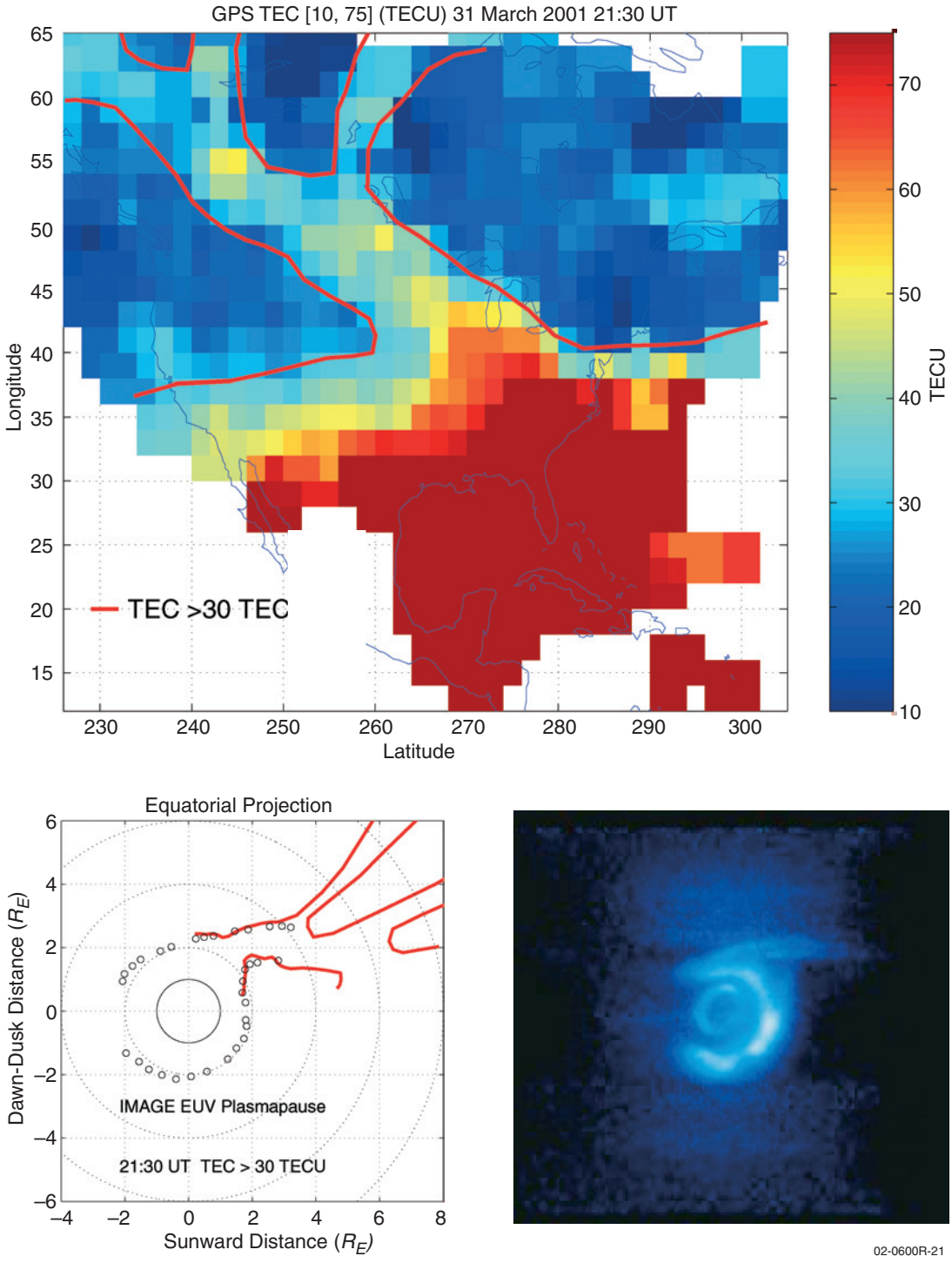

Figure 21. Plumes of elevated ionospheric total electron content (TEC) and storm enhanced density (SED), which result in significant mid-latitude ionospheric space weather effects, map directly into plasmaspheric tails. IMAGE observations of the plasmasphere (lower right) show a sunward-directed plasmatail. Simultaneous ground-based observations of TEC over the North American continent (top panel) show a pronounced band of storm-enhanced density extending from Florida through the Great Lakes region. A mapping of the plasmaspheric tail to the magnetic equator (lower left) and to the ionosphere (red lines) demonstrates the coupling of the inner magnetosphere to the ionosphere during a positive phase storm. (Foster et al., 2002)

equatorward in the longitude region in which the displacement of the magnetic pole is located. Such a process would generate a universal time dependence on the effectiveness of storm-time perturbations, but an effect may be additionally modulated by asymmetries in the longitude distribution of Joule heating and particle precipitation, which implies that the local time distribution of precipitation and Joule heating is also desired. Particle precipitation can be measured in situ along a spacecraft track and Joule heating can be estimated from ground observations combined with assimilative modeling techniques. Auroral imaging can be used to extend in situ and ground observations to a global (hemispheric) scale and will significantly improve the accuracy of assimilative models. ***To provide an adequate description of these processes, we must (a) discover the longitudinal extent over which the neutral wind and electric field each evolve and (b) determine the variation in latitudinal distributions of the winds and fields at different storm epochs.***

Regarding the first point, magnetic declination will provide a first-order internal longitudinal variation. However, other longitude variations, driven for example by the competition between magnetospheric and corotation fields, may also exist. Regarding the second point, large penetration jets are the most pronounced manifestation of storm-time influences. However, neutral wind surges and associated dynamo-driven electric fields will be much more commonly observed. At present, there is no information on the longitudinal scales in these features that we should strive to capture in a physics-based model.

In order to make progress in answering all of these questions, we must do the following:

- Make simultaneous measurements of the ionospheric electric field, the ion drifts, the neutral wind and composition, and the plasma density profile at middle latitudes, sampling adjacent longitude regions with a temporal resolution faster than an orbital period
- Accumulate such measurements during a storm to discover the evolutionary behavior of the polarization fields
- Assess the changes in the magnetospheric inputs associated with the described evolution of the electric fields, winds, and the plasma density distributions

2.3.2.2 What causes the transport of plasma from the equator to mid-latitudes during geomagnetic storms? (Objectives 2A.1b, 2B.1, 3A.1b)

Changes in the ion density at a given location are intimately associated with the transport properties of the plasma. A dramatic example of transport-driven changes in plasma density appears at low latitudes during storm times when the prompt penetration of electric fields lifts the F-region to much higher altitudes than expected. This lifting produces an overall increase in TEC because of the reduction in the chemical loss rates at higher altitudes. However, rather dramatic reductions in the density will occur near 500 km if the F-region peak is lifted above this altitude. The upward motion of the F region also transports plasma from lower to high latitudes as the upward and outward motion is accompanied by downward and poleward field-aligned diffusion. Subsequent interactions between this mid-latitude plasma enhancement and the magnetospheric penetration electric field could produce the previously described phenomenon of positive-phase ionospheric storms.

Mid-latitude evidence suggests a longitudinal confinement to the density enhancements (see preceding section), and **Figure 21** suggests that the ionospheric uplift itself may occur in a longitudinally confined sector. Why does the ionospheric uplift occur when and where it occurs? Is there a preferred local time or longitude?

These key questions must be addressed to provide an adequate physical framework for examining the evolution of the phenomenon. Both magnetospheric processes and those internal to the I-T system may be involved. The most straightforward explanation for a localized electrodynamic uplift is the existence of a zonal polarization electric field. Perhaps magnetospheric processes can produce a longitudinally confined electric field, which would eliminate the need to invoke internal processes. But if internal processes play a role, they would require a conductivity gradient across which a uniform current is driven. Polarization fields will result to maintain current continuity and the large-scale uniform current could be driven by magnetospheric penetration fields or by neutral winds, each with characteristic temporal scales.

To answer the question posed in the title of this section we need to understand (a) the connection of the mid-latitude density enhancements to the vertical ion transport at the equator and (b) the convection of density enhancements poleward and toward local noon.

Specifically, it is necessary to determine

- The roles of magnetospheric penetration fields and their interaction with corotating flows impressed upon the ionosphere
- The universal time dependence of the location of penetration fields with respect to the terminator
- The longitude variations of storm time electric fields causing uplift at the equator

To this end, during positive-phase storms the Baseline I-T Investigation will measure:

- Ion drift or electric fields from the equator through mid-latitudes on multiple, simultaneous paths, allowing their evolution during a storm to be described
- Ionospheric density as a function of altitude, latitude, longitude, and local time to determine the response of this parameter to the electric field and to identify density gradients that are proxies for conductivity gradients and sources of scintillation
- Thermospheric winds to determine their contribution to plasma transport and polarization electric fields

2.3.3 How Do Negative-Phase Ionospheric Storms Develop, Evolve, and Recover?

Another challenge for space weather research is to understand the aftermath of the dynamically driven phase of a geomagnetic storm. Many of the ionospheric perturbations result from coupling with the neutral atmosphere through changes in composition and dynamics. The upper atmosphere can remain perturbed for more than a day after a storm and can continue to deplete the ionospheric plasma. Understanding the interactions between the plasma and the bulky, inertially constrained neutral atmosphere is therefore one of the keys to predicting the evolution and spatial distribution of ionospheric depletions. ***One of the specific objectives of the Baseline I-T Investigation is to quantify how the interactions between the neutral atmosphere and the ionosphere affect the distribution of ionospheric plasma.***

Many of the processes responsible for depleting the ionosphere at mid-latitudes are well-known. Plasmaspheric flux tubes are stripped away by magnetospheric convection, thermospheric winds force ions to regions of increased loss rate, electrodynamic drift redistributes plasma, and the drastic changes in neutral composition create holes in the ionosphere. The neutral composition changes are long-lived and recover very slowly; understanding their growth and evolution is crucial for quantifying their role in negative ionospheric storms.

One example of an ionospheric depletion being created is shown in **Figure 22,** which depicts a large reduction in airglow intensity on the dayside of the Earth. The weaker airglow is associated with a reduction in the column abundance of atomic oxygen, and an enhancement in the proportion of neutral molecular species, which hastens the recombination rate of O^+. The airglow image, acquired with the far-ultraviolet imager on the Dynamics Explorer 1 (DE-1) spacecraft, and the ionosonde data are a vivid demonstration supporting a well-established theory for the negative phase of an ionospheric storm. However, DE-1 captured very few of these images, and the imager was not able to resolve the details in the composition structure or follow the time evolution with sufficient cadence.

We know little about the spectrum of scale sizes that characterize ionospheric depletions. Are the depletions localized and discrete or uniform over a widespread geographic area? Composition changes, direct neutral wind forcing of the ionosphere, and electrodynamics all contribute to electron density depletions. The Baseline I-T Investigation will not only characterize the scale sizes of the ionospheric depletions, but will also determine the relative contribution of each process. The improved understanding will dramatically improve our ability to predict and forecast the state of the system.

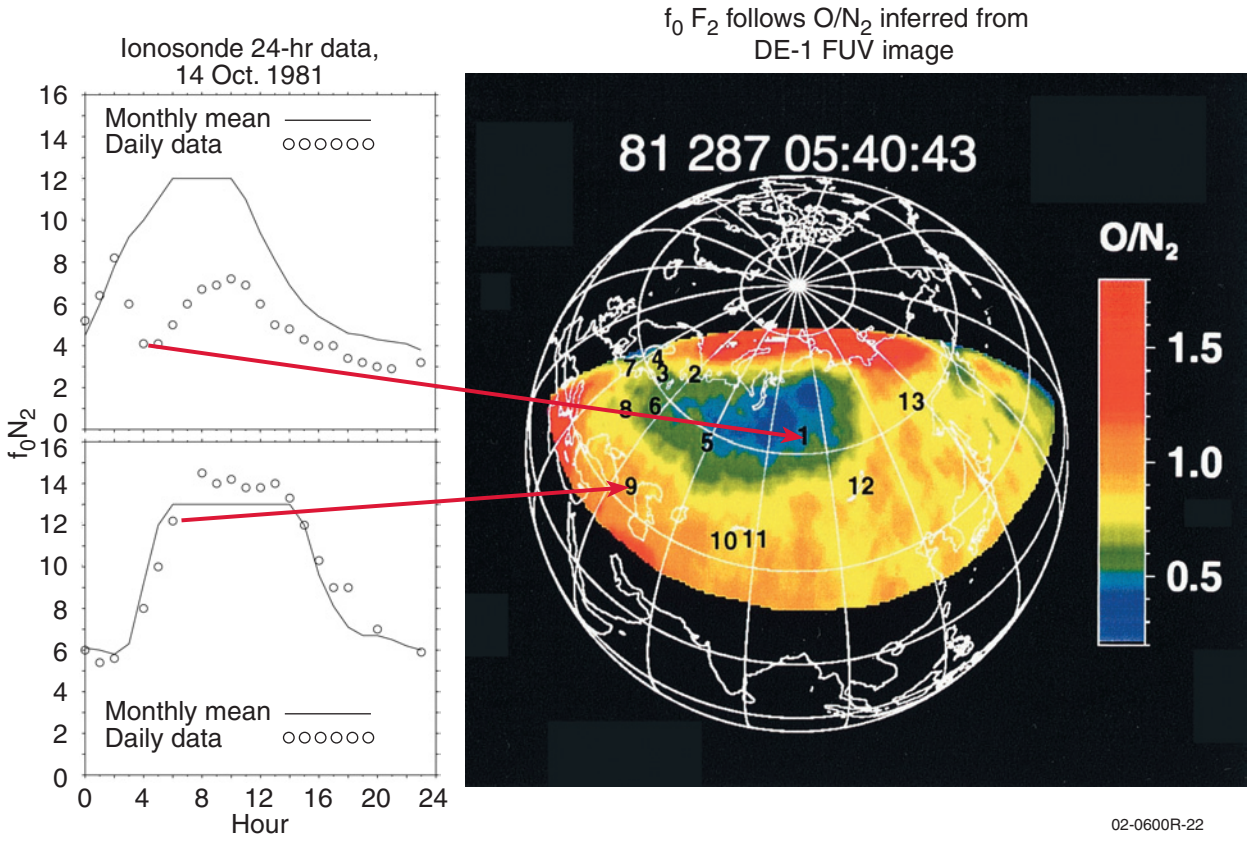

Figure 22. The O/N_2 ratio for a storm in October 1981 deduced from a DE-1 FUV satellite image showing a depleted region. The 24-hour ionospheric F2-region critical plasma frequency (left panels) demonstrates that the ionospheric electron density is depleted inside the depleted region while nominal outside. Further examination of a number of stations shows that the negative excursion of the critical plasma frequency is proportional to the O/N_2 ratio. This dependence demonstrates that ion chemistry dominates the production and loss of the electron density. (Figure adapted from Strickland et al., 2001)

2.3.3.1 How do the magnitude, spatial structure, and time history of storm-time Joule heating relate to the shape and size of neutral composition changes? (Objectives 2A.1b, 2A.2, 3A.1b)

Storm-time neutral composition changes are created when divergent winds force upwelling of the neutral gas from low to higher altitudes. Localized Joule heating and auroral particle heating drive the divergent wind. The thermospheric response is driven by the integrated vertical transport over several hours, so the size and structure of the composition changes will be a complex mix of the spatial and temporal history of the source. ***We currently have little knowledge as to whether the composition features result from large-scale convection or from the accumulation of many small-scale mixing cells.*** Imaging has clearly revealed the patchy nature of the auroral processes. However, the spatial scales of Joule heating, the primary driver of the heating and upwelling of the neutral gas, cannot be imaged directly. In situ and ground-based observations, combined with assimilative modeling, are typically used to provide maps of Joule heating. The accuracy of modeled Joule heating, however, can be significantly improved when combined with auroral imaging.

The divergent wind, which is an integral part of the upwelling process, forces the predominantly atomic oxygen thermospheric gas out of the way, first horizontally (usually equatorward) but also eventually downward. In the region of downwelling, the proportion of molecular neutral species actually increases, giving rise to reductions in ion loss rate and increases in ion density. The nature of the downwelling is unknown.

To understand the important scale-sizes in the growth of the composition disturbance zones and their relation to the scale-size of the source regions, the Baseline I-T Investigation will provide a combination of imaging and in situ measurements to:

- Determine the spatial structure and temporal evolution of Joule heating to specify the driving mechanism
- Measure the thermospheric horizontal and vertical neutral winds over different spatial scales at F-region altitudes during geomagnetic storms when the magnetospheric sources intensify and expand to mid-latitudes
- Measure the neutral temperature and the changes in number densities of the neutral species in response to the upwelling and downwelling
- Measure the scale sizes, expected to range from a kilometer to hundreds of kilometers, of the vertical motions and the composition response
- Sample the latitude and longitude structure over all local-time sectors

2.3.3.2 How does the composition evolve as it is transported by the wind field? (Objectives 2A.1b, 2A.2, 2A.3, 3A.2)

Neutral winds transport composition disturbances away from their source region as they gradually recover by molecular diffusion. The wind field itself is a superposition of the normal daily background circulation and the changes induced by the storm inputs. Dynamics can advect the features, change their shape, and produce structuring analogous to fluid turbulence. Physical models have been able to simulate the creation of the composition features, and have shown that transport by the global wind field can explain the general seasonal and diurnal characteristics of the ionospheric storm response at mid-latitudes. During summer, the prevailing summer-to-winter global circulation is very effective in transporting composition changes to mid-latitudes in the recovery phase of a storm. As a result, in summer, the mid-latitudes typically experience a negative phase, while the response at winter mid-latitudes is much more variable. During intense storms, the source re-

gion for the local upwelling and composition change penetrates directly to mid-latitudes. In these circumstances, the negative phase can be initiated very rapidly and does not rely on the gradual transport from higher latitudes before strong ionospheric depletions are produced. ***Understanding the balance between in situ generation and transport of composition from higher latitudes is crucial to tracking the development and evolution of the storm-time ionospheric response.***

In order to predict the characteristics of electron density during the recovery phase of a geomagnetic storm, the structure and depth of the neutral composition changes must be understood. It is essential to determine the scale-sizes of the composition features that produce the most severe ionospheric depletions. We must also understand how the features move under the influence of the global neutral wind field, and track their evolution as they gradually recover over the day or two following a geomagnetic storm.

By combining imaging and in situ observations the Baseline I-T Investigation will:

- Determine the extent of the regions of depleted atomic oxygen on the dayside of the Earth and follow their evolution
- Measure the in situ neutral species concentrations and temperature to relate the column integrated remote observations to the actual in situ properties of the gas
- Measure the neutral winds over different spatial scales to determine how the composition structure is transported by the wind field
- Measure how the scale-sizes of the composition features evolve through time and determine their relationship to the ion density depletions
- Resolve the question as to whether additional loss processes, such as vibrationally excited molecular nitrogen, are required to explain the plasma depletions during geomagnetic storms

2.3.3.3 How do changes in neutral dynamics during a storm affect the development, evolution, and recovery of ionospheric depletions? (Objectives 2A.1b, 2A.2)

The storm-time dynamics of the neutral gas are fundamental in the initial creation of the composition disturbance zones. When combined with the background wind fields, the storm-driven winds are also the source of the transport of the perturbations. Neutral winds also have a direct impact on the ionosphere, pushing plasma along the inclined magnetic field. Lastly, the dynamo action of the storm-time winds generate large polarization electric fields which directly transports plasma. It is therefore imperative that we understand the time-dependent storm dynamics and the latitude, longitude, and local-time dependence of the changes to the thermospheric circulation.

The evolution of the thermospheric circulation is highly time-dependent, being initiated by the rapid energy injection at high or mid-latitudes, and the development of neutral wind surges propagating around the globe. After the passage of the transient wind surges, a new circulation develops slowly, but is unlikely to ever reach a new equilibrium even for the simplest of storm forcing. The wind and waves continually slosh around the globe as the circulation decays under the action of viscosity and ion drag. The continually evolving wind field also drives electrodynamic polarization fields that are important in controlling the plasma distribution, particularly at low latitudes. ***How the wind and electrodynamic fields evolve during the storm is currently very poorly characterized, yet is fundamental in predicting the evolution of the ionospheric depletions.***

Knowledge of the time scales for the recovery of the global thermal structure is also important for following the dynamic changes during a storm. Changes in temperature and pressure gradients drive the global storm-time wind pattern initially, but the winds also advect energy and convert dynamics to heat through adiabatic processes. After the cessation of high-latitude storm heating, the latitude structure in the global energy balance is altered, and continues to drive storm winds.

To characterize the time history of the changes in neutral dynamics and thermal structure the Baseline I-T Investigation will:

- Measure the structure in the neutral wind surges over a range of spatial scales and determine their contribution to the low and mid-latitude dynamo electric field
- Determine the evolution of the thermospheric wind field and its impact on transport of composition features
- Measure the ion drift at mid-latitudes to determine the importance of dynamo processes in the electrodynamic redistribution of plasma
- Measure the latitudinal and longitudinal thermal structure to determine its importance in the recovery of the global circulation

2.3.4 What Are the Sources and Characteristics of Ionospheric Irregularities at Mid-Latitudes? (Objectives 2B.1, 2A.3)

The preceding discussion has focused on the large scale variability of the ionospheric plasma density. This plasma, however, can also vary widely in scale, with scale-sizes ranging from hundreds of kilometers to centimeters, which has profound effects on communication, navigation, and radar systems. The sources of free energy that drive the ionosphere unstable include electric fields, velocity shears, neutral winds, and other forcing functions, often operating in concert. A broad irregularity spectrum is created through the action of a hierarchy of plasma instability mechanisms, such as the Rayleigh-Taylor, the gradient drift, and cross-field instabilities. Some of these mechanisms operate more efficiently in certain distinct regions of the globe and at distinct local times. For example, the gradient drift instability at high latitudes, the Rayleigh-Taylor instability at equatorial latitudes, and possibly the gradient drift and/or Perkins instability at mid-latitudes. The societal impact of these irregularities depends on their absolute amplitudes, which in turn depend on the large-scale variability of the ionosphere and the ionospheric response to solar EUV irradiance. Hence, ionospheric variability and irregularities are closely related.

Irregularities have been studied most extensively at high and low latitudes. At high latitudes, for example, polar cap patches—plasma structures possibly originating at mid-latitudes—convect through the polar cap and form irregularities via the gradient drift instability. Irregularities at low latitudes are well known as equatorial spread F (ESF), produced in the post-sunset ionosphere by the Rayleigh-Taylor instability. In contrast to high- and low-latitude instabilities, plasma instability mechanisms at mid-latitudes are poorly understood. ***Our ability to characterize these irregularities and to understand their driving mechanisms suffers from a lack of basic measurements and from limited theory and modeling.***

Recent campaigns using the Millstone Hill incoherent scatter radar have demonstrated that intense mid-latitude electron density structures are created and evolve during magnetic storms as discussed in Section 2.3.2. The penetration of large storm-induced electric fields is likely to overpower the normally stable mid-latitude ionosphere. This process appears to occur dur-

ing positive storms, when dense equatorial plasma is transported poleward and subauroral ion drift flows move equatorward. The combination of density gradients and fast plasma flows produces electron density irregularities with scale lengths of tens of kilometers to meters, whose presence and intensity have been documented from ground-based scintillation and total electron content measurements. (See, for example, **Figure 23**, which shows GPS scintillations over central New York.) ***However, the spatial extent, temporal evolution, intensities. and spectral properties of these irregularities have not been characterized and in some cases never even measured. Their causes, evolution, and decay are completely unknown.***

Other large-scale mid-latitude plasma structures include spectacular cases of ionospheric "formations" that are observed at mid-latitudes in ground-based airglow images. **Figure 24** shows an airglow image obtained at Arecibo, PR, indicative of plasma depletions, which, at first glance, are strikingly similar to those observed during intense ESF. Unlike ESF, this type of

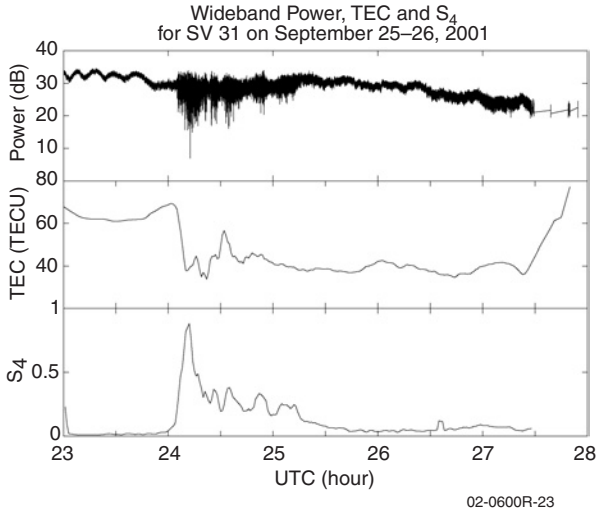

Figure 23. GPS scintillations during a modest geomagnetic storm. The largest-amplitude scintillations correspond to elevated TEC and steep gradients. Peak values of the S4 index of 0.9, coincident with the TEC gradient and representative of the largest amplitude scintillations, will cause many GPS receivers to fail.

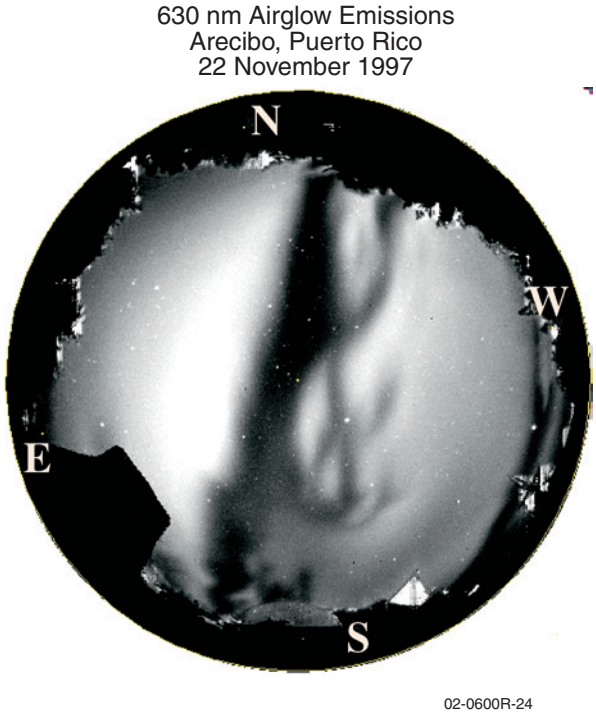

Figure 24. Wave-like structures in airglow emissions associated with large electron density perturbations during a geomagnetic storm. Such large-scale structures and their motions are commonly observed at mid-latitudes during storms but are not understood. These structures affect differential GPS corrections and radio wave propagation. (Kelley et al, 2000; courtesy American Geophysical Union)

structure, however, is not related to eastward zonal plasma flow and appears to be a different type of ionospheric "traveling" disturbance related to a poleward surge associated with global magnetic storms. Simultaneous GPS measurements indicate that such large-scale depletions contain strong sub-kilometer scale irregularities. In addition to airglow measurements, remarkable radar backscatter maps of 3-m irregularities at middle latitudes show structures that appear to be very similar to ESF. The intensity of the backscatter returns indicate that the medium has been driven hard by an underlying instability mechanism that has yet to be identified. Possible instability processes include the gradient drift instability or Perkins instability, although neither provides a very satisfactory explanation for these mid-latitude irregularity observations.

Scintillations have been almost solely studied from the ground, and we have only recently begun to appreciate their significance for orbiting platforms such as Shuttle and the International Space Station. GPS is increasingly being used in space. ***Since many low Earth orbit (LEO) spacecraft will see GPS signal paths through most of the F-region ionosphere, irregularities and associated scintillations at all latitudes must be studied from a viewpoint entirely different from that of ground-based measurements.*** The present state of scintillation theory and simulation is not adequate to predict the effects of irregularities on LEO scintillation receivers. Instead the properties of the irregularities must be measured and characterized. Only then can theories and models be developed and tested using these data.

Although the I-T Investigation focuses on mid-latitudes, it will also provide important data related to ESF itself and, in particular, will contribute to our understanding of how, and under what circumstances, the mid-latitude and low-latitude structures are related. Since strong ESF includes unstable flux tubes that may extend to geomagnetic latitudes of 20° or more, their effects will be observed to geographic latitudes as high as 30°, depending on the longitude. The dual satellite system proposed herein will thus help to characterize the location, magnitude, and temporal evolution of ESF, as well as use its unique instrumentation to advance our understanding of ESF irregularities and their drivers.

Mid-latitude plasma density irregularities cover an enormous range of scale sizes, from hundreds of kilometers to less than 1 m. They represent a real and very poorly understood class of phenomena that likely have numerous energy sources and instability mechanisms. Scintillations and other space weather effects associated with irregularities of scale lengths >100 m are significant and can, for example, be just as severe as those produced by ESF. It is thus a major objective of the I-T Investigation to understand both the conditions for the appearance and growth of such irregularities as well as the detailed properties of the waves themselves. This information will enable a direct understanding of how efficiently the irregularities scatter and disrupt communication, navigation, and radar systems.

To address the question posed in the title of this section, the Baseline I-T Investigation will:

- Characterize the morphology, extent, and amplitudes of mid-latitude irregularities
- Discover the sources of the free energy that generates the irregularities
- Characterize the spectral properties of mid-latitude irregularities that produce scintillations
- Determine the detailed electron density and electric field wave characteristics of irregularities, including wavelength, phase velocity, anisotropy, and nonlinear evolution

2.3.5 What Are the Space Weather Effects of Ionospheric Variability at Mid-Latitudes?

Our society uses radio waves to provide services, such as GPS navigation and satellite communication, and to assure defense through over-the-horizon radars, trans-ionospheric radars, and secure military HF communication. When the ionosphere changes during a magnetic storm, its ability to reflect HF signals is altered, its capability to absorb such signals increases, and it exerts degrading influences on ultra-high frequency (UHF) and L-band satellite signals through either group delay or diffraction (scintillations). During magnetic storms all of these technologies can be severely impacted in the normally benign mid-latitude region. Another storm-induced effect is the increased satellite drag due to enhanced neutral density.

Many technologies affected by ionospheric variability are designed to use signals from the GPS constellation of satellites. Designed and implemented to provide position and time information, the GPS constellation is being used by an ever-increasing set of applications. One major civilian application is the Wide Area Augmentation System (WAAS) being designed by the Federal Aviation Administration (FAA) to provide GPS-based navigation to aircraft. Another example is an upcoming system, where the position of a cell phone is determined by GPS signals. A military example is GPS-guided munitions. In space, GPS is being used for determining position, velocity, and attitude of LEO satellites, including the Shuttle and the International Space Station, and GPS receivers are being used for remote sensing of the properties of the atmosphere and oceans. All of these systems, as well as others that require accurate positions and timing, can fail to provide information due to tracking failure in their GPS receivers.

In the next decade, between solar maxima, the technical systems dependent on GPS will be deployed in a relatively benign space weather climate. During the next solar maximum, however, these systems will be fully exposed to the extremes of space weather for the first time. The Geospace investigations described in this report will be the only space assets to address this vulnerability.

Some of the effects of ionospheric variability on GPS signals during the most recent solar maximum can be studied by analyzing variations in the Total Electron Content (TEC), the number of electrons in a 1 $\times$ 1 m column between the receiver and the transmitting satellite that cause group delay. During the positive phase of a magnetic storm TEC can increase by 300%, introducing range errors of tens of meters in single frequency GPS L1 (1.575 GHz) navigation systems. (TEC is reported in TECU, where 1 TECU = 10^{16} electrons m^{-2}. A range error of 1 m is equivalent to a difference of 6.15 TECU.) **Figure 20** shows the drastic variations in range errors that were encountered over various stations during the magnetic storm of September 22–23, 1999, as a function of local time. The range errors were derived from TEC data obtained by the GPS stations of the International Geodynamic Service (IGS) network spanning the United States from north-east to south-west over a 4-day period covering the storm. The storm was produced by the material in the halo CME that launched from the Sun on September 20, 1999. It reached its highest activity level (as measured by the storm index Dst) at about 2400 UT on September 22, 1999, corresponding to between late afternoon and dusk over the east coast of the United States. (The minimum Dst was –167 nT.)

Following the drastic increase of TEC during the positive phase of the storm is a precipitous decrease of TEC. This decrease is accompanied by fluctuations in TEC that cause fluctuations of signal phase in GPS receivers. During the storm of September 22, 1999, TEC fluctuations during the day were very small. In the afternoon, however, fluctuations as large as ±5 TECU min^{-1} were observed for several tens of minutes over almost all the satellite ray paths visible from Westford, MA. Such fluctuations are produced by electron density irregularities with a scale-size of tens of kilometers in the presence of ionospheric motions with velocities of several hundred meters per second. ***In the presence of such TEC fluctuations, many GPS navigation systems may fail to provide information due to loss of tracking in GPS receivers or may be unable to use differential corrections.***

In addition to the tens of kilometer-scale irregularities that cause TEC fluctuations, magnetic storms also cause smaller irregularities at mid-latitudes in the range of sub-kilometer scales. These irregularities produce diffraction that causes rapid fluctuations in signal power (or

scintillations) in satellite communication links and GPS signals. Intense scintillations can introduce unacceptable message errors in satellite communication systems. During the magnetic storm of September 22, 1999, 250-MHz communication links from Hanscom Air Force Base, MA, to a geostationary satellite experienced intense scintillations. The storm-induced scintillations exceeded 25 dB, introducing unacceptable message errors and causing a total outage of that communication link.

Defense systems, such as UHF surveillance radar and any radio using HF bands, also encounter unexpected outages at mid-latitudes during magnetic storms. The storm-enhanced TEC and ionospheric scintillations introduce range errors and degrade target detection in UHF radars. The equatorward motion of the auroral oval also causes backscatter of radar signal and introduces severe clutter in mid-latitude systems. The Drug Enforcement Agency uses over-the-horizon HF radar to detect drug smuggling airplanes and ships by bouncing signals off the ionosphere. Over-the horizon HF radars are disrupted during magnetic storms by the variations of ionospheric electron density, spatial gradients of density, presence of ionospheric irregularities, and absorption.

Near-ground HF communication systems (ground-to-ground and aircraft-to-ground) that reflect signals off the ionosphere are severely impacted by magnetic storms due to drastic variations of ionospheric electron density and increased absorption. In areas where airlines depend on HF communications, flight disruptions can occur during outages of HF links under storm conditions. Military operations that require secure HF communications to rescue downed pilots may be delayed due to storm-time ionospheric conditions.

During the negative phase of a magnetic storm, characterized by decreased TEC and reduced strength of turbulence, trans-ionospheric communication systems are not as adversely affected. Navigation errors in single frequency GPS receivers may arise, however, due to overcorrection of ionospheric effects in the receiver. The gradual decrease of TEC during the negative phase can be accommodated by WAAS-like systems more easily if there are no significant gradients. However, large reductions in ionospheric density that then require drastic changes in the frequency plan seriously impact global HF communication circuits and over-the-horizon radar. In both phases of ionospheric storms the radar monitoring of spacecraft is disturbed.

Ionospheric fluctuations during the positive phase of large magnetic storms affect a wide range of DoD and civilian communication, radar, and navigation systems at normally benign mid-latitude locations. To characterize and understand these fluctuations, the Baseline I-T Investigation will measure the occurrence and magnitude of TEC enhancements, gradients, and small-scale irregularities during the positive phase of magnetic storms; resolve the local time and longitude dependences of ionospheric effects during the positive and negative phase of magnetic storms; and determine the consequences of irregularities and scintillations on LEO spacecraft. These objectives will be attained by measuring from LEO spacecraft the presence of irregularities, electron densities, scintillations, and the altitude profile of the electron density as functions of location and local time during geomagnetic storms and by imaging large-scale regions containing ionospheric enhancements, depletions, and gradients.

CHAPTER 3.
CLOSURE THROUGH GEOSPACE MODELING

3.1 The Role of Models in Living with a Star

Theory and modeling have come to play an important role in the spacecraft missions within the Sun-Earth Connections program. Models support missions in several ways:

- They aid mission design, providing estimates of conditions to be encountered for different scenarios.
- They provide a framework for interpreting observational data. This is particularly important for the geospace component of Living with a Star, which emphasizes multipoint measurements. LWS Geospace aims at quantitative representation of the near-Earth part of space, and understanding at a level that allows reliable prediction.
- They provide an organized and quantitative way to incorporate the new physical insights gained from the mission into the existing physical picture. Our most advanced understanding is nowadays usually expressed in terms of computer algorithms.

To be successful, the unique goals of Living with a Star must give rise to substantial improvement in space weather services in addition to expanding the frontiers of science. Much of the knowledge accumulated will be transferred to the space weather services in the form of scientific models, which will form the basis for operational models, design tools, and decision aids to be used by those concerned with designing around or operating through hazardous space weather conditions. ***Data sets acquired by the Radiation Belt Investigations and I-T Investigations are essential to drive the quantum improvements in the characterization and understanding of the dynamic environment that are needed to build the next generation of space weather models.***

Several types of models play essential roles in space weather research and services. The terminology used in this section to describe the differing types includes the following:

- *Climatological and empirical models* are based on long-term statistical information. Aimed more at characterizing the environment than on understanding it, they specify conditions in a broad sense over long time periods and are often based on historical data.
- *Nowcast models* (or real-time specification models) are used to provide an up-to-date picture of current conditions in the space environment. Nowcasting can range from simple characterization using empirical models driven by proxies to sophisticated data assimilation techniques requiring significant understanding.
- *Forecast models* advance an initial environmental specification ahead in time and provide predictions of potentially hazardous conditions. In general, forecasting requires understanding, though one class of models uses empirically derived algorithms driven by key proxies or data streams.
- *First-principles models* generally attempt to integrate the basic physical differential equations of the system forward in time. Scientists use them to test their understanding and to provide new insights. These models can be used for specification and forecast if the initial and boundary conditions are accurate.
- *Data assimilation models* combine measurements, empirical models, mathematical optimization methods and first-principles models to provide the most realistic possible picture of the present conditions or updates and corrections to the propagation of conditions forward in time. In this way these models improve both nowcasting and forecasting.

Models are essential to bringing closure to the Living with a Star program because of their capability for facilitating scientific understanding and as the means by which that understanding is transferred to users of space weather services. Most of this chapter is necessarily devoted to describing models, including present capabilities and advances needed to accomplish the goals of LWS. The discussion is not comprehensive; rather it outlines a minimal suite of models needed to bring science closure. The observational data from the Geospace Investigations are essential to needed model development, and the measurements described in Chapter 4 were designed with an eye toward satisfying the requirements of the models.

3.2 Models of the Radiation Belts and the Magnetospheric Environment

In what follows, there is more emphasis on the top-priority outer-belt electrons than on radiation-belt ions or inner-belt electrons, and the section on full-physics radiation-belt models deals exclusively with outer-belt electrons. However, many of the processes and underlying electromagnetic field drivers are also responsible for the ion dynamics. Thus the comprehensive understanding of outer zone electron dynamics that will be provided by the Radiation Belt Investigations and modeling effort will lead to improved ion specification and forecast capabilities.

3.2.1 Climatological Models of the Radiation Belts

Spacecraft that fly regularly through the radiation belts have to be designed to withstand the effects of radiation and plasma damage. Designers need to be able to calculate reliably the likely radiation environment that will be encountered by a spacecraft in a certain orbit for a given time period, including worst-case scenarios with probabilities of occurrence. Climatology models are also critical for improved scientific understanding in that they often provide global initial and boundary conditions for first-principles models.

NASA constructed the heavily used set of AP and AE radiation-belt models in the 1970s, using data sets from 1960s and 1970s satellite experiments. However, the CRRES mission, which took radiation-belt measurements in 1990 to 1991, showed that the earlier models were not necessarily correct and that the belts were much more dynamic than previously thought. **Figure 25** illustrates the differences between the NASA AE-8 Max and CRRESELE model predictions for ~2 MeV electrons. CRRES measurements indicate that the NASA model over-predicts the environment at geosynchronous orbit while under-predicting in the "slot" region. The enhanced flux levels shown in the slot were largely the result of a shock wave that hit Earth's magnetosphere in the magnetic storm of March 1991, suddenly changing the structure of the belts and then taking many months to return to normal. Unfortunately, the CRRES spacecraft lasted only 14 months and so covered only a small fraction

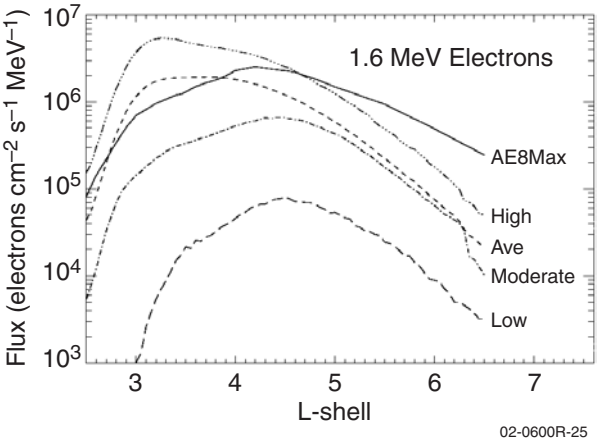

Figure 25. A comparison between the NASA AE8Max model and the CRRESELE model, representing the range of conditions encountered by the CRRES satellite during solar maximum. The discrepancies amount to more than a factor of 10 in some cases, illustrating the need for improved climatological radiation belt models, which are widely used in spacecraft design.

of a solar cycle. There has been no mission since CRRES in the critical geostationary transfer orbit (GTO) regime that has even begun to make the necessary measurements to improve the models.

With potential high-performance yet radiation-sensitive technologies being considered for space flight and the increasing demands for global coverage pushing constellations of spacecraft in radiation-intensive orbit regimes, a new generation of radiation belt climatologies is urgently needed. ***The Radiation Belt Storm Probes will enable development of these models by providing the highly resolved pitch-angle and energy spectrum measurements of energetic electrons and ions through the heart of the radiation belts.*** The upper part of **Table 4** summarizes the climatology models in terms of the GMDT science objectives and benefits to society.

3.2.2 Nowcast Models of the Radiation Belts

Spacecraft and manned space operations would greatly benefit from a model that could provide a continuous nowcast of the status of the radiation belts and plasma. Radiation belt situational awareness is currently provided by real-time data sources with little if any modeling to extrapolate to spatial locations or spectral regimes not directly sampled by the sensor. Examples of this include the NOAA Polar Operational Environmental Satellite (POES) particle flux maps and

Table 4. Models aimed at characterizing the radiation belts.

Type of Model	Radiation Belt Storm Probe Data Utilized	Use of Data	Science Objectives	Societal Benefits
Radiation-Belt Climatology	High Energy Electrons (20 keV–10 MeV, 2<*L*<6) Energetic Proton & Ion Composition (H^+, O^+, 20–600 keV, H^+ 1 MeV-20 MeV, 1.1<*L*<6) Very Energetic Protons (20–200 MeV (1.1 < *L* < 6)	Input	1.2c 1.4b 4	Reliable characterization of radiation environment for spacecraft design & mission planning
Data-Assimilating Radiation-Belt Nowcast Model	Same as climatology (see above)	Assimilation	1.2c 1.3c, 1.4b 4	Situational awareness of the radiation belts for mission operations and anomaly resolution
derived from				
Semi-empirical B-field model	Vector magnetic field (35,000 nT, DC-20 Hz, 1.1 < *L* < 6) Low Energy Ions and Electrons (30 eV –30 keV, 2 < *L* < 6) Energetic Proton & Ion Composition (H^+, O^+, 20–600 keV, 2<*L*<6)	Assimilation	1.3c	Required to extend local measurements to global scales

the Los Alamos National Laboratory (LANL) geosynchronous particle data available to the DoD in real-time. One important exception is the Magnetospheric Specification Model (MSM) being run by NOAA to provide a nowcast and short-term forecast of the inner magnetospheric plasma environment responsible for spacecraft surface charging. The input to MSM is primarily the K_p index with secondary inputs that include auroral boundary locations measured in real time by satellites. It is noteworthy that no real-time particle data are used in the model.

The key to progress in developing accurate nowcasts lies in physics-based data assimilation models. To specify the radiation belts it is not only necessary to assimilate particle measurements but also to capture the dynamic variation of the magnetic fields that govern the trapped particle motion. Current field models, such as the Tsyganenko models, are climatologies driven by proxy inputs (e.g., solar wind) and, though fast and convenient, do not provide reliable specifications, especially during storm times. ***Accomplishment of the Radiation Belt Investigation science objectives will provide not only the high-resolution, extended spatial and temporal measurements of the energetic particles, but also the measurements of the magnetic field and ring current drivers that are needed to achieve the understanding that will advance radiation belt nowcasting.*** The lower part of **Table 4** summarizes the nowcast models in terms of the GMDT science objectives, data needs, and benefits to society.

3.2.3 Forecast and First-Principles Models of the Radiation Belts

Present radiation belt forecasts are based mainly on experienced forecasters applying their intuition while viewing a small number of data streams. When quantitative algorithms are used, they tend to be climatological or mathematically optimized models driven by forecasts of proxy indices or solar wind data streams; an example is the NOAA model forecasting >2 Mev electrons at geosynchronous orbit using solar wind inputs. Space weather forecasters, however, desire something more akin to the current state of the art of tropospheric weather forecasting. In tropospheric forecasting, physics-based models with high-resolution spatial and temporal grids are marched in time starting from a data-derived initial condition to produce a detailed forecast over a broad region; sophisticated data-assimilation schemes are used to keep the models consistent with observations. It is major goal of the LWS program to provide the scientific understanding that will enable a transition to a true space weather forecasting capability. ***This will only be accomplished through the development of first-principles models motivated and validated with measurements from the Radiation Belt Investigations.***

A complex of models is needed to represent the physics of the radiation belts. The belts are controlled by the electromagnetic environment of the magnetosphere. Thus understanding the dynamics of the belts requires understanding of the underlying magnetospheric environment, including particularly the inner magnetosphere and ring current.

3.2.3.1 First-principles models of the magnetospheric environment

At present, the global MHD models provide the best theoretical representation of the global magnetospheric configuration. They calculate the time-dependent electric and magnetic field everywhere in the magnetosphere, including even the ULF waves. However, present global MHD models do not represent the ring current properly, including particularly the strong potential electric fields that inject ring-current ions into the inner magnetosphere to $L \sim 2.5$. The most promising approach to first-principles simulations of the inner and outer magneto-

sphere appears to be embedding a ring-current model that includes gradient/curvature-drift transport inside a global MHD model. First results are just now coming out for such combined simulations, which are complex and unproven.

The data utilization and closure aspects of coupled global-MHD/ring-current models are summarized in the central rows of **Table 5**. The basic input parameters for global-MHD, and thus for a coupled MHD/ring-current model, are pro-

Table 5. First-principles/forecast physical models.

Type of Model	Physics Included	Data Needed	Use of Data	Science Objectives	Societal Benefits
Radiation Belt Model					
Outer-Belt Electron Model (diffusive or bounce avg.drift)	Bounce-averaged drift in time-varying **E**, **B**	RBSP electrons (2.5<*L*<5.5, 20keV-10MeV,)	Validation, assimilation	1.1, 1.2, 1.3	Capability for optimal nowcasting and eventual prediction of outer-belt energetic electrons
		Electrons (*L*=6.6, 20keV-10MeV)	Boundary condition		
coupled to					
Models of Wave-Particle Interactions	Heating, transport mechanisms with violation of m, *J*	RBSP waves	Valid., assim.	1.1, 1.2a, 1.3	
		RBSP Electrons (2-5.5)	Valid., assim.		
		Electrons (6.6)	Valid., assim.		
		RBSP precip. electrons (20 keV-10MeV)	Validation, assimilation		
Coupled Magnetosphere Model					
Global MHD	Large-scale magnetospheric physics with coupling to solar wind	Solar wind *n*,*V*, **B**	Input	2A.2, 2B.3, 2B.4, 3A2,	Nowcasting, eventual prediction of magnetospheric structure, high-lat. ionospheric **E**.
		RBSP **B**	Valid., assim.	3B.3	
		RBSP electrons and ions (<20 keV)	Validation, assimilation		
coupled to					
Ring current model	Transport by guiding-center drift, charge exchange, ionospheric ions?, pitch-angle scattering	RBSP ionosph. plasma drifts	Validation, assimilation	1.4a, 3B.1, 3B.2, 3B.3	Nowcasting, eventual prediction of keV electrons (surface charging)
		RBSP **E**	Valid., assim.		
		RBSP Ring current ions (20-600 keV)	Validation, assimilation		
		ENA images	Valid., assim.		
		Geosynch. ions (20-200 keV)	Validation, assimilation		
Comprehensive Ionosphere-Thermosphere-Electrodynamic Model					
Data-Assimilating Coupled Thermosphere-Ionosphere-Electrodynamic Model	Full chemistry and fluid mechanics of thermosphere, ionosphere, with coupling to mesosphere	SDO Solar EUV	Input	2A.1, 2A.2,	Nowcasting and prediction of large-scale N_e (communications, navigation, radar), and neutral density (sat. drag)
		High-lat. and low-lat. FUV	Valid.,assim.	2A.3, 2A.4, 2B.1, 2B.2,	
		ITSP $N_e(h)$	Valid., assim.	2B.3, 3A.1,	
		ITSP N_e at spacecraft	Valid., assim.	3A.2, 3A.3,	
		ITSP plasma drift	Input, valid.	3A.4, 3B.1	
		ITSP thermosph.winds and composition	Validation, assimilation	3B.2	
coupled to					
Plasmasphere Model	Plasma exchange between ionosphere and plasmasphere	ITSP $N_e(h)$	Valid., assim.	2B.1	Nowcasting and prediction of midlatitude N_e
		ITSP N_e at spacecraft	Valid., assim.		
and					
Model of Irregularity Generation	Gravity wave seeding	ITSP $N_e(h)$ and conduct	Valid., assim..	2B.1, 2B.2,	Nowcasting and prediction of irregularities
	Self-consistent electrodynamics	ITSP plasma drift	Valid., assim.	2B.4	
	Field-line conductivity	ITSP thermospheric winds and waves	Valid., assim.		

vided by an upstream solar-wind monitor. ***Measurements of the magnetic field, ring-current ions, and electrons that are made by the Radiation Belt Storm Probes will provide crucial tests for the coupled model.*** ENA images from the IMAGE spacecraft are already providing useful tests of ring-current models, as discussed in Chapter 2 (Section 2.2.3). ***In the Living with a Star era, ENA images will complement the in situ measurements made by the Radiation Belt Storm Probes, providing information on the local-time dependence.*** The coupled model will also calculate global ionospheric electric fields, both in the driving high-latitude region and also in the low- and mid-latitude regions. If the coupled magnetosphere models are also joined to an active ionosphere-thermosphere model, as indicated by the double-headed arrows in **Table 5**, then neutral-wind and active-conductance effects can also be included in the calculation.

3.2.3.2 First-principles models of the radiation belts

The most highly developed approach to radiation-belt modeling is through diffusion-type codes, which represent the particle populations in terms of the three adiabatic invariants. Violations of adiabatic invariants are parameterized in terms of diffusion coefficients, which may be estimated from theory or adjusted to fit observations; algorithms for estimating sources, losses, and in situ heating are also included. A great deal of radiation-belt knowledge is incorporated in the coefficients and source and loss rates. Codes of this type have been extensively tested against observations.

During bounce and drift motions in the magnetosphere, energetic particles interact with various plasma waves, which cause violation of one or more adiabatic invariants. For stochastic scattering, the temporal evolution of the particle phase space density may be described in terms of diffusion coefficients in space and velocity space coordinates. ULF waves (with periods of a few minutes) cause third invariant violation and radial diffusion with a diffusion coefficient D_{LL}. VLF and ELF waves (with frequencies between a few hertz and several kilohertz) cause violation of the first and second adiabatic invariants and velocity space diffusion in pitch-angle $D_{\alpha\alpha}$ or energy D_{EE}. Each rate of diffusion depends on the spectral properties of the relevant resonant waves. The Radiation Belt Investigation will measure wave intensities, which can be converted into diffusion coefficients using well-established theoretical techniques. The Radiation Belt Investigation wave measurements will facilitate development of global models for the plasma wave environment, which are required for specification of the average diffusion coefficients (D_{LL}, $D_{\alpha\alpha}$, and D_{EE}) experienced by particles over their drift paths, coefficients that can be used in codes that simulate the temporal variability of the high-energy electron population during disturbed conditions.

To represent the relatively rapid evolution of the radiation belts during magnetic storms, modelers typically increase radial diffusion coefficients considerably above their quiet-time levels, usually adjusted for rough agreement with observed fluxes. A first-principles approach to representing storms would involve coupling diffusion models of the radiation belts to global MHD simulations. Radial diffusion coefficients could be calculated as a function of time through a storm by appropriate Fourier analysis of the electric fields computed by the MHD models.

One drawback of diffusion models is that, in the real magnetosphere, invariants are sometimes violated in ways that are not accurately characterized as diffusion, which considers the cumulative effects of many small, randomly phased events. In some cases, the radiation belts are changed by a very small number of strong events. For example, a single storm sudden commencement, which is a rapid compression of the

magnetosphere, can modify the belts significantly but cannot be accurately portrayed as diffusion. A more precise description of radial transport is provided by bounce-averaged-drift codes, which calculate violations of the third invariant in detail but use diffusion coefficients to estimate violations of the first and second invariants. Codes of that type were used very successfully to explain the rearrangement of the radiation belts that occurred March 24, 1991. A major challenge involves developing bounce-averaged-drift codes that treat the full range of pitch angles and are still fast enough to run through long events using reasonable computing time.

In the nominal model plan shown in **Table 5**, information on the electrodynamic environment flows from the coupled magnetosphere model to the radiation-belt model at the top of the table. Thus drift shells can be continuously adjusted to keep up with changing magnetic conditions. The radiation-belt model has two components, one to keep track of the overall population and one to calculate diffusion and heating coefficients. The outer boundary of the overall model is set at geosynchronous orbit, where data are normally available to constrain the time-dependent boundary condition. ***From a scientific point of view, measurements made by the Radiation Belt Storm Probes for modeled events will provide rich opportunities for testing the model. Comparing event simulations conducted for various theoretical assumptions with the satellite-measured particle fluxes and plasma waves will provide insight into the heating and diffusion processes (Objectives 1.1, 1.2, 1.3).*** That understanding should culminate in new algorithms for calculating heating and diffusion and heating coefficients, which should allow better nowcasting and predictions. In the most advanced state of the model, wave measurements could be fed into an automatic algorithm for calculating those coefficients.

3.3 Modeling of the Mid- and Low-Latitude Ionosphere and Thermosphere

3.3.1 Ionosphere and Thermosphere Climatology Models

The standard for empirical ionospheric electron density models is the International Reference Ionosphere (IRI). Although this model has a long heritage, it is only the latest version, IRI2000, that has included a geomagnetic activity dependence. Understanding of the storm phenomenon has only recently become sufficient to allow formulation of even a rudimentary empirical description. This first attempt targets the recovery phase but only captures part of the response and only in summer and equinox seasons. For both the initial large positive-phase response during the storm-driven phase and the recovery during winter, our level of understanding has not allowed formulation of an empirical description. Empirical models of total electron content suffer the same problem as electron density profiles, in that understanding has not allowed geomagnetic-activity dependence to be included in the empirical models. ***The observations of the ionospheric response to geomagnetic storms that will come from the LWS I-T Investigation measurements will improve characterization of the response.*** The combined observations of the ionospheric profiles, in concert with the electrodynamics and with thermospheric winds and composition, will provide the understanding of the physical processes, which will lead to development of substantial improvements in empirical ionospheric models.

The thermosphere models developed more than thirty years ago are still being used routinely for estimating lifetimes of low-Earth orbit spacecraft. The accuracy of the models is limited by our ability to predict the solar and geomagnetic input parameters, such as the F10.7 index, and the K_p or A_p indices. The Mass Spectrometer and Incoherent Scatter (MSIS) neutral atmosphere model, in addition to providing climato-

logical neutral density, also provides the standard for neutral temperature and composition structure. The Horizontal Wind Model (HWM), the newer of the thermospheric empirical models, has relied on considerably less data to characterize the dynamics. ***The neutral wind data from I-T Storm Probes promise the biggest and most needed improvement to the HWM, while the comprehensive multi-point LWS Geospace disturbed condition data sets will be crucial in making the under-sampled storm climatologies in MSIS and HWM realistic.***

3.3.2 Assimilation Models of the Ionosphere and Thermosphere

Data assimilation comes in two distinct forms. The first is a snapshot assimilation in which current observations are assimilated to produce an improved specification. Examples of this are the high-latitude electrodynamics produced by the Assimilation Model of Ionospheric Electrodynamics (AMIE) and the JPL Global Ionospheric Maps (GIM). In both cases, observations from often more than 100 separate locations are input into an assimilation model to adjust an initial 2-D climatological distribution to produce a revised pattern. These models produce a more realistic 2-D snapshot of the electrodynamics (AMIE) and the ionosphere in total electron content (GIM).

The second method of assimilation often uses a physical model to propagate the state forward in time and so capture the dynamics of the I-T system. This approach uses the dynamics, as captured in the prior observations and the model, to produce realistic temporal changes in the system. This type of assimilation model will test our understanding of the physical processes either by determining unknown parameters in the physics (e.g., model time constants) or by how well a specific set of modeled processes matches the storm observations. In either case, the combination of the physical model, I-T Investigation data, and the assimilation tool are essential to better understanding of the physical processes. The blending of the observed I-T weather and our understanding of the I-T processes can be done in a Kalman filter. If the observed weather and modeled physics are in agreement, the Kalman errors are small. However, if they are not, the Kalman provides the tool by which the incorrect physics can be analyzed.

There is currently a strong effort sponsored by the DoD to develop the first data assimilation models for the ionosphere. The Global Assimilation of Ionospheric Measurements (GAIM) is utilizing Kalman filters with a sophisticated physical model of the ionosphere and plasmasphere to propagate the ionospheric state forward in time. A variety of existing and soon-to-be-existing data sources are utilized to include ionosondes, TEC measurements, and Defense Meteoroligical Satellite Program (DMSP) in situ and remote ultraviolet (UV) sensors. Integral to the GAIM program is the need to specify the neutral atmosphere composition. To follow the storm-time changes in thermospheric composition a separate Kalman filter is being developed. ***These types of models will be designed to incorporate the many new data sources expected from the SDO and Geospace Investigations.***

The current I-T assimilative models are standalone, analogous to the situation of physical models 20 years ago. The challenge in the coming decade is transition to self-consistent coupled assimilative models of the thermosphere, ionosphere, and electrodynamics. ***By measuring the neutral, ionospheric, and electrodynamic components simultaneously, the I-T Investigation will make this transition feasible.***

3.3.2.1 Application to nowcasting

Nowcasts of ionospheric electron density profiles and scintillation are vital to effective operations of satellite communication, HF communication, and GPS navigation. The U.S. Air Force currently runs the Parameterized Real-

time Ionospheric Specification Model (PRISM), which ingests data from a worldwide suite of ground sensors and the DMSP satellite to adjust climatological model coefficients and produce a global map of the electron density profile every hour. This first-generation model has yet to complete an operational-level validation; the model is useful, but there is much room for improvement. ***These new assimilative models of the thermosphere-ionosphere-electrodynamic system will depend heavily on both the observations provided by the I-T Investigation, and the model advances expected from the improved understanding of the physical processes.***

A nowcast of HF absorption due to solar flares is currently produced by NOAA using empirical correlations between x-ray levels and measured absorptions mapped onto the dayside with simple algorithms. Flare absorption is currently based on simple empirical formulas that lack accurate quantitative estimation. ***The comprehensive LWS measurements of EUV flux will provide substantial improvements for this type of nowcast.***

Large solar EUV events and geomagnetic storms can raise havoc for those responsible for tracking space objects. Nowcasts of the neutral density are routinely employed to estimate drag for satellite propagation algorithms. Recent advances in using actual drag measurements as an estimate of the density into the Jacchia climatological model have led to the High Altitude Satellite Drag Model (HASDM) being transitioned to operations. Daily average location errors have been reduced from 15% to 5% with this model, but there is still no ability to forecast or incorporate sudden changes due to space weather events. ***Neutral dynamics and density measurements from the I-T Investigations will provide much needed data for improving data assimilation techniques for the neutral thermospheric wind and density, consequently both reducing nowcast errors and providing an accurate initial condition for forecast models.***

3.3.2.2 Application to forecasting

The discussion of magnetospheric forecast models in Section 3.2.3 applies equally well here. With the advances in understanding and the availability of data afforded by the Geospace I-T Investigations, the assimilative models will form the basis for forecasting the state of the thermosphere and ionosphere. With empirical or physical models, forecasting the space environment conditions currently relies on accurate estimation of the primary inputs to the model, typically solar indices, such as F10.7, and geomagnetic indices, such as A_p. An assimilative model also relies on an accurate specification of the current conditions. For a short-term forecast, the current conditions will dominate the accuracy of the forcing. In the longer term, the impact of uncertainties in model forcing functions will begin to dominate the accuracy of the forecast. In some cases, such as during the recovery to a storm, the forecast may be reliable for up to a day. On the other hand, if a solar storm is approaching Earth, the response will be so dominated by the forcing that initial conditions become less significant.

The first I-T challenges for the Geospace Investigations are therefore to improve the understanding of the physical system and to provide the appropriate data for the assimilative models to improve the capability for nowcasting. The additional major technical challenge lies in predicting solar and magnetospheric inputs with which to drive the I-T models. Part of that process will involve the development and use of coupled magnetosphere-ionosphere-thermosphere models, as discussed in Section 3.4.

3.3.3 First-Principles Models of the Ionosphere, Thermosphere, and Electrodynamics

Coupled first-principle ionosphere-thermosphere models have reached a reasonable level of sophistication. They have been able to dem-

onstrate the importance of the interaction between the neutral particles and plasma in controlling the response of the upper atmosphere to geomagnetic storms. Although some aspect of the "climatology" of storms can be captured and understood by the simulations using the coupled I-T models, the response to particular storms is highly dependent on specification of the electrodynamic drivers of the system, both from the magnetosphere and from the internal-dynamo-driven changes in electric fields. Both have been difficult to specify with sufficient accuracy that would allow even a perfect model to predict the I-T response correctly. The evolution of the internal dynamo processes during a geomagnetic storm is also poorly understood.

The current theoretical understanding is represented by many physical models of both the ionosphere and thermosphere separately, and by the coupled ionosphere-thermosphere models. These models are driven by inputs representing the other regions of geospace and include solar EUV, solar-wind/magnetosphere-controlled and generated electric fields and auroral precipitation, and the terrestrial lower atmosphere. Calculation of internal dynamo electric fields is possible in the coupled models where dynamics and conductivity changes are calculated self-consistently. The validation of these models using observations indicates that our theoretical understanding is reasonable during "quiet" non-weather conditions, but very inadequate during "disturbed" conditions. ***The Geospace I-T Investigation, providing both in situ measurement and global imaging of the I-T system, together with the SDO EUV irradiance measurements, will make it possible to test and validate our models during quiet and disturbed periods for the first time.***

Understanding of disturbed-time electrodynamics is inadequate, with regard both to coupling to the magnetosphere and to the internal I-T dynamo. LWS and especially its Geospace Investigations will provide much-needed observational evidence to resolve this present-day theoretical limitation. In particular, the evolution of the neutral wind together with the plasma structure is essential for validation of the physical models.

The current versions of the physical models represent the interaction of the thermosphere and ionosphere with the plasmasphere in a fairly rudimentary way. For instance, the boundaries between open and closed drift paths remains static in the current model. Allowing for the dynamic changes in this boundary will significantly influence the plasmapause location, its longitude structure, and its interaction with the I-T system at mid-latitudes during storms. ***The rich variety of measurements from the Geospace Investigations will provide essential information for improving the coupling of the plasmasphere with the I-T models.***

Other areas that are in their infancy are the numerical simulation of ionospheric irregularities and the self-consistent coupling of the I-T models with the magnetosphere. The latter will be discussed in Section 3.4. Current physical models for the formation of ionospheric irregularities are two-dimensional and rely on field-line-integrated quantities. First attempts at a full three-dimensional solution are in progress, but the interaction and dependence on the background state of the ionosphere have not been considered. ***With guidance from the data, and understanding provided by the LWS Geospace Investigations, the possibility of full coupling of the global models with a nested, high-resolution irregularity module is quite feasible.*** In particular, observations of the wind and waves that act to seed the generation of plasma irregularities will begin to elucidate the triggering mechanism. Some of the sources for the wind and wave field originate from the lower atmosphere, and not only drive dynamo processes, but also can be the source of gravity waves that trigger ionospheric irregularities.

The lower part of **Table 5** highlights the data needed from the Geospace Program for development of the next-generation first-principle coupled models of the thermosphere, ionosphere, electrodynamic system.

3.4 Coupled Magnetosphere-Ionosphere-Thermosphere Models

As described in Chapter 2, the mid- and low-latitude ionosphere suffers violent disturbances during major storms, and these disturbances have major space-weather effects. Total electron content is dramatically disturbed across wide swaths at middle latitudes. The equatorial ionosphere can be transported rapidly upward, and the ionization of the equatorial ionosphere is transported to higher latitudes in a strengthened Appleton anomaly. These effects are, to a large extent, driven by disturbances in the mid- and low-latitude ionospheric electric field, which represents a particular challenge for modeling. Those disturbance electric fields involve the magnetosphere, ionosphere, and thermosphere all coupled together, where each element acts actively on the others.

Physical modeling of these events will involve coupled magnetosphere-ionosphere-thermosphere models. Solar-wind/magnetosphere coupling is important as the basic coupling to the energy source. Realistic representation of the plasmasheet/auroral-ionosphere field lines is crucial, because that is where the major transfer of energy from magnetosphere to ionosphere and thermosphere occurs, resulting in the disturbance neutral winds. Realistic treatment of the inner magnetosphere and ring current is essential, because recent observations make it clear that the ring current dramatically affects electric fields in the subauroral ionosphere during major storms. Disturbances in total electron content are due, in large part, to evolution of the plasmasphere, which therefore must be included in the model, along with the transfer of plasma along the field line. Rearrangement of the ionosphere during the storm affects conductances, which act back on the electric fields.

The LWS Geospace Investigations, with its suite of electric field and ring current measurements through the inner magnetosphere and the comprehensive lower-altitude measurements of electric field and density, is well designed to test the big, coupled models. **Table 5** shows the data needed for a nominal suite of coupled, physical models of the magnetosphere-ionosphere-thermosphere system.

3.5 Summary Comments

The LWS Geospace Program is crucial to the success of the national effort to improve space weather services. New data streams from LWS will serve as prototypes for eventual operational capabilities and will generate the comprehensive databases required for model performance validation. Successful execution of the LWS Geospace Program, including its modeling component, will lead to greatly improved space weather services, imparting a substantial benefit to our spacefaring society during the next solar cycle. Several specific conclusions can be drawn:

- Near-equatorial measurements of the radiation belts and ring current, remote sensing of the ring current, in situ and remote-sensing measurements of the I-T system, and correlative measurements of EUV spectral irradiance will provide the data needed for a vastly improved climatological model of the radiation belts and of the ionosphere and thermosphere, particularly if the measurements cover an entire solar cycle.
- Development of a data-assimilating radiation-belt model, validated by comparison with data from the Radiation Belt Investigations, will provide capability for effective nowcasting of the radiation belts from real-time radiation-belt measurements.

- Development of data assimilative models of the coupled thermosphere-ionosphere-electrodynamic system, utilizing the comprehensive I-T Investigation measurements, will be the foundation of future nowcast and forecast operational models.
- Development of comprehensive first-principles fully-coupled models of the magnetosphere-ionosphere-thermosphere system will improve understanding of magnetic storm effects in both the radiation belts and ionosphere.
- If data from the LWS Geospace Program are to be fully utilized, much effort will be needed in development of data assimilating models.

Some of the model-development work needed to support LWS is being funded by NASA's Community Coordinated Modeling Center (CCMC), the DoD-sponsored Multi-University Initiatives (MURIs), and the anticipated National Science Foundation's Science and Technology Center for Space Weather Modeling (CISM). However, significant funding will be needed for modeling within LWS to ensure support of areas that are not included in the other efforts. Careful coordination of the variously sponsored space weather modeling efforts will be essential for the success of LWS.

CHAPTER 4.
GEOSPACE SCIENCE INVESTIGATIONS

4.1 Overview

In developing investigations to address the priority scientific objectives set forth in the two preceding chapters, the Geospace Mission Definition Team (GMDT) endeavored to be realistic in its assessment of the resources likely to be available for the implementation of the geospace components of Living With a Star (LWS). At the same time, the Team felt it was important to present the full range of measurements required to address fully and completely, with the maximum scientific yield and societal benefit, the scientific priorities that it had defined. The Team therefore organized the investigations that it considered in four categories. **Baseline** science investigations are designed to lead to a robust understanding of the priority phenomena and processes within the regions of geospace under study. Within both the Baseline Radiation Belt and the Baseline I-T Investigations, the Team identified a set of science measurements that constitute the **Core** science investigations. As defined by the Team, the Core investigations are investigations that are feasible from an engineering standpoint, are consistent with a prescribed resource envelope, and will allow significant progress to be made toward accomplishing the LWS Geospace priority scientific objectives.[5] Possible **Augmentations** to the Baseline investigations were also identified. These consist of enhancements of the in situ measurement capabilities of the radiation belt and I-T spacecraft that will significantly enhance the science return of the two investigations. Finally, the Team considered several **Network-level** investigations. By collecting data over an entire solar cycle, by providing increased spatial and local time coverage, or by investigating additional regions of geospace, the Network-level investigations will enable expanded understanding of the geospace environment as a coupled system.

[5]The measurements to be made by the in situ spacecraft envisioned for the Core science investigations were used to develop strawman payloads for mission feasibility studies performed by the GMDT support staff at the Johns Hopkins University Applied Physics Laboratory. The results of these studies are presented in Appendix 2. It should be noted that these studies were preliminary in nature and that the measurements and payloads used in the studies do not preclude other measurements identified in the Baseline investigations.

4.2 Radiation Belt Investigation

The LWS Geospace Radiation Belt Investigation was designed to achieve three primary goals:

- Discover which processes, singly or in combination, accelerate and transport radiation belt electrons and ions and under what conditions
- Understand and quantify the loss of radiation belt electrons and determine the balance between competing acceleration and loss processes
- Understand how the radiation belts change in the context of geomagnetic storms

The Baseline Radiation Belt Investigation comprises three components: (1) in situ measurement from two spacecraft of radiation belt particles and fields and of ring current H^+ and O^+ in a highly elliptical orbit; (2) measurement of precipitating particles from low Earth orbit; and (3) global energetic neutral atom imaging of the ring current. The Core investigation consists of a subset of the Baseline in situ measurements. The following five sections describe the Baseline and Core Radiation Belt Investigations and outline possible augmentations to the Baseline investigation. Network-level Radiation Belt Investigations are discussed in Section 4.4.

4.2.1 Radiation Belt Storm Probes (RBSPs)

The RBSPs are two spacecraft in nearly identical, low-inclination, highly elliptical orbits with apogee inside geosynchronous orbit. One spacecraft will be fully instrumented for in situ measurement of radiation belt particles, the fields that act on them, and the plasma environment. The second spacecraft will carry a subset of those instruments needed to make simultaneous multipoint measurements of the particle distributions within the radiation belts.

4.2.1.1 RBSP measurements

In order to understand radiation belt acceleration, transport, and loss during geomagnetic storms and other conditions, it is necessary to measure radiation belt particles, electric and magnetic fields from DC to VLF, ring current particles, and the low-energy plasma that acts as a source population for the radiation belt and ring current populations and determines wave modes influencing particle acceleration and loss. This set of measurements allows a full characterization of the local particle population and their local interaction with quasi-static and wave fields.

Radiation belt electrons. The RBSPs need to measure electrons from 20 keV to ~10 MeV in order to identify both the high-energy "tail" of the distribution in the heart of the radiation belts and the source population of lower-energy particles which are accelerated to form the radiation belts (Objectives 1.1, 1.2a, 1.2b, 1.2c, 1.3b). Good pitch-angle coverage is needed to distinguish among different types of acceleration processes and to determine the invariants of particle motion. The time resolution for three-dimensional distributions should be better than 1 minute.

Vector magnetic field. Three-axis vector magnetic field measurements are required to determine particle pitch angles and to calculate phase space densities and for the development or constraint of medium-to-large-scale, storm-time, magnetic field models (Objectives 1.1, 1.2a, 1.2b, 1.2c, 1.3a, 1.3b, 1.3c). Such measurements are typically made by flux gate magnetometers. The measurements should be valid from 1 to 35,000 nT with 0.1 nT resolution at 20 Hz.

DC and AC electric fields and AC magnetic fields. AC magnetic fields need to be measured from 1 pT to 3 nT for frequencies from 100 Hz to 10 kHz. Three-axis measurements are required. DC electric fields from 0.1 to 500 mV/m and at frequencies up to 20 Hz should be measured in two dimensions. The AC electric fields should be measured up to frequencies of 10 kHz (Objectives 1.1, 1.2a, 1.2b, 1.2c, 1.3b). The Baseline Investigation requires that the electric and AC magnetic fields measurements be made by only one of the two RBSP spacecraft.

Ring current particles. The RBSPs must measure the ions that carry the bulk of the current density and that produce the largest perturbations on the magnetic field during geomagnetic storms (Objectives 1.3c, 1.4a). At a minimum, H^+ and O^+ with energies from 20 to 600 keV must be resolved.

Energetic ions. Proton (or total ion) measurements at energies above the range of the ring current particles (e.g., >0.6 MeV) are highly desirable. It is often possible to make ion measurements with detectors designed for clean electron measurements with little or no added cost, and it is recommended that this option be strongly considered. Measurements of ions with energies from 1 to 200 MeV are needed to characterize the ion component of the radiation belts and to develop a new generation of proton radiation models (Objectives 1.3c, 1.4b). For these measurements it is sufficient to measure omnidirectional fluxes (i.e., not pitch-angle resolved), and it is not essential to distinguish ion composition. We note that typically this energy range

cannot be covered by a single detector but may need to be split into separate detectors measuring, e.g., 1 to 20 MeV and 20 to 200 MeV. The Baseline Investigation requires that the energetic ion measurements be made by only one of the two RBSP spacecraft.

Low-energy electrons and ions. Measurements of low-energy (~30 eV to ~30 keV) particles are needed to fully characterize the source population for radiation belt electrons and ring current ions (Objectives 1.2a, 1.3b). Such measurements are also needed to characterize the plasmasphere and its relationship to the wave fields that strongly influence radiation belt electrons. The low-energy particles measurements are needed on only one of the two RBSP spacecraft.

4.2.1.2 The two-spacecraft RBSP configuration

A two-spacecraft configuration is the minimum configuration necessary to understand radiation belt dynamics and is a critical part of the Radiation Belt Investigation. This will be the first multi-spacecraft science mission in the inner magnetosphere. The spacecraft, orbit, and measurements have been designed to provide the first quantitative tests between observation and theories of inner magnetosphere dynamics by enabling fundamentally new measurements and discoveries.

As discussed above, dramatic changes in the radiation belts take place during geomagnetic storms. The main phase of a geomagnetic storm lasts from a few hours to tens of hours. This is comparable to or less time than an orbital period. A single well-instrumented spacecraft can measure the processes that produce acceleration and transport of radiation belts particles, but at least two spacecraft are required to actually measure the acceleration and transport—one in the region the particles are transported from and one in the region that the particles are transported to.

The amount of radial transport is likely dependent on geomagnetic conditions and, possibly, on particle energy. Therefore it is not possible to design a single, optimal separation. Rather, a variety of radial separations of the spacecraft over the mission lifetime is needed.

Similarly, the two-spacecraft configuration provides the ability to investigate the temporal, the azimuthal, and the radial spatial structure of the field variations responsible for acceleration of particles. The particle and fields information also enables construction of radial profiles of particle fluxes as a function of energy, electric and magnetic field structure, and phase space density profiles as a function of the adiabatic invariants. These radial profiles will be obtained at varying time intervals but with two spacecraft will occur as often as every 2 hours.

The two-spacecraft configuration can be achieved with a single launch vehicle that puts both spacecraft into an identical elliptical orbit. After orbital insertion, spacecraft separation will be achieved by means of springs, which give the two spacecraft slightly different orbital periods. The small spatial separation then grows over time, providing a continuum of spatial separations and allowing the full radial dynamics of the radiation belts to be characterized and understood statistically.

4.2.1.3 Orbital design considerations

The ideal place to measure both the radiation belt particles and the fields that act on them is at the magnetic equator. Measurements at the magnetic equator

- Can obtain the full equatorial pitch-angle distribution, including 90° equatorial mirroring particles
- Simplify calculation of the phase space density at fixed adiabatic invariants
- Do not need to be mapped along magnetic field lines to obtain equatorial values

- Capture wave fields that can be strongly confined to the near-equatorial region

For these reasons, the RBSP science calls for placing the two spacecraft into a near-equatorial orbit.

In practice the magnetic equator is both inclined and non-planar, making it impossible to make continuous measurements exactly on the magnetic equator. Additional resources are also required to continuously change the inclination of the spacecraft orbit. The requirement for the RBSP mission is thus to obtain the best near-equatorial measurements that can reasonably be achieved given launch constraints. We also note that there is only marginal value in bringing the inclination below 10° geographic because the near-equatorial coverage does not increase.

The RBSP orbit also needs to cover a broad range of L-shells within the inner magnetosphere. Therefore the orbit should be elliptical. There is a trade-off between altitude of apogee, which determines the maximum L-shell measured, and the orbital period, which determines how often a given L-shell is measured. The radiation belts extend to the magnetopause but have their peak fluxes near 4 R_E. Geosynchronous orbit at ~6.6 R_E. is an important region for both physical and practical reasons, but it is also anticipated that there will be ongoing energetic particle measurements from the GOES and LANL series of satellites. Therefore we recommend apogee for the RBSP satellites be located just inside geosynchronous orbit at ~5.5 R_E, which gives an orbital period of ~9 hours.

4.2.2 Precipitating Particle Measurements from Low Earth Orbit

In order to measure the loss of particles from the radiation belts it is necessary to measure particles in the loss cone as well as the trapped population (Objective 1.2a). The Baseline Radiation Belt Investigation therefore includes measurement of the loss cone population by a low-altitude, high-inclination (>65° latitude) spacecraft, which could be a mission of opportunity. The critical measurement needs are for pitch-angle distributions of electrons from 20 keV to 10 MeV and of ions from 20 to 200 MeV. The precipitating particle measurements should be made simultaneously with RBSP measurements of the trapped population.

4.2.3 Energetic Neutral Atom Imaging

As discussed in the preceding chapter (Section 3.2.3), global imaging of the ring current is a highly desirable complement to the two-point in situ measurements of ring current ion composition to be made by the RBSP spacecraft. Therefore the Baseline Investigation also includes energetic neutral atom (ENA) imaging that will measure energetic neutral H from 10 to 200 keV and O from 40 to 400 keV. (The results of a feasibility study for an imaging platform in a circular near-polar orbit with a radius of 9 R_E are given in Appendix 2.) ENA imaging of the ring current contributes to radiation belt science objectives in two specific areas:

Global magnetic and electric fields. To specify and predict radiation belt particle fluxes during disturbed periods requires accurate modeling of the structure of the global magnetic and electric fields in the inner magnetosphere (Objective 1.3c). ENA imaging of the global ring current energy density and dynamics will provide valuable inputs to models from which the global magnetic and electric fields will be derived.

Radiation belt dynamics. Ring current interactions with the plasmasphere generate both ULF and electromagnetic ion cyclotron waves that can accelerate, pitch-angle scatter, and diffuse radiation belt particles (Objective 1.1). By knowing the global distribution of the ring current population those physical processes responsible for radiation belt dynamics can be included in the development of predictive models.

Ring current coupling to the ionosphere. In addition to its influence on radiation belt dynamics, the ring current is likely critical to mid-latitude ionosphere-magnetosphere coupling. Development of the ring current during geomagnetic storms is asymmetric, and pressure gradients produce mid-latitude ionospheric electric fields and currents that may penetrate to the equatorial ionosphere (Objective 2A.1b). Imaging of the ring current will show where the fields and currents mapping to the ionosphere occur, and, if pressure gradients can be estimated, the resulting ionospheric electric fields will be determined.

4.2.4 The Core Radiation Belt Science Investigation

As defined by the GMDT, the Core Radiation Belt Investigation consists of only the two RBSPs and a subset of the Baseline in situ measurements. **Table 6** summarizes the Baseline measurements as discussed above. The subset, defined as the Core measurements, is shown in bold. The measurements in this subset are those that the Team considered essential for making substantial progress in achieving the LWS Geospace priority science objectives. Ideally, both RBSP spacecraft would be identically instrumented, but realistic cost constraints make even this approach unlikely. Therefore, one spacecraft will be instrumented to make the complete set of Core measurements; the other spacecraft will measure only those parameters for which gradients are most necessary. These measurements were used by the GMDT support staff to develop a strawman payload for the feasibility study presented in Appendix 2.

4.2.5 Augmentations to the Baseline Measurements

The LWS GMDT also considered measurements that are not part of the Baseline Investigation but would significantly enhance the science return. The measurements that were identified are:

- Addition of AC magnetic field and DC/AC electric field measurement capability to spacecraft B identical to that on spacecraft A
- Addition of an electric field measurement capability in a third dimension to one or both RBSP to provide true vector electric field measurements

4.3 Ionosphere-Thermosphere Investigation

The LWS Geospace Ionosphere-Thermosphere Investigation was designed to achieve five primary goals:

- Understand the mean and dynamic I-T response to a variable EUV source

Table 6. RBSP Baseline measurements with Core subset indicated in bold.

Measurement	Platform
Radiation belt electrons	RB Storm Probes A & B
Vector magnetic field	RB Storm Probes A & B
Ring current particles	RB Storm Probes A & B
AC magnetic fields	RB Storm Probe A
DC/AC electric fields	RB Storm Probe A
Radiation belt ions	RB Storm Probes A & B
Inner belt protons	RB Storm Probe A
Low-energy ions and electrons	RB Storm Probe A
Energetic neutral atom imaging	High-altitude, high-latitude spacecraft
High-energy electrons and protons	Low-altitude, high-latitude spacecraft

- Discover and characterize the processes leading to positive phase ionospheric storms
- Characterize and understand the processes leading to negative phase ionospheric storms
- Discover and characterize the sources of mid-latitude ionospheric irregularities
- Characterize and understand scintillations from an orbital viewpoint

The Baseline and Core I-T Investigations both consist of two key elements: (1) in situ (and limited remote sensing) measurements in the I-T system and (2) imaging of the global low- and mid-latitude I-T system from a high-altitude platform. The Core investigation differs from the Baseline investigation only in that it involves a reduced set of in situ measurements. In addition, monitoring of solar EUV irradiance is of critical importance to the accomplishment of the objectives of the I-T Investigation. We therefore include this measurement in the following discussion of the Baseline and Core I-T Investigations, even though we anticipate that it will be made by the LWS Solar Dynamics Observatory (SDO) rather than by an LWS Geospace asset. Augmentations to the Baseline investigation are discussed later in this section. A Network-level I-T Investigation is discussed in Section 4.4.

4.3.1 Solar EUV Monitoring

Measurement of the solar EUV flux is required to understand the principal source both of ionospheric plasma and temperature and of neutral atmospheric dynamics. Typically, proxies are currently used to estimate this source function, but operational and assimilative models of the ionosphere-thermosphere system require an accurate specification of the solar EUV flux incident on the atmosphere simultaneous with the in situ measurements. Accurate EUV spectral measurements will enable I-T models to differentiate the importance of other sources that influence the plasma number density distribution and I-T dynamics.

EUV flux variation time scales range from minutes to a solar cycle. The required cadence of measurements varies from 10 minutes (to achieve minimum geospace goals) to once per second (meeting both geospace and solar goals). Spectral coverage from 1 to 200 nm at 0.1-nm resolution is sufficient for geospace goals in the ionosphere and thermosphere.

Such solar EUV measurements will be provided by the LWS SDO, which is planned for launch in 2007. ***A complete understanding of the ionosphere-thermosphere system requires that solar EUV spectral irradiance be measured at the same time as the response of the I-T system to that radiation. It is therefore of critical importance that the Baseline I-T Investigation take place during the SDO mission lifetime.*** Since the most significant geoeffective variability occurs near solar maximum (expected to occur around 2010), concurrent monitoring of the solar EUV flux and measurement of the I-T system's response during this period is of particular importance.

4.3.2 The Ionosphere-Thermosphere Storm Probes (ITSPs)

The I-T Storm Probes are two spacecraft in nearly identical, 60°-inclination, circular orbits at altitudes at a nominal altitude of 450 km. This orbit permits the satellites to be close to the F-region peak altitude, to be at sufficiently low altitudes to permit in situ measurements of the neutral gas properties that couple with ionospheric plasma, and yet to be at high enough altitudes to be consistent with a mission lifetime of at least 3 years. Both spacecraft are identically instrumented to characterize the dynamic response of the I-T system to variable solar EUV flux and geomagnetic storms as well as to measure the sources and properties of mid-latitude irregularities. Separation of the spacecraft ascending nodes by about 10° to 20° will make it possible to characterize I-T longitudinal behav-

ior and coherence scales, to identify sources and sinks, and to understand transport mechanisms. A more detailed discussion of the two-spacecraft mission scenario and orbits can be found below, in sections 4.3.2.2 and 4.3.2.3.

4.3.2.1 Baseline ITSP measurements

In order to characterize and understand the ionospheric-thermospheric response to geomagnetic storms, it is necessary to determine the state of the I-T system before, during, and after the storm main phase. The magnetospheric coupling to the ionosphere through electric fields must be determined as well. In characterizing the I-T response, it is important that mid-latitude irregularities, along with their sources, be characterized and mapped. To achieve this understanding, we should measure ionospheric density and height profiles, density irregularities, in-orbit scintillations, plasma drifts (or electric fields), and neutral density, composition, and winds. These are essentially the same measurements that are needed to characterize the I-T system's response to variations in the solar EUV flux.

Plasma density and irregularity measurements. Plasma density must be monitored both in situ and remotely. The in situ measurements will determine ionospheric gradients and characterize the latitudinal and longitudinal distribution of the bulk ionospheric plasma, while remote sensing will yield altitude profiles of density and spatial gradients as well as definitive measurements of the F-peak altitude and density, which are critical for the model input. The measurements are required to characterize the response of the ionosphere to changes in solar EUV, the redistribution of ionospheric plasma during geomagnetic storms, and the identification of source regions that produce scintillation. In addition to bulk plasma density measurements, plasma density irregularity measurements are required to characterize the scattering volumes that produce scintillations. These measurements should be adequate to determine the absolute density fluctuations and the wave number spectra (Objectives 2A.1a, 2A.1b, 2A.2, 2A.3, 2B.1, 2B.2a).

DC electric fields or ion velocity measurements. DC electric fields or plasma flow velocity measurements are required to characterize the transport of plasma (e.g., from the equator to mid-latitudes and poleward); to determine how the interaction of neutral and plasma gases create internal electric fields that influence plasma structure and drive both storm-time and quiet ionospheric currents; and to identify the electric fields that map down from the magnetosphere, such as in the sub-auroral nighttime ionosphere, where strong polarization fields are common (Objectives 2A.1b, 2A.2, 2A.3, 2B.1, 2B.2a). DC electric fields are also important as a source of free energy to drive mid-latitude irregularities, as well as a consequence of large-scale ionospheric structuring (e.g., depletions) associated with magnetic storms. In essence, almost every objective in the I-T section requires an accurate determination of the electric field or ion velocity.

Neutral density, composition, and temperature. The neutral density, composition, and temperature are required to determine how the upper atmosphere responds to variations of both the solar EUV irradiance and magnetic storms (Objectives 2A.1a, 2A.2, 3A.1a, 3A.1b). The number density and temperature provide a measure of the scale height which varies with the EUV input. The composition data will reveal how the upper atmosphere responds to a variety of variable energy inputs, for example from magnetic storms that create large changes in the O/N_2 ratios. These neutral atmosphere measurements have a direct bearing on the important space weather phenomena of satellite drag and will also be used to evaluate in detail the decay of the orbits of the I-T Storm Probes themselves.

Neutral wind measurements. Vector neutral wind measurements are required to establish how the atmosphere moves in response to both the EUV irradiance and magnetic storms (Objectives 2A.1b, 2B.1, 2A.2, 2B.2a). The neutral wind can redistribute ionospheric plasma through tidal motions and in response to geomagnetic storms and is likely responsible for the daily variability of equatorial spread F. In the presence of conductivity gradients, neutral winds will create electric fields that may compete with magnetospherically generated fields.

In-orbit scintillations. Scintillations are the consequences of an electromagnetic signal propagating through plasma density irregularities and are a principal space weather concern for society (Objectives 2B.1, 2B.2a). Compared with ground-based measurements of scintillations, the relative movement of the signal path through the irregularities will be much faster, 2 to 3 km/s instead of 100 m/s, implying much faster time scales. Both GPS signal amplitude and phase scintillations must be measured because different scale length irregularities are responsible for these two phenomena. Since the GPS signal architecture will be changing over the next decade, the measurements must accommodate the evolving and not entirely agreed-upon code and signal protocols currently being considered for GPS system upgrades. In addition a design approach for measuring scintillations while the scintillations simultaneously degrade reception quality is required.

Electron precipitation. Precipitating energetic (~20 eV to 20 keV) electrons observed at subauroral latitudes indicate the presence of strong geomagnetic activity and provide a measure of local energy input into the I-T system (Objective 2A.1b). Furthermore, electron precipitation within this energy range creates thermal plasma as the impacting energetic electrons ionize the neutral atmosphere. Precipitating electrons also provide clear evidence of geophysical boundaries, such as the equatorward extent of auroral oval and reveal how these boundaries respond to solar variability and storms.

Magnetic fields. Inference of ionospheric currents from magnetic field measurements on two satellites will yield insight into the disturbance dynamo and the disruption of the Sq current pattern by storms. In addition, such inferences, together with electric field measurements, will yield estimates of Joule heating, which are important for understanding negative phase ionospheric storms (Objectives 2A.1b, 2A.2). The two satellite measurements spaced relatively close together enable the geometry of the current sources (e.g., sheets, one-dimensional jets, etc.) to be much better ascertained than with a single satellite, which is essential for the correct interpretation of the current from inferred curl in the magnetic field data. Magnetic field measurements on the ITSP would be a significant cost factor that must be resolved.

AC electric fields. Vector measurements of the electric field spectrum of mid-latitude irregularities are needed for understanding this phenomenon (Objective 2B.1). The complete spectrum, from about 100 km to about 10 m, can help demonstrate where energy is injected and decays through the spectral shape and the frequencies (wavelengths) where the wave vectors shift from anisotropic to isotropic distributions. Together with the measurements of the plasma density irregularities, the vector electric field is important for determining the wave dispersion relation and generation mechanisms—making it possible to determine, for example, whether these mechanisms obey a Boltzman relation at short wavelengths.

4.3.2.2 The two-spacecraft ITSP configuration

A two-spacecraft configuration is the minimum configuration necessary to understand mid-latitude ionospheric storm-time dynamics. This will

be the first multi-spacecraft science mission in the ionosphere. The spacecraft, orbit, and instrument suite have been designed to provide the first quantitative tests between observation and models of ionospheric and thermospheric dynamics by enabling fundamentally new measurements and discoveries.

As discussed above, dramatic changes in the mid-latitude ionosphere take place during the main phase and recovery of geomagnetic storms. The main phase of a geomagnetic storm lasts several hours during which the positive phase ionospheric storm responds over local times from noon to post dusk. The recovery phase lasts from tens of hours to days during which the negative phase ionospheric response develops, evolves and is transported equatorward. These times are significantly longer than a low Earth orbital period so that the dynamic ionospheric response to geomagnetic storms can be followed with multiple passes. Multiple spacecraft are required because we have no measurements whatsoever of coherence scales in the disturbed thermosphere including winds, composition and density. For the ionosphere many of the processes that have societal consequences, such as mid-latitude irregularities, depend on gradients in plasma density or flows that must be spatially characterized. In addition, the coupling of magnetospheric fields downward has only been implied, and characterizing longitudinal gradients, especially near the dusk terminator, is essential for understanding polarization and direct electric field generation causing positive phase storms.

From the viewpoint of modeling, one spacecraft produces a one-dimensional trace that is adequate to develop and validate one-dimensional models. For higher-dimension models, more dimensions must be measured. An excellent example is the validation of Thermospheric General Circulation Models (TGCM) in which the I-T response to solar EUV variability is modeled. The gradients measured with two spacecraft will provide the necessary constraints to achieve understanding.

Finally, understanding the orbital scintillation environment requires the interpretation of spacecraft-measured time domain variations that have a spatial origin on many length scales. The largest length scales will be investigated with a dual-spacecraft strategy to distinguish convecting irregularities from propagating structures.

4.3.2.3 Orbital design considerations

The I-T Storm Probes must investigate

- Ionospheric plasma originating near the equator and moving poleward across mid-latitudes during positive phase storms
- Thermospheric composition changes during geomagnetic storms, their equatorward drift, and the ionospheric response
- Thermospheric winds and tides responding to geomagnetic storms and impulsive solar EUV events
- Irregularities and the I-T conditions leading to irregularity formation especially at mid-latitudes
- The orbital scintillation environment to be encountered by low Earth orbit spacecraft

The optimal altitude for the I-T Storm Probes is determined by the need to characterize the response of the I-T system to geomagnetic storms, solar EUV variability, irregularities and typical spacecraft orbits using scintillation-sensitive GPS technology. On average, the ionospheric peak density, called F-peak, occurs near 350 km but is highly variable and is frequently driven to higher altitudes. The thermospheric winds most responsible for driving ionospheric drifts are typically found near and below F-peak and thermospheric densities responsible for problematic orbital prediction are typically found below 500 km. The irregularities with the most significant societal impact typically occur in the regions of

largest density, F-peak, and in-orbit scintillations are most problematical for Space Shuttle, International Space Station, and low-altitude DoD assets typically near or below 400 km. On the other hand, the altitude distribution of ionospheric flows, gradients, irregularities, and thermospheric winds is relatively smooth in the altitude range near F-peak so that downward extrapolation is possible. In most cases, diffusive equilibrium is a reasonable assumption. The required altitude is as low as possible, certainly below 500 km, consistent with a 3-year lifetime. The ability to permit orbital decay followed by boosting is highly desirable to investigate the I-T state as low in altitude as possible.

The inclination of the orbits is determined by the science objectives focusing on mid-latitudes and the recognition that missions by other agencies will be investigating the equatorial and high latitude I-T system. The inclination is set by the need to observe the I-T state disturbed by geomagnetic storms. The highest latitude phenomena of interest is thermospheric compositional changes initiated by auroral processes. An inclination of 60° has been chosen to allow observations of these changes directly during major storms and to allow observation of the equatorward drift of the disturbed thermosphere during minor magnetic storms. Additionally, this choice permits the observation of subauoral ionospheric drifts during storms and poleward flow of positive phase ionospheric plasma perhaps acting as a source for polar cap patches.

The separation of the two spacecraft ascending nodes is driven primarily by the need to observe the coherence lengths and gradient scales of a diverse range of I-T phenomena. A strawman design of 10° to 20° has been chosen but this should be re-considered during Phase A studies. Also a variable separation is possible if orbital propulsion is employed and this should be investigated in more detail later.

4.3.3 Mid- and Low-Latitude Ionosphere-Thermosphere Imaging

Valuable information about the global state of the I-T system can be derived from the imaging of airglow emissions. Remote sensing of these emissions is important for accomplishing critical science objectives of the I-T Investigation, such as establishing the consistency between the solar EUV radiative energy input and the global state of the ionosphere and thermosphere, tracking the global response of the I-T system to geomagnetic storms, and studying the behavior of the tropical ionosphere (Objectives 2A.1a, 2A.1b, 2A.2, 2B.2a). Moreover, global imaging of the I-T system provides important contextual information for the in situ observations made by the I-T Storm Probes (Objective 2B.1). Apart from their scientific value, global images of the ionosphere-thermosphere will, like the SOHO images of the Sun and the IMAGE and POLAR images of the magnetosphere, serve to stimulate the interest of the general public in solar-terrestrial research and educate them about the importance of space weather. ***The GMDT therefore recommends inclusion of an I-T imager on a non-LWS geosynchronous spacecraft as an important component of the Core I-T Investigation.***[6]

Particularly useful diagnostic information can be obtained about thermospheric composition and dynamics by taking the ratio of the emission rates of atomic oxygen and molecular nitrogen. This ratio varies strongly in response to geomagnetic storm activity, and thus imaging of the O and N_2 emissions offers a means of tracking space weather storms and dynamical patterns in the ionosphere, much as meteorological remote sensing tracks hurricanes and jet streams in the troposphere. Moreover, in regions where photochemistry is a rapid process, the electron density is proportional to the O/N_2 ra-

[6] An alternative to I-T imaging from geosynchronous orbit—combined auroral and mid-/low-latitude imaging from a satellite in a circular, high-inclination orbit with a radius of 9 R_E—is considered below, in Section 4.4.1.

tio. Ionospheric conductivities can be derived from O/N_2 data and absolute solar radiances.

In addition to compositional information, height-integrated global neutral density and temperature can be extracted from high spectral resolution measurements of molecular nitrogen emissions.

For the ionosphere, the usual remote-sensing approach is to measure recombination radiation from $O^+ + e \rightarrow O^* \rightarrow h\nu$. The electron density can be inferred from this measurement since in the F-region of the ionosphere, the oxygen ion density nearly equals the electron density, so the intensity becomes proportional to the square of the electron density. Line radiation and continuum radiation from radiative recombination are readily seen at night and have been used in the past to obtain information about the ionosphere. During the day, other emission processes, such as photoelectron excitation, obscure ionospheric recombination radiation. When the ionosphere peaks at high altitudes (above dayglow altitudes) and is viewed on the limb, however, it may be possible to separate dayglow and recombination radiation. These measurements must be made at very high spectral resolution during the day (<0.1 nm) in order to identify and remove nearby contaminating emission lines.

Global imaging from geosynchronous orbit would satisfy the mid- to low-latitude science objectives. A resolution of the order of 25 to 50 km would be sufficient to track global variations in the thermosphere. Other considerations are spectral resolution, sensitivity, integration time, and measurement cadence. If temperature information is desired, spectral resolution of better than 0.1 nm is required. To resolve emissions at the Earth limb, spatial resolution should be somewhat better than a scale height, or of order 10 to 20 km.

In summary, the imager should be of sufficient resolution and sensitivity to be able to measure global ionospheric neutral composition and temperature, conductivities, and electron density, and thermospheric variations.

4.3.4 The Core I-T Science Investigation

Table 7 summarizes the ITSP Baseline measurements. The subset, defined as the Core set, is shown in bold. As noted above, measurement of solar EUV spectral irradiance by SDO is of fundamental importance for the Core I-T Investigation; we therefore include it here as one of the Core measurements. The Core measurements remove the electron precipitation, magnetic field, and AC electric field measurements from

Table 7. ITSP Baseline measurements with Core subset indicated in bold.

Measurement	Platform
Solar EUV	Solar Dynamics Observatory
O/N_2, N_e^2 from global mid-latitude imaging	Non-LWS Geospace geosynchronous spacecraft
Plasma density and fluctuations	I-T Storms Probes 1 and 2
Plasma density altitude profile	I-T Storms Probes 1 and 2
DC electric fields	I-T Storms Probes 1 and 2
Neutral density & mass composition	I-T Storms Probes 1 and 2
Neutral temperature	I-T Storms Probes 1 and 2
Vector neutral wind	I-T Storms Probes 1 and 2
Scintillations	I-T Storms Probes 1 and 2
Low-energy electrons	I-T Storms Probes 1 and 2
Magnetic field	I-T Storms Probes 1 and 2
AC electric field	I-T Storms Probes 1 and 2

the Baseline set. The results of a feasibility study for the Core I-T Storm Probes are given in Appendix 2.

4.3.5 Augmentations to I-T Baseline Science Investigation

The GMDT also considered measurements that are not part of the Baseline investigation but that significantly enhance the science return. The measurements that are identified are:

- Ion mass composition
- Electron temperature
- Ion temperature

4.4 Network-Level Investigations

Network-level investigations are those missions and experiments that enable an understanding of geospace at the system level and that are not being addressed by other agencies or the International LWS Program now (see Chapter 5 for the integration of LWS Geospace with other programs). The GMDT notes that the Network-level investigations elevate our understanding to include coupling between different regions in some cases, while in other cases they expand our perspectives over greater regions of geospace or a greater range of solar activity and the solar cycle. Network-level investigations considered by the GMDT are discussed in the following sections.

4.4.1 High-Latitude Imaging

From its inception, the GMDT has recognized the vast potential of two-dimensional remote sensing (high-latitude FUV imaging, mid-latitude ionospheric-thermospheric imaging, and ENA imaging) to meet Geospace science priorities. ENA imaging is included in the Baseline Radiation Belt Investigation, and mid-latitude I-T imaging is a component of the Core I-T Investigation.

Auroral imaging has been identified as a key Network-level investigation. The I-T thrust of investigating the ionospheric response to storm time inputs will be greatly aided by the improved specification of high-latitude energy sources and ionospheric drivers. For example, as noted in Section 2.3.3, studying the negative phase ionospheric storm response requires knowledge of asymmetries in particle precipitation and Joule heating. Similarly, investigation of thermospheric composition changes benefits from a knowledge of the spatial structure and temporal evolution of the Joule heating patterns. In addition, the two-dimensional distribution of ionospheric conductivity in the auroral region impacts study of current closure through the ionosphere.

High-altitude auroral imaging either provides this information directly or significantly improves the estimation of these parameters, for example by improving the accuracy of assimilative models of Joule heating. Global-scale (hemispheric) imaging also provides context for I-T in situ measurements, provides strong constraints on models, and can ultimately be used to constrain global space weather assimilation models. Simultaneous imaging is thus a natural adjunct to in situ observations for investigating the mid-latitude storm-time ionospheric response to magnetospheric storm-time inputs. By providing context and extending discrete observations, an auroral imaging investigation will contribute significantly to Objectives 2A.2, 2A.3, and 2B.3. High-latitude auroral imaging contributes to the objectives by providing the following:

- **Global measurement of relatively impulsive energy inputs to the ionosphere and thermosphere from particle precipitation and Joule heating.** FUV auroral imaging provides information on the energy characteristics and spatial distribution (longitudinal structure and temporal history) of electron precipitation, which is an important energy source for ionospheric modifications and thermospheric heating.

- **Instantaneous local time knowledge of the boundaries of the equatorward edge of the auroral zone and its temporal morphology.** Many ionospheric characteristics change at the equatorward boundary of the aurora and an instantaneous specification of this boundary is important to modeling studies and interpretation of observations.
- **Size of the polar cap.** This is a direct measure of the amount of magnetic energy stored in the magnetotail, much of which is released episodically into the auroral ionosphere and thermosphere to be propagated to mid- and even low-latitudes.

The best way to provide the remote sensing measurements that follow from the LWS science priorities is through dedicated instrumentation and observing platforms for each measurement need, that is, dedicated spacecraft for ENA, mid-latitude imaging, and high-latitude FUV imaging. However, it may be possible to place two or more imagers on a common viewing platform. Furthermore, while the measurement needs for mid- and high-latitude imaging differ considerably, there is considerable similarity between the instrumentation required to meet these needs. This raises the possibility that a composite FUV imaging package could conceivably be used to meet all I-T and auroral measurement needs. This composite imager could then be included with the ENA imager on a common viewing platform in a suitable orbit. A detailed mission analysis of a proposed high-altitude, high-latitude, circular orbit option combining multiple imagers is presented in Appendix 2.

4.4.2 Inner Belt and Slot Investigation

The Baseline RBSP configuration contains energetic electron and proton instruments that should allow unambiguous measurements of particles in the inner belt, slot, and outer belt regions. However, the specific objective to characterize and model the inner belt and solar protons is not as high a priority as the objective of understanding outer zone electron dynamics. Indeed, the orbit of the RBSP mission optimizes the outer zone residence time while minimizing the time spent in the inner belt. Though scientifically a lower priority than understanding outer zone dynamics with the LWS Geospace arena, there is much not characterized or understood about the inner zone and slot regions, including the energetic electron spectrum, penetration of solar protons, variation of proton fluxes with changes in neutral density and the internal Earth's magnetic fields, and the decay and formation of slot region proton belts. Furthermore, protons pose a severe hazard to spacecraft and astronauts even in low Earth orbit through the South Atlantic Anomaly. Improving models of inner zone protons is a top priority for the satellite design and operations community as they attempt to expand their orbit options to higher and higher altitudes. LWS should take advantage of opportunities to fly energetic proton and electron detectors with a magnetometer on missions that go through the inner belt. An orbit in the range $1.1 < L < 3$ would provide for optimal coverage.

4.4.3 Geosynchronous Phase Space Density Investigation

Currently there exist sources of particle and magnetic field data on geosynchronous orbit spacecraft, for example, the GOES and LANL sensors. Unfortunately, neither of these provides the spectral and/or pitch-angle resolution required to establish the phase space density of the particle population. With the apogee of RBSP at L ~5.5 R_E, there is a clear gap in coverage. Opportunities to fly the RBSP energetic electron sensors with a magnetometer on a geosynchronous satellite would give a valuable outer boundary condition to constrain the models in a region of great commercial interest.

4.4.4 Additional RBSP for Enhanced Local Time and Solar Cycle Coverage

The RBSP mission will yield a major advance in the understanding of radiation belt processes.

There are two clear paths to building upon this advance. The first approach is to expand solar cycle coverage of the RBSP. The strawman mission study for this report assumes a 2-year mission lifetime. Current radiation belt models are static and only exist for solar maximum and solar minimum. If the RBSPs are flown at solar maximum, they will yield improved specification models appropriate for the most intense radiation belts. By extending the RBSP lifetime either with more robust spacecraft or a new set of spacecraft, dynamic specification models can be generated for the full range of solar activity.

The second approach is to increase the local time coverage by conducting one or more additional Radiation Belt Storm Probes (or possibly a mission of opportunity piggyback) simultaneously with the investigation defined herein, but in a different local time region. This approach would yield a fuller set of constraints and validation parameters for modeling the acceleration and loss of radiation belt particles by providing much better local time asymmetry information.

4.5 Options Table

The Living with a Star Program (LWS) represents a long-term investment. No one mission or small set of missions will deliver all of the understanding that is needed to achieve the broad LWS goals. In that context, the Geospace Program defined herein is highly robust. Given that resources are always limited and uncertain, the Geospace Program is designed to deliver substantial and highly valuable progress at various levels of investment. The robustness of the Geospace Program is captured here in what is termed the "Options Table" (**Table 8**). The options table summarizes many of the discussions of this section. It shows, in a graphical manner, the GMDT's assessment of the level of understanding that will be achieved for the identified science objectives. It also illustrates the effect of deletions from and/or additions to the Geospace Baseline investigations.

The center panel of the table shows the general and specific objectives (cf. **Table 3 in Chapter 1**) in an abbreviated form; the first columns on either side indicate how well the Baseline investigation fulfils the objectives. The table is designed to assess the impact on each of the Specific Geospace Objectives when a key element of the Baseline investigation is removed. The form of the table is differential, i.e., each deletion is considered stand-alone. The left side of the table shows the consequences of deleting measurements, with the leftmost column showing the cumulative effect of implementing a set of deletions so that the remaining measurements represent a "Core" investigation. The color-coding signifies the degree to which each of the objectives is fulfilled by the individual measurements, with blue denoting the overall goal for the Geospace Investigations. The gray boxes indicate when deleting a measurement does not significantly impact the science objectives.

The table demonstrates that the Baseline investigations fulfill very well 10 out of the 17 highest-priority objectives, with substantial progress being made on a further four. Following the chart through to the left for each of the specific objectives shows how deleting a particular measurement impedes progress. For example, Specific Objective 1.1 (acceleration and transport of radiation belt electrons) is "well fulfilled" (blue) by the Baseline investigation. Removing the high-latitude ENA imaging degrades this assessment to "substantial progress" (green). The chart also represents well the effect of deletions on clusters of science objectives, represented with vertical groupings. For example, the Baseline investigation "well fulfills" the ITSP Objectives 2A.2, 2A.3, and 2B.1. If the precipitating electron (10 eV to 20 keV) measurement is removed, the degree to which these objectives are met is degraded to green or "substantial progress."

Removing each of the measurements on the left side of the table enables us to consider a subset

of the Baseline investigation, the Core investigation, and to assess its ability to fulfill the objectives. The table shows that even the Core investigation will provide "well fulfilled" in 1 and "substantial progress" in 9 out of the 17 highest-priority objectives, with "limited progress" being made in a further 6. Only 2 of these objectives show no possible progress should the Core investigation be flown.

Finally, the right side of the table shows additions to the Baseline, where a "+" indicates a value-added measurement providing enhanced scientific understanding of the objectives. The options here are either Augmentations to the Baseline investigations or Network-level investigations. It is anticipated that these major additions represent areas where inter-agency, intra-agency, and international collaboration can make major contributions. The rightmost column shows the cumulative effect of adding all of the options to complete the Geospace Program.

Table 8. LWS Geospace Options table. See text for explanation of format and color coding.

CHAPTER 5.
LWS INTEGRATION WITH OTHER PROGRAMS

The Baseline Geospace Investigations, described in Chapter 4, together with the Augmentations and Network-level investigations, constitute the LWS Geospace Program. As explained above, the Baseline investigations will address the highest priority science objectives of the Geospace Program, while the broader set of Network-level Investigations will enable understanding of the geospace environment as a coupled system. The implementation of the Geospace Program thus conceived will rely on a number of NASA and other U.S. and international programs as well, both to provide simultaneous data during the Geospace Investigations and also to provide information addressing gaps in understanding and enabling improved space weather models in support of LWS goals. This chapter describes those programs that (1) are **essential** to the fulfillment of LWS Geospace objectives and (2) will **complement and expand the scope of** the Geospace Investigations by providing additional data. Summary descriptions for many of the programs falling into the above categories are presented in the following sections; estimated operational timelines are given in **Figure 26.** The chapter concludes with a brief discussion of the importance of close coordination of the Geospace Program with existing and developing space weather programs supported by other national and international agencies.

5.1 Essential Measurements from Other Programs

The Geospace Program will rely on six types of essential measurements from other programs.

- Solar EUV spectral irradiance
- Solar wind parameters
- High-latitude magnetospheric energy input to the I-T system during moderate magnetic storms
- Magnetospheric seed populations for the high-energy electron radiation belts
- Global distribution of ULF waves
- Measurements of low-latitude ionospheric irregularities

If any of these expected measurements were not available, progress on the relevant scientific objective(s) would be affected unless other means were found to obtain equivalent measurements.

5.1.1 Solar EUV Spectral Irradiance

Understanding the I-T response to variable solar EUV irradiance requires a set of well-calibrated measurements with a cadence capable of following the fastest variations of the flux that have geospace effectiveness. ***As stated above, in Section 4.3, the LWS Geospace Program expects that an EUV spectral irradiance monitor will be included in the SDO payload to fulfill this requirement and that EUV measurements will significantly overlap the I-T Storm Probes mission***. While other flight programs will provide solar EUV observations (see Complementary Programs), none of these measurements have the spectral resolution and continuous coverage that will satisfy the Geospace I-T requirements.

5.1.2 Solar Wind Parameters

A basic assumption of the LWS Geospace Program is that measurements of the interplanetary magnetic field and solar wind plasma will be available during the Radiation Belt and I-T Storm Probe missions. The platform providing these measurements must be near the Earth–Sun line. Measurements of solar wind velocity and density and the interplanetary magnetic field are absolutely necessary for the success of the LWS Geospace Program. For the next 10 years, Advanced Composition Explorer (ACE) is the pri-

Figure 26. Timeline for complementary programs and missions.

mary solar wind monitor, with Wind a backup. Triana, currently in storage, could be activated to provide these measurements.

5.1.3 High-Latitude Magnetospheric Energy Input into the I-T System

Joule heating from the magnetosphere-ionosphere current system, and to a lesser but important degree, auroral particle precipitation, are the two dominant forms of high-latitude magnetospheric energy input to the I-T system. The high-latitude heating modulates the dynamo electric fields. Substorm and storm-time Joule heating and particle precipitation represent an impulsive heat source that drives thermospheric disturbances that propagate to low latitudes. ***This is believed to be the source of the negative ionospheric storm*** (Objective 2A.1b and Section 2.3.3). During major magnetic storms the I-T imager on a geosynchronous spacecraft will view auroral inputs. During moderate magnetic storms knowledge of auroral energy sources will be obtained from a variety of other facilities.

NPOESS. Beginning in about 2008 the National Polar-Orbiting Environmental Satellite System (NPOESS) operated by the Departments of Commerce and Defense will maintain several near polar orbiting, Sun-synchronous satellites that will make extensive measurements of the energy input to the high-latitude ionosphere as well as specifications of the ionospheric parameters themselves. Measurements include magnetic field perturbations from field-aligned currents, a complete particle precipitation environment, and two-dimensional auroral imaging in UV.

SuperDARN. An international network of high-frequency coherent scatter radars, the Super Dual Auroral Radar Network (SuperDARN) provides continuous Doppler measurements of plasma convection in the high-latitude ionosphere, along with other observables. Data from the nine existing radars in the northern hemisphere cover up to 75% of the auroral oval and polar cap and can be used to study the spatial and temporal evolution of the high-latitude convection pattern. These convection patterns can be combined with model ionospheric conductance patterns or those derived from FUV auroral imaging to estimate the spatial and temporal evolution of Joule heating within the polar I-T system. The polar cap potentials are also used in models to estimate auroral energy input.

GEC. The Global Electrodynamic Connections (GEC) mission of NASA's Solar Terrestrial Probe Program is expected to overlap the I-T Storm Probe mission to furnish both magnetic field and auroral precipitation data comparable to NPOESS. It will especially determine how the I-T system responds to magnetospheric forcing, thus addressing the Geospace objectives related to the high-latitude ionosphere and thermosphere (General Objective 2A and Specific Objectives 2.B.3 and 3A.2).

Auroral imager. If a global FUV auroral imager is flown (cf. Section 4.4.1), it would permit inference of the precipitating energy flux, from which Joule heating could be estimated when combined with polar cap convection patterns. The strength of an auroral imager would be in its global coverage and high time resolution. Concurrent precipitation observations would aid in calibration and validation of the calculated auroral energy flux.

5.1.4 Magnetospheric Seed Populations for the High-Energy Electron Radiation Belts

Since the majority of processes that have been proposed to account for radiation belt enhancements conserve the first adiabatic invariant and therefore involve some form of radial transport of plasma (see Section 2.2.1), ***simultaneous measurement of the source plasma at an outer boundary to the radiation belts is very important; of particular importance is determination of the phase space densities.*** Geospace RB Storm

Probes can expect some access to these measurements from at least one long-range program.

GOES. Currently, two NOAA GOES satellites are stationed over the east and west coasts of the United States in geosynchronous orbits. These satellites carry space environment monitors (SEMs) that include measurements of energetic particles and the magnetic field. The next generation of GOES satellites, to be launched in the 2004 time frame, will extend the measurements of energetic particles to lower energies (80 keV for protons and 30 keV for electrons). Planning is in progress for another generation GOES spacecraft, the GOES R+ series, which should be ready for launch in 2012 during the LWS RB mission. They will contain similar particle and fields measurements. However, the particle measurements on GOES will not have adequate energy or pitch angle resolution to provide the desired phase space densities of the seed populations for energetic particle acceleration mechanism studies.

MMS. The science objective of the Magnetospheric Multiscale (MMS) mission is to characterize the basic plasma processes which control the structure and dynamics of the Earth's outer magnetosphere, using four identical spacecraft. At times MMS will be in a position to provide measurements of the ultimate electron source populations just outside the inner magnetosphere where the Radiation Belt Investigation is focused. Its current launch date would allow an overlap with RBSP.

Geosynchronous phase space density measurements. As noted, in Section 4.4.2, the GMDT recommends inclusion of LWS Geospace provided instrumentation to measure phase space density on a geosynchronous spacecraft. With the lack of quality phase space density measurements in the outer magnetosphere during the RBSP mission, the flight of such instrumentation as a mission of opportunity becomes very important for the fulfillment of radiation belt science objectives (Objective 1.1).

5.1.5 Global Distribution of ULF Waves

ULF wave power in the inner magnetosphere is greatly enhanced during geomagnetic storms and may be a key parameter to distinguish storms that produce radiation belt enhancements from those that do not. These ULF waves lead to enhanced rates of radial diffusion compared to classical diffusion resulting from impulsive changes in the convection electric field. ***The global ULF wave distribution is required for individual event analysis and for first-principles models of the radiation belts*** (cf. Section 3.2.4). Recently, data from ground-based magnetometer chains have been used to derive the global distributions of ULF waves. It is expected that this important data source will remain available through the RBSP mission.

5.1.6 Measurements of Low-Latitude Ionospheric Irregularities

Understanding the conditions that lead to the formation of equatorial spread-F to enable nowcasting of their location and magnitude is a high-priority space weather problem (Objective 2B.2). ***The Baseline I-T Storm Probes are designed primarily to address the problem of storm-time mid-latitude irregularities. This strategy is feasible*** because the Communications Navigation Outage Forecasting System (C/NOFS), a planned Air Force satellite in a 700-km low-inclination orbit, is designed for specifying and forecasting equatorial ionospheric irregularities. The C/NOFS mission objective is to understand the fundamental physics governing space weather at low latitudes. For this mission, the satellite will carry a wide range of sensors. These data will be available for LWS Geospace analysis and will be ingested into a Coupled Ionosphere Scintillation Model (CISM), which is expected to provide nowcasting and 6-hour forecasting of the background equatorial ionosphere and the onset and magnitude of scintillations.

5.2 Complementary Programs

5.2.1 Radiation Belt Particle and Seed Population Measurements

A number of U.S. government agencies will sponsor spacecraft before, during, and following the RB Storm Probe mission that will provide complementary data; these data will be especially valuable for characterizing the radiation belts over a solar cycle.

LANL-GEO and GPS. The Los Alamos National Laboratory provides comprehensive energetic particle and plasma space environment instruments on Global Positioning System (GPS) and multiple geosynchronous (LANL-GEO) satellites. The whole GPS constellation of 26 satellites is expected to carry radiation environment instruments during the LWS Geospace Program. These satellites, which cover $L \geq 4$, will expand the local time coverage inside geosynchronous orbit while the LANL-GEO will continue to provide measurements at multiple local times just outside the nominal RBSP satellite apogees. Without magnetic field measurements, these data sets cannot provide phase space densities.

DoD/MEO and HEO. Medium Earth orbit (MEO) and high Earth orbit (HEO) platforms flown by commercial satellite operators and DoD will provide energetic proton and electron measurements and radiation dose measurements. The MEO data will come from a moderate inclination circular orbiting satellite that makes measurements for $L \geq 3$. HEO satellites have 63° inclination, elliptical orbits with apogees of 7.2 R_E. Both will have significant spatial coverage overlap with the Radiation Belt Investigation and will add to the phase space density measurements needed for particle acceleration and transport studies.

NASA/MAGCON. The goal of the NASA Magnetospheric Constellation (MAGCON) mission is to understand the interactions between the localized and time-dependent drivers of magnetospheric dynamics, both locally and globally. It will orbit tens of autonomous micro-satellites in the magnetotail, which for LWS will be making measurements of the source population region for the energetic population.

TWINS. The Two Wide-angle Imaging Neutral-atom Spectrometers experiment will make stereoscopic images of the ring current and plasma sheet over the energy range of 1 to 100 keV. The instruments will be launched into two separate Molniya orbits beginning in 2003, with the mission lasting until 2007. Although this mission will not overlap the Geospace Investigations, the TWINS experiment will advance both the modeling of the ring current and our understanding of the potential for using the ENA technique to estimate geoeffective quantities such as pressure gradients.

DoD/Space Test Program. The Space Test Program has requirements to assess the radiation effects on space technology. In performing that mission, it may cover local time sectors and spatial regions complementary to but different from those covered by the Radiation Belt Investigation. For example, planned instrumentation on SBIRS-Low (the DoD's Space-Based Infrared System Low) will monitor low-altitude particles.

5.2.2 Ionospheric Parameters

In addition to measurements of the energy input to the high-latitude I-T system, the NPOESS set of spacecraft will make observations of ionospheric irregularities, ionospheric plasma parameters (although at a significantly higher altitude than I-T Storm Probes), and two-dimensional thermospheric UV luminosity. These sets of observations are sufficiently complete that the I-T Investigation can plan a unique attack on the mid-latitude large- and small-scale variability, with NPOESS data earmarked for objectives related to the polar region (e.g., Objectives 2B.3, 2B.4, and 3A.2). However, the imaging will not fulfill

the global imaging needs for I-T objectives described in Section 4.4.1 because of the relatively low, circular orbit of 833 km.

The total electron content (TEC) along the line-of-sight between a GPS satellite and a GPS receiver can be deduced from the effect of the intervening electrons on the signal. Recently an array of ground-based GPS receivers, including the network of the International GPS Service for Geodynamics (IGS) stations and the Air Force Research Laboratory scintillation network, have begun providing ionospheric TEC maps by combining the deduced TEC along many satellite-receiver paths. Since global descriptions of such perturbations would pertain to General Objective 2B, the extent of these networks would hopefully grow to enable even better coverage during the LWS I-T Investigation, although they will not cover the oceans.

From space, the set of six COSMIC satellites from Taiwan, and EQUARS, a Brazilian low-altitude satellite complementary to COSMIC, will contain GPS receivers for ionospheric soundings of TEC. These flights may occur concurrently with the I-T Investigation.

The Canadian Enhanced Polar Outflow Probe, scheduled for launch in 2005, will contain an array of detectors to obtain ionospheric parameters, especially in the polar region. While the primary interest is in the acceleration and outflow of the polar wind plasma to the magnetosphere, it will also obtain basic ionospheric and thermospheric parameters, the magnetic field, waves and images from a fast auroral imager.

The DoD Space Test Program is planning to place a high-resolution FUV imager (Ionospheric Mapping and Geocoronal Experiment, IMAGE) into geosynchronous orbit to image ionospheric density, gradients, and large-scale irregularities. It will have a regional field of view that can be operated in a raster mode to yield global images and would be highly complementary to the I-T Investigation.

5.2.3 Ground-Based Observations

The four incoherent scatter radars supported by the National Science Foundation, along with others operated by Europe, Japan, and Russia, are particularly important in providing a wealth of information about the space environment. They should prove particularly useful in providing ground truth for the remote sensing of the ionospheric density distribution by imaging components of the I-T Investigation. Furthermore, they represent sites at which other ground-based instruments are clustered, allowing detailed study of phenomena occurring in a localized region. In addition, the National Science Foundation (NSF) is developing an Advanced Modular Incoherent Scatter Radar (AMISR) that will enable incoherent scatter radars to be moved to different locations to support specific scientific objectives.

In addition to the line-of-sight Doppler measurements of plasma convection, the ten SuperDARN radars in the northern hemisphere and the five in the southern hemisphere also provide information about the spatial distribution of ionospheric irregularities, regions of velocity turbulence, and the neutral winds at 90 to 100 km altitude. These more globally distributed observations will provide contextual information for the in situ measurements from the two I-T Storm Probes.

The NSF supports a wide array of other ground-based instrumentation that complements the LWS program. These include lidars, passive optical systems, and small radio-wave instruments that remotely measure important ionospheric and thermospheric parameters, particularly neutral and charged particle densities, temperatures, and winds. The NSF also provides ongoing support for ground-based magnetometer chains that can be used to study magnetic substorms and storms and their effects.

5.2.4 Complementary Solar EUV Flux and Other Solar Observations

The Solar Terrestrial Relations Observatory (STEREO) mission, to be launched in late 2005, is important for the LWS Geospace Program because it is designed to trace the flow of energy from the Sun to Earth through stereoscopic imaging of coronal mass ejections (CMEs) and tracking interplanetary shocks by radio triangulation. Such data are especially pertinent for the development of forecast models for the radiation belts (see Sections 3.2.3 and 2.2.4).

The next generation of GOES satellites in geosynchronous orbits, to be launched in the 2004 timeframe, will include new instruments to measure the whole-disk integrated solar EUV flux in five wavelength bands.

Another solar observing satellite, Solar-B (led by Japan's Institute of Space and Astronautical Science, ISAS), is being designed to reveal the mechanisms that give rise to solar variability and study the origins of space weather and global change. The spacecraft will make coordinated measurements at optical, EUV, and x-ray wavelengths and will provide the first measurements of the full solar vector magnetic field on small scales.

Coordination with complementary programs, both space-flight and ground-based, will work best if these programs are integrated with the LWS Geospace Investigations well before implementation. Therefore, collaboration should be arranged and key investigators from collaborating programs should be involved in the science operations planning for the Geospace Investigations. Examples of excellent past and current collaborative programs are the Dynamics Explorer program, the International Solar Terrestrial Physics Program (ISTP), and the Thermosphere, Ionosphere, Mesosphere, Energetics and Dynamics Program (TIMED).

5.3 Coordination with Other Space Weather Programs

To maximize the contributions of the Radiation Belt and I-T Investigations to our understanding of the response of the geospace environment to solar variability, the Geospace Program, along with other LWS activities, should be closely coordinated with other space weather research programs, both those conducted or sponsored by other U.S. agencies and those undertaken by the space agencies of other countries. Of particular importance in this context is the International Living with a Star (ILWS) program, which will provide a means for communicating and coordinating strategic plans of individual space agencies. Members of the ILWS will consist of scientific and technical program representatives from national and international agencies planning to contribute to ILWS space missions. Typical contributions may include space instrumentation and/or space missions that will directly address important LWS objectives.

Among programs sponsored by different U.S. agencies, there are a number of modeling initiatives related to the Geospace Program and especially to its theory and modeling component. These include the multi-agency Community Coordinated Modeling Center, the DoD's Multi-University Research Initiative, and through the NSF's Science and Technology Center, the Center for Integrated Space Weather Modeling.

Other national programs and initiatives relevant to the LWS Geospace Program include the multi-agency National Space Weather Program (NSWP), the DoD's National Security Space Architect's Space Weather Architecture, and the three continuing NSF-sponsored science programs that study the entire space weather system from the Sun to Earth: the Coupling, Energetics and Dynamics of Atmospheric Regions (CEDAR), Geospace Environment Modeling (GEM), and Solar, Heliospheric, and INterplanetary Environment (SHINE) programs.

CHAPTER 6.
SOCIETAL BENEFITS

The region of the Earth's space environment targeted by the LWS Geospace Program extends from the upper atmosphere into the heart of the radiation belts. Here, solar disturbances are most effective in producing geospace storms The vast majority of satellites used by both government and industry operate in this region and just beyond, in geosynchronous orbit, and are vulnerable to the increases in energetic particle fluxes that occur there during geomagnetic storms. This region presents risks to astronauts as well: the International Space Station's 51.6° inclination orbit brings it to geomagnetic latitudes where exposure to both relativistic electron fluxes and solar energetic protons is a serious concern. Finally, communications and navigation systems are profoundly influenced by the state of the ionosphere, which in turn is influenced by conditions in the inner magnetosphere. The number of our nation's technical systems dependent on space assets will increase during the next solar cycle; at the next solar maximum (2010), these systems will be stressed by extreme space weather for the first time and will be especially vulnerable.

The Geospace Investigations and the Storm Probes are the only programs designed to mitigate the vulnerability of important elements of our technological infrastructure to space weather through the improved scientific understanding of the radiation belts and ionosphere-thermosphere system. Therefore the Geospace Investigations will benefit many sectors of society, including the Department of Defense and other government agencies such as the Federal Aviation Administration, industry, and the general public, whose activities can be affected in numerous subtle and non-so-subtle ways by disturbances in the geospace environment. Many of the key societal benefits to be derived from the Geospace Investigations have already been discussed, in Sections 2.2.4 and 2.3.5 of Chapter 2. Some additional benefits are described in the following sections.

6.1 Operational Model Development and Validation

One of the specific benefits of the Geospace Program is its contribution to the development of models (cf. Chapter 3). The Geospace Investigations will yield the physical understanding of the radiation belts and I-T regions needed for the development of sophisticated new models of the geospace environment and will provide the data required to run and validate the models. These models will:

- Specify the nominal and extreme cases of space environments
- Provide assessments of those environments during specific periods of interest (now casting), and ultimately
- Predict future environments

Specification or ***empirical*** models are of great value both to the developers of technology and to the users of new technologies that are being developed. This user community includes, for example, designers and manufacturers of spacecraft, communications systems, and navigation systems. Also included are those responsible individuals and agencies that must decide which technologies to implement. An example is the use of Global Positioning System (GPS) receivers in air transportation.

Nowcasting models are needed in operational settings to understand events and anomalies. Operational military facilities must understand, for example, whether an out-of-specification event is the result of enemy action or simply the result of transient disturbances in the natural environment. Similarly, air transportation operators must

assess the probabilities that the loss of communication with an aircraft is the result of a security breach or, again, the result of natural phenomena.

Predictive models are needed for planning future activities. Spacecraft operators, and some ground system operators, need warning about natural events so that they can, for example, make decisions about the operation of spacecraft assets. NASA needs such warnings of disturbances in the space environment to plan astronaut activities, such as extravehicular activities associated with the maintenance of the International Space Station.

The development and refinement of specification models will be a near-term benefit, as such models often can be derived with relatively straightforward assimilation of the data. The transition from specification to nowcasting to predictive models requires increasing levels of deep understanding of physical processes. Progress will be made at all of these levels, but the development of fully predictive models is a long-term program. The Geospace Investigations will make unprecedented, multipoint measurements needed to advance our modeling capabilities to the predictive level. Furthermore, the inclusion of imaging in the Geospace Investigations will accelerate substantially the development of nowcast and predictive models. Global imaging will help establish the connection between locally quantified physical processes and the large-scale manifestations of those processes. Developing an understanding of that connection is one of the most important applications of the models.

6.2 Real-Time Data

Although LWS is not an operational program, a subset of the data provided by the Geospace Investigations will be useful for both government and commercial space weather operations, including NASA's manned space flight program and military and civilian space weather forecast centers. Such data should be considered for transmission in real time. Geospace data might be used, for example, to construct the first-ever real-time or near-real-time maps of the radiation environment in near-Earth space, maps analogous to the familiar global maps of cloud cover from weather satellites. In situ data might also be assimilated into models to create global views of the space environment, while global images of the high-latitude aurora and Earth's ring current will reveal essential details of the near-Earth space environment important for understanding geospace conditions. In addition to their operational value, real-time data are also valuable for basic space physics research. For example, real-time data from the ACE and IMAGE satellites are being used both for scientific studies and for space weather forecasting. Global maps can be used for displays that will enable scientists to assess data quality and instrument operations, and will make excellent survey plots that will simplify browsing through large amounts of data. Finally, the great public interest in seeing real-time data and watching events that are "happening now" should be noted. Thus, besides their importance for both operations and research, real-time data have significant "public relations" value as well.

Instrument teams involved in the Geospace Investigations will provide scientifically valid data to all users as rapidly as possible after receipt of telemetry. Each investigation will deliver data in accordance with the requirements of the data access system that will be developed for the Geospace Program.

6.3 Trailblazing

Agencies, individuals, and organizations responsible for operational systems that are affected by the highly variable space environment require the ability to monitor that environment. The questions of what to monitor and where to monitor it are nontrivial. In the past, scientific and technol-

ogy research spacecraft and investigations have been "trailblazers" for the development of operational satellites that monitor the geospace environment. For example, such NASA technology research missions as ATS-1 and ATS-6 (Applications Technology Satellites 1 and 6) performed the fundamental research on the space environment of the geosynchronous region that was a necessary precursor to the development of such operational spacecraft as the GOES (Geostationary Orbit Environmental Satellites) constellation. Those satellites, in turn, monitor the environment where a broad spectrum of communications satellites reside and provide nowcasting for operators concerned with the radiation effects throughout the Earth's magnetosphere.

The increase in the sophistication of our use of space will require the use of new and more advanced monitoring techniques and facilities. The Geospace Investigations will serve as trailblazers for the monitoring techniques and satellites that will be needed in the future. For example, the Radiation Belt Investigation may discover that near-equatorial, radial profiles of selected particle intensities, delivered at the cadence available in a sub-geosynchronous transfer orbit, may provide the most useful near-real-time assessment of the radiation environment of the inner magnetosphere. Other opportunities for developing monitoring techniques may be identified based on the in situ measurements made within the heart of the hard radiation regions when these data are combined and correlated with the simultaneously obtained global imaging products. The Geospace Investigations will discover the critical parameters that can serve as proxies to a host of complicated geophysical processes and phenomena, and they will point the way to where those assets must reside.

6.4 Education and Public Outreach

The LWS Geospace Program has a unique potential for meaningful educational and public outreach because of its significant societal benefits. Space weather conditions can have dramatic effects on our everyday lives because of the disruption of personal activities associated with communications, navigation, and security. These effects will engender a parallel interest on the part of the public in the region of space where the phenomena occur that produce these disruptions. The migration of models into operational environments will place before the public concepts and images that will be new to a large portion of the affected public.

Thus public outreach will be an integral element of the LWS Geospace Program. One facet of the Program's public outreach effort will be to target museums and science centers to raise awareness of the exciting scientific results of the Geospace Investigations and to educate the public about how space weather affects their lives. The LWS Program will explore avenues for the broad dissemination of real-time geospace data to the general public, along with the output of models running simultaneously to illustrate the geospace response in an easily understandable format.

Space and the phenomena that occur there are exciting and capture the imagination of students. The science of the Sun and its effects on Earth fit well into daily curricula for K-14 students. A robust formal education component will thus be included in the LWS Geospace Program. This educational component will invoke both traditional and nontraditional methods to communicate the exciting science to students of all ages. Since the phenomena of space lend themselves as practical, curiosity-fulfilling, and timely examples of fundamental physical processes, it is relatively easy to integrate them into the core curriculum through traditional classroom activities and innovative web-based programs.

APPENDIX 1.
TRACEABILITY MATRIX

This traceability matrix is one of several tools used to develop the Geospace science program and the implementation strategies. The matrix is included here to inform the reader as to the direction of the committee's reasoning during deliberations. It is not represented as being comprehensive or definitive. The quantitative numbers in the matrix are guidelines only and should not be interpreted as requirements.

The traceability matrix begins with columns showing the general and specific science objectives, as in **Table 3** of Chapter 1. Following are columns that identify general **Approaches** for achieving the specific objectives, more detailed **Techniques** for implementing the approaches and finally the **Measurement Parameters** that the Geospace program must provide to carry out the techniques. Not included in the measurement parameters column are the parameters that are to be obtained by existing (non-Living With a Star) assets. These "assumed from other programs" parameters are presented in a separate table that follows the main traceability matrix.

Note that within the main traceability matrix, no prioritization has been performed for the entries within the Approach, Technique, and Measurement Parameters columns.

Specific objectives for the highest priority geospace investigations derived from the general objectives. Groups of specific objectives are prioritized within each general objective.

LWS/Geospace General Objective	Specific Objectives:
Priority 1: Understand the acceleration, global distribution, and variability of energetic electrons and ions in the inner magnetosphere. SAT report: WG1-5 and 6, WG2-4	**Priority 1:** **1.1***:* Differentiate among competing processes affecting the acceleration and transport of outer radiation belt electrons.
	Priority 2: **1.2a***:* Differentiate among competing processes affecting precipitation and loss of outer radiation belt electrons. **1.2b***:* Understand the creation and decay of new electron radiation belts. **1.2c***:* Develop and validate physics-based data assimilation and specification models of outer radiation belt electrons.
	Priority 3: **1.3a***:* Understand the role of "seed" or source populations for relativistic electron events. **1.3b***:* Quantify the relative contribution of adiabatic and nonadiabatic processes on energetic electrons. **1.3c***:* Understand the effects of the ring current and other storm phenomena on radiation belt electrons and ions.
	Priority 4: **1.4a***:* Understand how and why the ring current and associated phenomena vary during storms. **1.4b**: Develop and validate physics-based and specification models of inner belt protons for solar cycle time scales.
Priority 2A: Determine the effects of long and short term variability of the Sun on the global-scale behavior of the ionospheric electron density. SAT report: WG1-1, WG2-1	**Priority 1:** **2A.1a***:* Quantify the relationship between the magnitude and variability of the solar spectral irradiance and the global electron density. **2A.1b**: Quantify the effects of geomagnetic storms on the electron density.
	Priority 2: **2A.2***:* Quantify how the interaction between the neutral atmosphere and the ionosphere affects the distribution of ionospheric plasma.
	Priority 3: **2A.3***:* Discover the origin and nature of propagating disturbances in the ionosphere.
Priority 2B: Determine the solar and geospace causes of small scale ionospheric density irregularities in the 100 km to 1000 altitude range. SAT report: WG1-2, WG2-2	**Priority 1:** **2B.1***:* Characterize and understand the origin and evolution of newly-discovered storm-time mid-latitude ionospheric irregularities.
	Priority 2: **2B.2a***:* Understand the conditions leading to the formation of equatorial spread-F irregularities, and their location, magnitude, and spatial and temporal evolution. **2B.2b**: Understand the conditions leading to the formation of polar patches and their high latitude irregularities.
	Priority 3: **2B.3***:* Enable prediction of the onset, location, and development of E-region irregularities.
Priority 3A: Determine the effects of solar and geospace variability on the atmosphere enabling an improved specification of the neutral density in the thermosphere. SAT report: WG1-3, WG2-3	**Priority 1:** **3A.1a***:* Determine the variability in the neutral atmosphere attributable to the solar EUV spectral irradiance. **3A.1b**: Determine the variability in the neutral atmosphere attributable to magnetospheric inputs.
	Priority 2: **3A.2***:* Determine the variability in the neutral atmosphere attributable to internal processes.
	Priority 3: **3A.3***:* Determine the variability in the neutral atmosphere attributable to atmospheric waves from below.

LWS Geospace General Objective: Priority 1: Understand the acceleration, global distribution, and variability of energetic electrons and ions in the inner magnetosphere.			
Specific Objectives	**Approach**	**Technique**	**Measurement Parameters**
Priority 1: 1.1: Differentiate among competing processes affecting the acceleration and transport of outer radiation belt electrons.	• Differentiate importance of radial diffusion vs. impulsive transport as a function of solar wind parameters.	• Obtain simultaneous phase space density (PSD) distributions along multiple L-shells • Characterize E and B to distinguish stochastic and coherent propagating structures. • Characterize ULF and stochastic electric fields and magnetic fields (>minute scale) during a number of storms. • Compare radial diffusion rates with impulsive transport rates as a function of upsteam solar wind driving forces.	Electron differential flux j(E,α, L) Energy: 20 keV to 10 MeV Vector magnetic field Electric field Wave electric field Wave magnetic field
	• Determine relative importance of convective transport by improving empirical models of global electric fields.	• Measure the electric field in the equatorial region for a variety of interpletary conditions to provide statistical data for the global models. • Obtain simultaneous PSD distributions at multiple L-shells and along at least two local times to test model veracity. • Compare convection transport rate with diffusive and impulsive transport rates.	Electron differential flux j(E,α, L) Energy: 20 keV to 10 MeV Electric field Vector magnetic field
	• Distinguish adiabatic from non-adiabatic energization during transport, for example betatron versus shock-drift acceleration.	•Obtain simultaneous PSD distributions at multiple L-shells and along at least two local times. • Measure plasma wave E and B spectrum • Compare the various energization efficiencies as a function of upsteam solar wind driving forces.	Electron differential flux j(E,α, L) Energy: 20 keV to 10 MeV Vector magnetic field Electric field Wave electric field Wave magnetic field
	• Determine distribution of source populations present over a variety of solar wind conditions to document the limits of energization possible through radial transport.	• Develop statistical models for the global distribution of seed population electrons.	Electron differential flux j(E,α, L) Energy: 1 keV to several MeV Vector magnetic field
	• Analyze specific scenarios over a variety of solar wind conditions using data-driven procedures and models based on different mechanisms (e.g., diffusion equation fitting, MHD, global guiding center transport, resonant ULF drift, etc.)	• Refine global magnetic field models to accurately represent a variety of dynamic conditions. • Assess existing data-driven procedures and models for calculating transport and acceleration based on different mechanisms. • Refine/update data-driven models to a level of fidelity needed to discriminate between mechanisms for different conditions.	n/a

LWS Geospace General Objective:
Priority 1: Understand the acceleration, global distribution, and variability of energetic electrons and ions in the inner magnetosphere.

Specific Objectives	Approach	Technique	Measurement Parameters
Priority 2: 1.2a: Differentiate among competing processes affecting precipitation and loss of outer radiation belt electrons.	• Establish accurate loss rates vs. energy and location for wave induced pitch-angle scattering mechanisms and their variability.	• Measure power spectral density of waves responsible for scattering throughout outer zone electron regions (vs. L and LT); use existing knowledge to determine wave modes (ES vs EM) • Develop statistical models for global distribution of wave properties. • Measure full electron energy-dependent pitch-angle distributions and intensities throughout outer zone regions. • Derive theoretical quasi-linear pitch-angle diffusion rates as a function of energy, pitch angle and location. • Establish wave modes most important for losses across regions and conditions.	Electron differential flux j(E,α, L) Energy: 20 keV to 10 MeV Vector magnetic field Electric field Wave electric field Wave magnetic field
	• Establish accurate loss rates vs. energy and location for current sheet scattering and its variability.	• Determine extent storm-time ring current distorts global E and B field topology. • Measure higher energy electron pitch-angle distributions at higher L values for the outer zone region. • Develop theoretical models for current sheet scattering rates.	Electron differential flux j(E,α, L) Energy: 1 MeV - 10 MeV Vector magnetic field
	• Establish accurate loss rates vs. energy and location for magnetopause shadowing and its variability.	• Use existing data to refine theoretical models for location and variability of magnetopause and global B distortion due to enhanced storm-time ring current. • Develop models for magnetopause shadowing rate for all solar cycle phases.	Vector magnetic field
	• Establish accurate loss rates vs. energy and location for Coulomb scattering and its variability.	• Refine models of neutral exospheric gas densities using existing data. • Refine time-averaged model of plasmaspheric ion densities using exiting data for various solar cycle conditions. • Develop theoretical models for rate of Coulomb scattering and variability for ions and neutral scattering processes.	n/a
	• Derive comprehensive precipitation/loss model reflecting the relative importance of various proposed mechanisms.	• Measure electron PSD profiles at high altitude and use analysis to estimate electron losses versus L-shell. • Measure losses using detectors on low altitude, polar orbit spacecraft. • Compare the estimated and measured losses for each loss process type. • Assimilate a global distribution of electron loss and its variability and compare with measured loss rates.	Electron differential flux j(E,α, L) Energy: 20 keV to 10 MeV Vector magnetic field

LWS Geospace General Objective: Priority 1: Understand the acceleration, global distribution, and variability of energetic electrons and ions in the inner magnetosphere.			
Specific Objectives	**Approach**	**Technique**	**Measurement Parameters**
Priority 2: 1.2b: Understand the creation and decay of new electron radiation belts.	• Understand how shocks or solitary structures propagate through the inner magnetosphere.	• Develop models, analytic or MHD, of the global electric and magnetic fields produced by interplanetary shocks. • Establish strength, polarization, k-vector and duration of accelerating E fields.	Vector magnetic field Electric field Wave electric field Wave magnetic field
	• Quantify relative limits of impulsive and diffusive transport as a function of solar wind parameters.	• Obtain measures of the plasma source population at different local times • Characterize ULF and stochastic electric fields and magnetic fields (>minute scale) during a number of storms.	Electron differential flux j(E,α, L) Energy: 1 keV to few MeV Magnetic field Electric field Wave electric field Wave magnetic field
	• Determine the role of non-adiabatic processes (e.g., electrostatic wave interactions) in energizing the new population.	• Obtain PSD profiles as a function of energy and magnetic coordinates for slot over several storms. • Measure plasma wave electric spectrum • Idenitfy wave modes and interactions as a function of energy.	Electron differential flux j(E,α, L) Energy: 20 keV to 10 MeV Vector magnetic field Electric field Wave electric field Wave magnetic field
	• Characterize time scale and efficiency of acceleration as a function of source population energy range.	• Obtain PSD profiles as a function of energy and magnetic coordinates for slot over several storms.	Electron differential flux j(E,α, L) Energy: 20keV - 10 MeV
	• Determine loss rates vs. energy for pitch-angle scattering and diffusion mechanisms for the new belts.	• Measure power spectral density of waves responsible for scattering throughout slot region (vs. L and LT); use theory to determine wave modes (ES vs. EM). • Develop statistical models for global distribution of plasma wave properties. • Measure full electron energy-dependent pitch-angle distributions and intensities throughout new belt region. • Derive theoretical quasi-linear pitch-angle diffusion rates as a function of energy, pitch-angle and location. • Establish wave modes most important for losses for different conditions.	Electron differential flux j(E,α, L) Energy: 20 keV to 10 MeV Vector magnetic field Electric field Wave electric field Wave magnetic field
	• Model evolution of particle populations as shocks or solitary structures propagate through inner magnetosphere.	• Develop models, analytic or MHD, which include realistic global electric and magnetic fields produced by interplanetary shocks.	n/a
Priority 2: 1.2c: Develop and validate physics-based data assimilation and specification models of outer radiation belt electrons.	• Develop parameterized statistical model of the electron population in the inner magnetosphere including representation of variations related to interplanetary and disturbance conditions.	• Obtain PSD profiles as a function of energy and magnetic coordinates for slot and outer belt regions over several solar cycles. • Measure the electric field in the equatorial region for a variety of interpletary conditions to provide statistical data for the global models. • Define particle parameters associated with changing E and B fields. • Develop statistical relationships between observables and boundary conditions. • Continuously test and update model against new observations.	Electron differential flux j(E,α, L) Energy: 20 keV to 10 MeV Vector magnetic field Electric field
	• Form hybrid MHD and kinetic data assimilation models suitable as prototype for nowcasting.	• Review existing models to determine which are the most important observables and the best techniques in order to provide the most realistic and responsive output.	n/a
	• Develop global physics-based models suitable for comprehensive testing of acceleration, transport and loss processes occuring through the inner magnetosphere.	• Review existing models to determine which are the most important observables and the best techniques in order to provide the most realistic and responsive output.	n/a

LWS Geospace General Objective: **Priority 1: Understand the acceleration, global distribution, and variability of energetic electrons and ions in the inner magnetosphere.**			
Specific Objectives	**Approach**	**Technique**	**Measurement Parameters**
Priority 3: 1.3a: Understand the role of "seed" or source populations for relativistic electron events.	• Determine distribution of source populations present over a variety of solar wind conditions.	• Develop statistical models for the global distribution of seed population electrons.	Electron differential flux j(E,α, L) Energy: 1 keV - few MeV Vector magnetic field
	• Determine ion injection and energization processes during storm development.	•Develop storm-time dependent E-field models for ring current and near-tail region. •Determine injection locations. •Distinguish between convective and in situ energization processes by comparing phase space densities in source and ring current regions. •Determine role of ULF and VLF waves in energizing ring current plasmas.	O and H ENA images 10-400 keV Ion differential flux j(E,α, L) Energy: 20-600keV Electric field Wave electric field Wave magnetic field
	• Model evolution of particle populations as shocks or solitary structures propagate through inner magnetosphere.	• Develop models, analytic or MHD, which include realistic global electric and magnetic fields produced by interplanetary shocks.	n/a
Priority 3: 1.3b: Quantify the relative contribution of adiabatic and nonadiabatic processes on energetic electrons.	• Measure and model the adiabatic processes conserving the 3 energetic electron invariants.	• Measure the PSD of energetic electrons during dynamic processes. • Construct displays of the temporal sequence of the PSD vs. L.	Electron differential flux j(E,α, L) Energy: 20keV - 10 MeV Vector magnetic field
	• Measure and model the nonadiabatic processes that violate the third invariant while conserving the first two invariants leading to radial diffusion.	• Measure the PSD of energetic electrons during dynamic processes. • Construct displays of the temporal sequence of the PSD vs. L. • Measure fluctuating ULF waves with periods comparable to electron drift period; use as input to model radial diffusion evolution. • Compute electron pitch-angle distributions caused by radial transport and compare with observed profiles.	Electron differential flux j(E,α, L) Energy: 20keV - 10 MeV Vector magnetic field Electric field
	• Measure and model the nonadiabatic processes that violate all three adiabatic invariants that cause pitch-angle scattering, stochastic energy diffusion and radial diffusion.	• Measure the PSD of energetic electrons during dynamic processes. • Construct displays of the temporal sequence of the PSD vs. L. • Measure high frequency VLF and ELF waves that violate m. • Extend local wave measurements using a global wave distribution model. • Compute average rates of pitch-angle scattering and energy diffusion.	Electron differential flux j(E,α, L) Energy: 20keV - 10 MeV Vector magnetic field Wave electric field Wave magnetic field

LWS Geospace General Objective: **Priority 1: Understand the acceleration, global distribution, and variability of energetic electrons and ions in the inner magnetosphere.**			
Specific Objectives	**Approach**	**Technique**	**Measurement Parameters**
Priority 3: 1.3c: Understand the effects of the ring current and other storm phenomena on radiation belt electrons and ions.	• Understand the ring current effects on those external electric and magnetic fields that cause diffusion of radiation belt particles.	• Measure 3D ring current particle pressure distributions throughout outer zone for storm and non-storm time periods using combined in situ and global measurements. • Measure statistical properties of electric field and magnetic field values and variations throughout outer zone for storm and non-storm time periods. • Model the effectiveness of various frequency bands of measured electric and magnetic field variations in causing radial transport for storm and non-storm time periods. • Correlate the distributions (radial and azimuthal) of the statistical properites of the electric and magnetic fields with the statistical distributions of particle pressures to ascertain the role of the pressure distributions in shielding and/or enhancing the most transport-effective electric and magnetic fields.	Ion differential flux j(E,α, L) with composition Energy: 20-600keV O and H ENA images with composition Energy: 10-400 keV Vector magnetic field Electric field Wave electric field Wave magnetic field
	• Quantify the storm-time wave phenomna affecting the energization of radiation belt particles.	• Measure the electron PSD L-profiles for storm and non-storm conditions. • Analyze PSD profiles to estimate non-adiabatic energization accompanying the radial transport. • Measure spectra of electrostatic and electromagnetic waves throughout outer zone for storm and non-storm time periods. • Correlate non-adiabatic energizations w/ wave properties for storm and non-storm periods to ascertain role of storm-driven waves in modifying characteristics of outer zone electrons.	Electron differential flux j(E,α, L) Energy: 20keV - 10 MeV Pitch angle distribution Vector magnetic field Wave electric field Wave magnetic field
	• Quantify storm- time wave phenomena affecting the loss of radiation belt particles.	• Measure electron PSD L-profiles for storm and non-storm conditions. • Estimate losses by analyzing PSD profiles for storm and non-storm periods. • Measure the losses of electrons using low-altitude polar orbiting spacecraft for storm and non-storm periods. • Measure spectra of electrostatic and electromagnetic waves throughout outer zone for storm and non-storm time periods. • Correlate the estimated and measured losses with wave properties for storm and non-storm periods to ascertain role of storm-driven waves in modifying the characteristics of outer zone electrons.	Electron differential flux j(E,α, L) Energy: 20keV - 10 MeV Vector magnetic field Wave electric field Wave magnetic field

LWS Geospace General Objective: **Priority 1: Understand the acceleration, global distribution, and variability of energetic electrons and ions in the inner magnetosphere.**			
Specific Objectives	**Approach**	**Technique**	**Measurement Parameters**
Priority 4: 1.4a: Understand how and why the ring current and associated phenomena vary during storms.	• Characterize the ring current source plasma to understand the dependencies of storm evolution on internal and external conditions.	• Measure PSD of ring current source for a large number of storms. • Measure PSD and composition of ring current populations for a large number of storms. • Develop storm-time dependent E-field models in ring current and near-tail. • Develop statistical description of ring current source as function of internal & external drivers.	Ion differential flux j(E,α, L) Energy: 20-600keV Electric field
	• Determine ion injection and energization processes during storm development.	•Develop storm-time dependent E-field models for ring current and near-tail region. •Determine injection locations. •Distinguish between convective and in situ energization processes by comparing phase space densities in source and ring current regions. •Determine role of ULF and VLF waves in energizing ring current plasmas.	O and H ENA images 10-400 keV Ion differential flux j(E,α, L) Energy: 20-600keV Electric field Wave electric field Wave magnetic field
	• Measure the global dynamics of the ring current to determine the time history, locus, composition and energy of ring current ions.	• Obtain global temporal and spatial history of ring current populations. • Test for adiabatic processes via phase space density.	O and H ENA images 10-400 keV Ion differential flux j(E,α, L) Energy: 20-600keV Vector magnetic field
	•Differentiate among competing loss processes as a function of time and external solar wind conditions.	• Improve geocoronal models. • Assimilate a global distribution of ion loss and its variability. • Measure ion cyclotron waves in ring current region.	Ion differential flux j(E,α, L) Energy: 20-600keV Vector magnetic field O and H ENA images 10-400 keV Composition
	• Improve models that predict the ring current development and electric and magnetic field dynamics in the inner magnetosphere based on solar wind and solar irradiance conditions.	• Development of self-consistent time -dependent global magnetospheric models with realistic E-fields. • Determine how the asymmetric configuration of the perturbation magnetic field and electric field are modified by the storm-time ring current. • Development of data driven ring current models using self consistent and realistic B and E fields (input to model may include solar wind conditions, particle source populations, local magnetic and electric fields).	Electric field Vector magnetic field
Priority 4: 1.4b: Develop and validate physics-based and specification models of inner belt protons for solar cycle time scales.	• Improve parameterized statistical models of the proton population in the inner magnetosphere including the location and intensity of the South Atlantic Anomaly (SAA) at LEO altitudes.	• Obtain ion PSD profiles as a function of energy and magnetic coordinates for the inner belt region over the course of a solar cycle. • Obtain corresponding ion phase space densities at low-altitudes in the L-shells corresponding to the inner belt. • Develop statistical relationships between the observables and the secularly varying magnetic field. • Develop program to continuously test and update model against new observations.	Ion differential flux j(E,α, L) Energy: 1-400 MeV Vector magnetic field
	• Improve physics-based models of the inner belt to account for secular changes in the global magnetic field.	• Develop techniques to quantitatively map inner belt fluxes to LEO altitudes. • Capture and refine models of neutral exospheric gas densities using existing data. • Develop theoretical models for rate of Coulomb scattering and variability. • Characterize particle lifetimes in terms of ULF spectral properties and stochastic electric and magnetic fields. • Validate models by comparing LEO and inner belt observations for variety of conditions.	n/a

LWS/Geospace General Objective: **Priority 2A: Determine the effects of long and short term variability of the Sun on the global-scale behavior of the ionospheric electron density**			
Specific Objectives	**Approach**	**Technique**	**Measurement Parameters**
Priority 1: 2A.1a: Quantify the relationship between the magnitude and variability of the solar spectral irradiance and the global electron density.	• Directly compare observed changes in the ionosphere with EUV flux (10% accuracy) – time scales of ~1 day to ~11 years.	• Measure the solar EUV spectral irradiance. • Measure ionospheric densities at mid-latitudes during magnetically quiet periods. • Apply statistical correlation methods to ascribe the proportion of ionospheric variability attributable to the EUV source magnitudes and/or spectral changes.	Solar EUV Spectral Irradiance O/N_2 ratio and n_e^2 column density Electron density (height profiles) Electron density (in situ)
	• Validate and improve models of the quiet time ionosphere and thermosphere driven by continuous measurements of solar EUV irradiance and constrained by I & T measurements.	• Measure the solar EUV spectral irradiance. • Measure ionospheric densities at mid-latitudes during magnetically quiet periods. • Compare day-to-day changes in TEC, NmF2 and electron density profiles with physical model predictions using observed EUV flux. • Provide an accurate model for storm studies.	Solar EUV Spectral Irradiance O/N_2 ratio and n_e^2 column density Electron density (height profiles) Electron density (in situ) Neutral density Neutral Temperature Neutral Composition Neutral velocity Ion drift or electric field
	• Evaluate the effects of intense EUV and X-ray solar irradiance events on the IT system - time scales less than a day.	• Identify events with solar observations from SDO. • Measure ionospheric densities at mid-latitudes during magnetically quiet periods. • Compare response of ionosphere and neutral atmosphere during EUV changes. • Compare measured response with those predicted using models driven with solar spectral irradiance.	Solar EUV Spectral Irradiance O/N_2 ratio and n_e^2 column density Electron density (height profiles) Electron density (in situ) Neutral velocity
	• Improve understanding of IT chemistry.	• Experimentally measure poorly known rate constants and cross sections in the lab or calculate from first principles. • Derive necessary reaction rates and collision frequencies from first principles. • Measure all relevant properties in situ, in the photochemical equilibrium region.	n/a

LWS/Geospace General Objective: **Priority 2A: Determine the effects of long and short term variability of the Sun on the global-scale behavior of the ionospheric electron density**			
Specific Objectives	**Approach**	**Technique**	**Measurement Parameters**
Priority 1: 2A.1b: Quantify the effects of geomagnetic storms on the electron density.	• Determine the character and origin of mid-latitude positive IT storms.	• Characterize their longitudinal and/or local time structure and its causes (local vs. transport). • Determine the contribution of local uplift of equatorial ionospheric plasma to mid-latitude positive IT storms. • Determine the causes of local uplift - (internal or external - compare E and neutral wind). • Determine the origin of the associated electric fields and/or neutral winds. • Determine the cause of the prompt response of the ionosphere at mid-latitudes (less than 10 minutes).	Solar EUV Spectral Irradiance O/N_2 ratio and n_e^2 column density Electron density (height profiles) Electron density (in situ) Neutral density Neutral Temperature Neutral Composition Neutral velocity Ion drift or electric field Ring current electric field
	• Determine the character and origin of mid-latitude negative IT storms.	• Characterize and determine the causes of their spatial structure. • Determine the contribution of Joule heating and auroral electron precipitation to changes in neutral composition. • Differentiate the effects of high latitude Joule heating, mid-latitude Joule heating, and circulation on mid-latitude chemistry and electron density. • Determine possible global changes to thermospheric circulation. • Determine the spectrum of scale sizes in the neutral composition that impact the plasma density. • Determine how wind surges are damped and how important are they for ionospheric transport.	Solar EUV Spectral Irradiance O/N_2 ratio and n_e^2 column density Electron density (height profiles) Electron density (in situ) Neutral density Neutral Temperature Neutral Composition Neutral velocity Ion drift or electric field High-latitude FUV imaging Auroral electron precipitation
	• Characterize the temporal evolution of positive and negative IT storms, their relationship with each other and with their drivers.	• Determine the effects of storm-time penetration electric fields on the global ionospheric electron density. • Evaluate the effects of variable global convective flows, enhanced conductivities and ionospheric currents at high latitudes. • Examine the recovery of the thermosphere to its undisturbed state.	Solar EUV Spectral Irradiance O/N_2 ratio and n_e^2 column density Electron density (height profiles) Electron density (in situ) Neutral density Neutral Temperature Neutral Composition Neutral velocity Ion drift or electric field High-latitude FUV imaging Auroral electron precipitation
	• Further develop physics-based IT simulation models.	• Develop assimilation techniques for use in nowcasting and initializing predictive simulations. • Compare simulation predictions with observations (following appropriate initialization and using accurately specified drivers) in order to validate models and provide event characterization.	n/a
Priority 2: 2A.2: Quantify how the interaction between the neutral atmosphere and the ionosphere affects the distribution of ionospheric plasma.	• Determine the dynamical rearrangement of ionospheric plasma that is driven by neutral winds.	• Compare ionospheric wind measurements from in situ satellites with the observed propagation in global images of O/N_2 ratio.	O/N_2 ratio and n_e^2 column density Electron density (height profiles) Electron density (in situ) Ion drift or electric field
	• Determine the rearrangement of ionospheric plasma that is driven by chemical reactions.	• Compare ionospheric density measurements from in situ satellites with that predicted from accurate models that assimilate the global images of O/N_2 ratio.	O/N_2 ratio and n_e^2 column density Electron density (height profiles) Electron density (in situ)
Priority 3: 2A.3: Discover the origin and nature of propagating disturbances in the ionosphere.	• Determine the climatology and drivers of propagating disturbances in the ionosphere.	• Determine the existence and properties of propagating disturbances from global images of the O/N_2 ratio. • Distinguish the propagating disturbances from their phase velocity and horizontal wavelength as well as their waveform. • Verify existence of propagating disturbances with in situ satellite and ground-based measurements.	O/N_2 ratio and n_e^2 column density Electron density (height profiles) Electron density (in situ) Ion drift or electric field High latitude FUV imaging

LWS Geospace General Objective: **Priority 2B: Determine the solar and geospace causes of small scale ionospheric density irregularities in the 100 km to 1000 altitude range.**			
Specific Objectives	**Approach**	**Technique**	**Measurement Parameters**
Priority 1: 2B.1: Characterize and understand the origin and evolution of newly-discovered storm-time midlatitude ionospheric irregularities.	• Understand the context in which midlatitude ionospheric irregularities develop.	• Characterize ionospheric and thermospheric dynamics as functions of latitude, local time, and longitude, at large and small scales; emphasize the regions of large gradients in ionospheric density. • Distinguish between dynamical conditions in absence and presence of storms. • Determine the storm-time electric field configurations necessary to generate irregularities.	Ion drift or electric field n_e gradients n_e amplitude fluctuations electric field fluctuations
	• Characterize when and how mid-latitude ionospheric irregularities develop.	• Assemble and characterize ground and space based measurements of ionospheric irregularities. • Characterize irregularities by their intensity, duration and occurence rate. • Measure in-orbit scintillations • Describe irregularities by their relationship to the background.	Ion drift or electric field n_e gradients n_e amplitude fluctuations electric field fluctuations in-orbit scintillations
	• Develop assimilative models of the midlatitude storm-time ionosphere; validate using data.	• Establish coherence lengths at all local times by examining the variation with longitude. • Develop assimilative model of the I/T that include the storm-time drivers of midlatitude irregularities. • Develop theories that can predict the onset, spectrum, and time dependence of midlatitude irregularities from a knowledge of the ionospheric and magnetospheric states.	Ion drift or electric field n_e gradients n_e amplitude fluctuations electric field fluctuations
Priority 2: 2B.2a: Understand the conditions leading to the formation of equatorial spread-F irregularities, and their location, magnetitude, and spatial and temporal evolution.	• Understand the context in which equatorial spread-F and associated ionospheric depletions develop.	• Characterize ionospheric and thermospheric dynamics as functions of local time and longitude, at large and small scales. • Distinguish between dynamical conditions in absence and presence of structures. • Characterize penetrating electric fields	Thermospheric neutral winds Ion drift or electric field
	• Characterize the ionospheric depletions.	• Assemble and characterize ground and space based measurements of ionospheric depletions, spread-F, and scintillation. • Establish coherence scales at different local times by examining persistence in longitude. • Determine coherence scales as a function of local time and longitude. • Characterize depletion regions by intensity, duration and periodicity. • Describe depletion motions and their relationship to the background.	Ion drift or electric field n_e gradients n_e amplitude fluctuations electric field fluctuations in-orbit scintillations Thermospheric neutral winds
	• Develop assimilative models and validate using data.	• Develop global I-T models that include formation of spread-F and compare with measurements. • Develop theories that predict the spectrum of irregularities produced by different forms of spread-F, including their spation andd temporal evolution and cross-scale coupling, and compare to observations.	n/a
2B.2b: Understand the conditions leading to the formation of polar patches and their high latitude irregularities.	• Investigate smooth flow and transient flow of plasma flux tubes and cusp precipitation as competing processes for formation of polar cap patches with enhanced F-region plasma density; establish solar EUV control of plasma density in patches.	• Measure the solar spectral irradiance that drives the polar ionosphere and the properties of the polar ionosphere and neutral atmosphere. • Measure solar wind, interplanetary magnetic field and their variations to establish the role of magnetic reconnection in polar cap patch formation. • Measure flow patterns of plasma and flux tubes in the polar cusp region associated with transiting polar cap patches. • Model smooth flow patch formation with a tongue of ionization and large flows; model patch formation by transient (~min) flows; model patches from cusp precipitation; model patch trajectories; compare models.	Solar EUV spectral irradiance Ion drift or electric field
	• Investigate plasma structuring in polar cap patches and asses effects on communication and navigation systems in the polar region.	• Run 3-dimensional plasma instability models to characterize plasma density and electric field structures in patches. • Validate model with scintillation and range error measurements.	n/a
Priority 3: 2B.3: Enable prediction of the onset, location, and development of high latitude E-region irregularities.	•Develop assimilative models and validate using data.	• Develop global models of the I/T that provide accurate scenarios to use in studying high-latitude sporadic E irregularities.	n/a

LWS Geospace General Objective:
Priority 3A: Determine the effects of solar and geospace variability on the atmosphere enabling an improved specification of the neutral density in the thermosphere.

Specific Objectives	Approach	Technique	Measurement Parameters
Priority 1: 3A.1a: Determine the variability in the neutral atmosphere attributable to the solar EUV spectral irradiance.	• Directly compare observed changes in the thermosphere with EUV flux (10% accuracy) – time scales of ~1 day to ~11 years.	• Measure the solar EUV spectral irradiance. • Measure thermospheric densities at mid-latitudes during magnetically quiet periods. • Apply statistical correlation methods to ascribe the proportion of thermospheric variability attributable to the EUV source magnitudes and/or spectral changes.	Solar EUV Spectral Irradiance O/N2 ratio and ne2 column density Electron density (height profiles Electron density (in situ)
	• Validate and improve models of the Thermosphere driven by continuous measurements of solar EUV irradiance and constrained by I & T measurements.	• Measure the solar EUV spectral irradiance. • Measure thermospheric densities at mid-latitudes during magnetically quiet periods. • Compare day-to-day changes in neutral atmosphere parameters with physical model predictions using observed EUV flux.	Solar EUV Spectral Irradiance O/N_2 ratio and n_e^2 column density Neutral density Neutral temperature Neutral composition Neutral velocity Ion drift or electric field
	• Evaluate the effects of intense EUV and X-ray solar irradiance events on the thermosphere - time scales less than a day.	• Identify events with solar observations from SDO. • Measure thermospheric properties at mid-latitudes during magnetically quiet periods. • Compare measured response with those predicted using models driven with solar spectral irradiance.	Solar EUV Spectral Irradiance O/N_2 ratio and n_e^2 column density Neutral density Neutral temperature Neutral composition Neutral velocity Ion drift or electric field
	• Improve understanding of IT chemistry	• Experimentally measure poorly known rate constants and cross sections in the lab or calculate from first principles. • Derive necessary reaction rates and collision frequencies from first principles. • Measure all relevant properties in situ, in the photochemical equilibrium region.	n/a
Priority 1: 3A.1b: Determine the variability in the neutral atmosphere attributable to magnetospheric inputs.	• Determine the effects of mid-latitude positive and negative storms on the thermosphere.	• Characterize their longitudinal and/or local time structure and its causes (local vs. transport). • Determine the contribution of local uplift of equatorial ionospheric plasma to changes in the mid-latitude thermosphere. • Determine the cause of the prompt response of the thermosphere at mid-latitudes (less than 10 minutes).	O/N_2 ratio and n_e^2 column density Neutral density Neutral temperature Neutral composition Neutral velocity Electron density (height profiles Electron density (in situ) Ion drift or electric field
	• Determine the effects on the thermosphere of magnetospheric inputs in the auroral and polar cap regions.	• Determine the contribution of Joule heating and auroral electron precipitation to changes in neutral composition. • Differentiate the effects of high latitude Joule heating, mid-latitude Joule heating, and circulation on mid-latitude chemistry and neutral parameters. • Determine possible global changes to thermospheric circulation. • Determine the spectrum of scale sizes in the neutral composition that impact the plasma density. • Determine how wind surges are damped and how important are they for thermospheric transport.	O/N_2 ratio and n_e^2 column density Magnetic field (currents) Neutral density Neutral temperature Neutral composition Neutral velocity Ion drift or electric field High-latitude FUV imaging Auroral electron precipitation
	• Further develop physics-based IT simulation models.	• Develop assimilation techniques for use in nowcasting and initializing predictive simulations. • Compare simulation predictions with observations (following appropriate initialization and using accurately specified drivers) in order to validate models and provide event characterization.	O/N_2 ratio and n_e^2 column density Neutral density Neutral temperature Neutral composition Neutral velocity Ion drift or electric field

LWS Geospace General Objective: **Priority 3A: Determine the effects of solar and geospace variability on the atmosphere enabling an improved specification of the neutral density in the thermosphere.**			
Specific Objectives	**Approach**	**Technique**	**Measurement Parameters**
Priority 2: 3A.2: Determine the variability in the neutral atmosphere attributable to internal processes.	• Determine the effects of plasma temperature and composition on the neutral atmosphere. • Quantify the effects of ion-neutral chemistry on the thermosphere.	• Determine the existence and properties of propagating disturbances from global images of the O/N_2 ratio.	O/N_2 ratio and n_e^2 column density Neutral density Neutral temperature Neutral composition Neutral velocity
Priority 3: 3A.3: Determine the variability in the neutral atmosphere attributable to atmospheric waves from below.	• Determine the energy that is transported into the thermosphere from below.	• Compare thermospheric wind measurements from in situ satellites with the observed propagation in global images of O/N_2 ratio.	O/N_2 ratio and n_e^2 column density Neutral density Neutral temperature Neutral composition Neutral velocity
	• Determine the chemical rearrangement of thermospheric material affected by the transport of material from below.	• Compare thermospheric measurements from in situ satellites with that predicted from accurate models that assimilate the global images of O/N_2 ratio and account for changes in catalytic compounds such as HOx, NOx, and NOy.	O/N_2 ratio and n_e^2 column density Neutral density Neutral temperature Neutral composition Neutral velocity

Assumed from other programs.

General Objective	Assumed from Other Programs
Priority 1: Dynamics of energetic electrons	Solar wind B, v, and n (1 min. res.)
	B, v, and n of solar wind shock (30 sec. resolution)
	Electron phase space densities in magnetosphere L < 10
	Prior satellite and ground wave data
	Ion and electron particle distributions from GEO and STP missions as available
	Global distribution of ULF waves from ground-based magnetometers
	Inner belt ion phase space densities as available
	SAA mapping from NPOESS
	Solar EUV fluxes
	AE, Dst indices
	Global model of electron density to calculate resonant energies
	Dynamics models of magnetospheric variability during storm conditions
	International Geophysical Reference Field (IGRF) updated
	Empirical geoelectric field models
	Ring current models with plasmaspheric boundary conditions
	LWS theory and modeling to derive scattering rates
Priority 2A: Effects of solar variability on global ionospheric electron density	Solar spectral irradiance
	Ground-based dual-frequency GPS measurements
	Ground-based incoherent scatter radar data
	Limb profiles of O and N_2
	SuperDARN convection maps
	Auroral boundary conditions from magnetospheric inputs
	Solar wind B, v, and n (1 min. res.)
	GEC data
	DMSP/NPOES polar cap data
	Specification of thermosphere
	High-latitude FUV images
	Mesopause energy input
	GPS TEC distributions
Priority 2B: Solar and Geospace causes of irregularities	Solar spectral irradiance
	Solar wind B, v, and n (1 min. res.)
	GPS TEC distributions
	Radio wave scintillations
	Low-latitude irregularity measurements from CNOFS
Priority 3A: Effects of solar variability on the neutral atmosphere	Solar spectral irradiance
	Solar wind B, v, and n (1 min. res.)
	Ground-based incoherent scatter radar data
	Auroral boundary conditions from magnetospheric inputs
	Laboratory measurements of cross sections and rate constants

APPENDIX 2.
FEASIBILITY STUDIES OF NOTIONAL CORE RADIATION BELT STORM PROBES, IONOSPHERE-THERMOSPHERE STORM PROBES, AND HIGH-LATITUDE IMAGING PLATFORM

Radiation Belt Storm Probes

Mission Summary

Core Radiation Belt Storm Probes will consist of two spacecraft in nearly identical, highly elliptical orbits. The primary spacecraft will carry the full instrument package, while the secondary spacecraft will host a reduced instrument suite that excludes the fields and waves instruments. The orbits are designed such that the smaller of the two spacecraft completes approximately one "lap" with respect to the larger one every year. This approach enables the spacecraft to evaluate many spatial scales over the course of the mission. A 12° inclined, 500 × 30,600 km altitude orbit is depicted in **Figure 2-1.**

The two spacecraft can be launched together on a single Taurus launch vehicle on a mission originating from the Kwajalein Atoll, which is part of the Marshall Islands in the Pacific Ocean. The slight difference in the two orbits is achieved by the relative velocity imparted by the springs used to separate the spacecraft from the launch vehicle.

The objectives of the Geospace mission drive a desire for a long-life mission; however, the selected orbit imposes a harsh radiation environment on the spacecraft. **Figure 2-2** shows the dose-depth curve for a variety of mission durations.

Based upon the high shielding requirements, a mission life of 2 years has been selected. In case the environmental prediction is overly pessimistic, the satellites carry 5 years of consumable items in order to maximize the potential for an extended mission. In an effort to constrain development costs, the spacecraft uses a 100-krad radiation design level. This implies a total shielding requirement of about 625 mils of aluminum. In general, the spacecraft body and other components provide 100 to 125 mils of shielding, but this still leaves electronics units with half-inch (1.3-cm) wall thicknesses. This high shielding mass is a significant spacecraft design driver. The 100-krad total dose requirement is also a spacecraft cost driver.

Radiation Belt Spacecraft Summary

The design of the two radiation belt science spacecraft is driven by the instrument and mission requirements. The key mission requirements are summarized in **Table 2-1.** Since the instrument suite is different for the two spacecraft, different

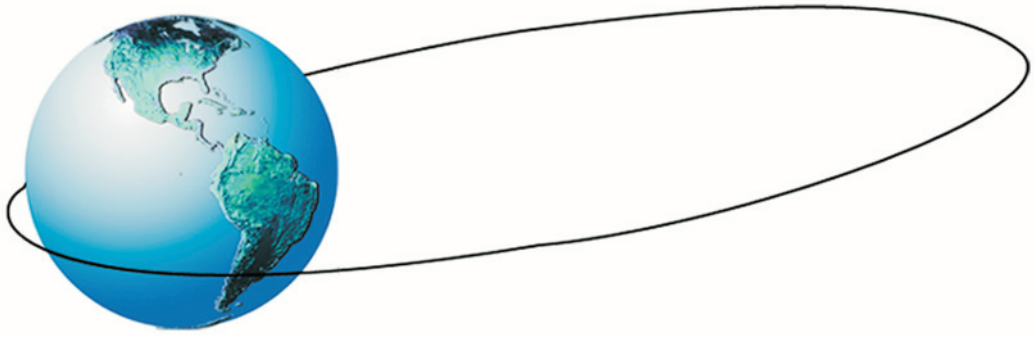

Figure 2-1. Radiation belt science element orbit.

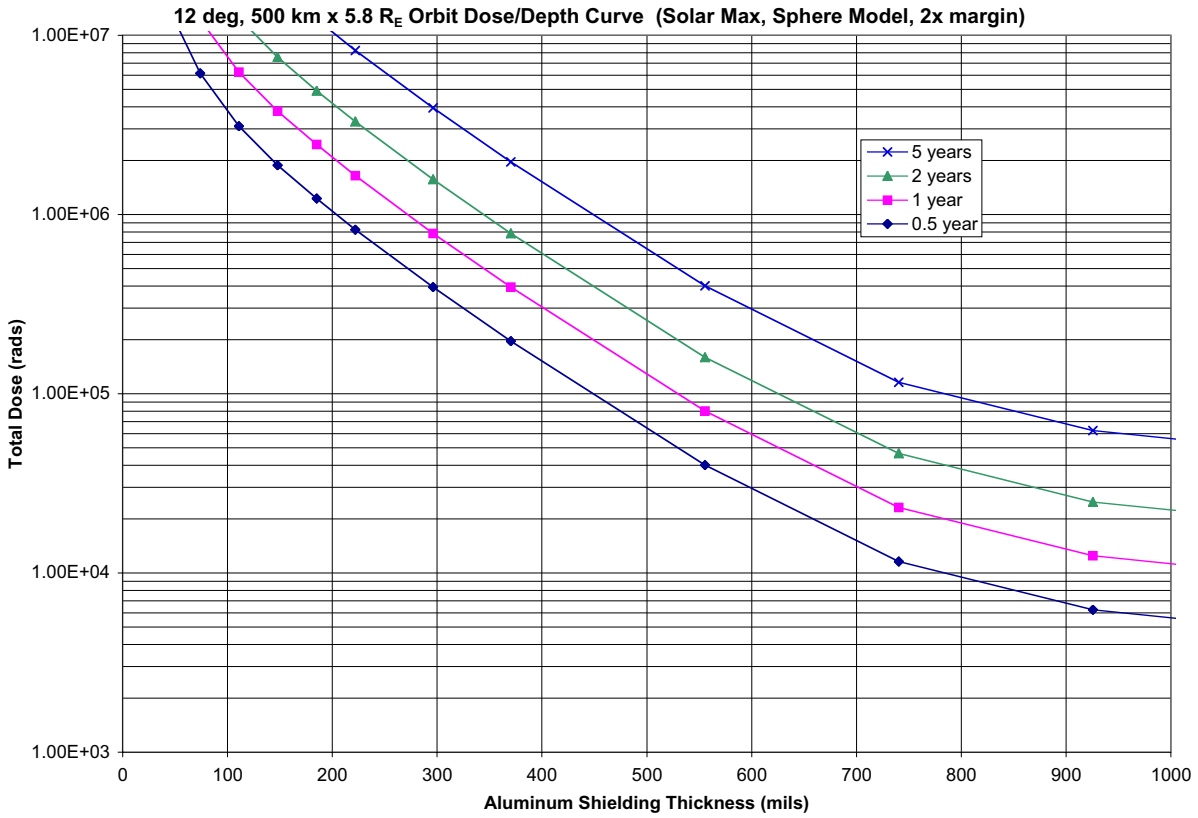

Figure 2-2. Radiation belt satellite dose-depth curves for various mission durations

designs are produced for each satellite. However, in Phase A, a trade study will be conducted to determine whether it is more cost-effective to build two identical spacecraft or to build one spacecraft with the full instrument suite and one with a reduced instrument suite.

The instrument accommodation requirements are summarized in **Tables 2-2** and **2-3**. Instrument performance parameters reflect typical values for the selected instruments based upon similar instruments flown on previous missions.

Attitude Control: The attitude control system (ACS) is driven by the need to be spin-stabilized with the spin axis pointed within 15° of the Sun. The attitude control requirement is largely met by the gyroscopic stiffness of the

Table 2-1. Key radiation belt mission requirements.

Parameter	Value	Driver
Mission life	2 yr, 5 yr expendables	Radiation shielding
Orbit	500 × 30,600 cm <18° inc., 12° goal "chasing" orbits	Magnetic L-shell coverage Particle distribution measurements
Orientation	Spinner Spin axis <15° from Sun Spin rate about 5 rpm	Simplify solar array design *E*-field measurements need even lighting on two sensors
Attitude knowledge	1°, 0.3° goal, 3σ	Flux gate magnetometer Search coil magnetometer
Attitude control	2°, 3σ	Spin axis <15° from Sun
Cleanliness	Magnetically clean Electromagnetically clean	Magnetometers Search coil magnetometer

Table 2-2. Instrument accommodation requirements for primary radiation belt spacecraft.

	Mass	Power	Data Rate	
			Burst	Normal
	kg	W	kbps	kbps
Instrument package	42.8	17.6	42.1	4.6
Radiation shielding	6.5			
Margin	14.7	8.8		
Primary S/C Total	**64.0**	**26.4**	**42.1**	**4.6**

Table 2-3. Instrument accommodation requirements for secondary radiation belt spacecraft.

	Mass	Power	Data Rate	
			Burst	Normal
	kg	W	kbps	kbps
Instrument package	11.2	8.1	20.1	1.3
Radiation shielding	3.3			
Margin	4.2	4.1		
Secondary S/C Total	**18.7**	**12.2**	**20.1**	**1.3**

spacecraft. The spacecraft must be rotated about 1° per day to keep the spin axis pointed toward the Sun. This is performed using torque rods near perigee where the Earth's magnetic field is the strongest. The ACS includes a passive nutation damper to minimize wobble.

A fine Sun sensor mounted on the Sun-facing spacecraft disk provides primary attitude knowledge. By keeping the spin axis slightly off the center of the Sun, the Sun sensor can also be used to gauge the spin rate. A horizon crossing indicator (HCI), mounted normal to the spin axis, provides yaw knowledge. A Kalman filter takes over this function when the HCI does not see the Earth. A coarse Sun sensor suite and magnetometer are provided for contingency operations.

Mechanical: Due to the spin-stabilization and the need to launch both spacecraft on a single launch vehicle, the satellites are designed as flattened cylinders. The primary spacecraft is on the bottom of the launch stack with the secondary satellite affixed to it. Separation hardware is mounted between them.

The spacecraft mass is driven by the high levels of radiation shielding required for the spacecraft and instrument electronics. The mass budget for the two spacecraft is shown in **Tables 2-4** and **2-5**. The subsystem masses in the table include all shielding mass and indicated margins. The selected margins are commensurate with the conceptual nature of the design.

Power: Spacecraft power is supplied by Sun-facing body-mounted solar cells. The primary spacecraft requires 1.0 m^2 of cell area, while the secondary spacecraft needs just 0.8 m^2. Both can easily fit within the available area. Some additional cells are placed on the anti-sun side and cylinder to provide power in an attitude emergency.

Table 2-4. Primary radiation belt spacecraft mass and power budgets.

	Mass		Power	
	Mass	Margin	Power	Margin
	kg	%	W	%
Instruments	64.0	30.0	26.4	50.0
Structure	40.0	23.6		
Attitude control	28.5	20.0	21.7	20.0
Power	33.1	20.0	14.4	20.0
Thermal	9.4	23.6	22.5	50.0
C&DH	41.6	20.0	36.0	20.0
Harness	18.8	23.6	2.4	30.6
Subtotal	235.5	23.6	123.5	30.6
Reserve	23.5	10.0	12.3	10.0
Total	**259.0**	**36.0**	**135.8**	**43.6**

Table 2-5. Secondary radiation belt spacecraft mass and power budgets.

	Mass		Power	
	Mass	Margin	Power	Margin
	kg	%	W	%
Instruments	18.7	30.0	12.2	50.0
Structure	24.9	26.5		
Attitude control	24.3	20.0	19.3	20.0
Power	24.2	20.0	9.6	20.0
Thermal	5.9	26.5	18.0	50.0
C&DH	36.8	20.0	27.0	20.0
Harness	11.7	26.5	1.7	29.0
Subtotal	146.4	26.5	87.8	29.0
Reserve	14.6	10.0	8.8	10.0
Total	**161.1**	**33.5**	**96.6**	**42.0**

The highly elliptical orbit will frequently avoid eclipses entirely; however, the worst-case eclipse lasts nearly 2 hours. The spacecraft carry lithium-ion batteries to provide power during this period. Batteries of 16.4 A-hr and 11.7 A-hr can meet this need with a maximum depth of discharge of 65%. Most eclipses will be significantly shorter, so the typical depth of discharge will be much smaller.

Command and Data Handling (C&DH): The C&DH subsystem is driven by the instrument and spacecraft data throughput requirements. The data budgets for the two spacecraft are provided in **Table 2-6 a**nd **2-7**. The two spacecraft generate 916 Mb and 305 Mb per day. The solid-state recorders are sized to hold at least two days of science and housekeeping data.

The downlink rate is limited by the communications geometry. Since the spacecraft is spinning with its spin axis toward the Sun, the relative position of the ground station can be at any angle in spacecraft coordinates. Therefore, the communications system must be capable of closing the uplink and downlink over most of a full sphere.

Table 2-6. Primary radiation belt spacecraft data budget.

	Burst		Normal		Avg.	Com-	Net
	Rate	Duty	Rate	Duty	Rate	press.	Avg.
	kbps	%	kbps	%	kbps	Factor	kbps
Instruments	42.1	10	4.9	90	7.7	0.75	6.1
Spacecraft bus			1.0	100	1.0	1.0	1.0
Data required					8.7	0.8	7.1
Margin						30%	2.1
Subtotal							9.2
Pkt. overhead						15%	1.4
Total Average Rate							**10.6**
Daily Data Volume (Mb)							**916**

Table 2-7. Secondary radiation belt spacecraft data budget

	Burst		Normal		Avg.	Com-	Net
	Rate	Duty	Rate	Duty	Rate	press.	Avg.
	kbps	%	kbps	%	kbps	Factor	kbps
Instruments	21.1	10	1.6	90	3.2	0.6	1.9
Spacecraft bus			0.5	100	0.5	1.0	0.5
Data required					3.7	0.6	2.4
Margin						30%	0.7
Subtotal							3.1
Pkt. overhead						15%	0.5
Total Average Rate							**3.5**
Daily Data Volume (Mb)							**305**

The S-band communication system uses circularly polarized quadrifilar or patch antennas on the two spacecraft disks. In order to maximize the data rate, the spacecraft uses a switch to direct the transmitter output to the antenna with the better view of the ground station. Together, these antennas provide coverage in excess of 90% of 4π steradians. The primary spacecraft uses a 9-W transmitter to achieve a 250 kbps downlink, while the secondary spacecraft uses a 5-W transmitter to achieve a 140 kbps downlink rate. Both links have a worst-case margin in excess of 3 dB assuming a 13-m ground antenna at a 10° elevation angle.

With these data rates, it takes 61 min/day to downlink data from the primary spacecraft. Only 36 min/day is needed for the secondary spacecraft. It is anticipated that data will be downlinked during two daily passes approximately 12 hours apart. Keeping the downlink time short simplifies ground station scheduling. However, the spacecraft are capable of operating with just one longer pass per day.

Ionosphere-Thermosphere Storm Probes

Mission Summary

The Core Ionosphere-Thermosphere Storm Probes will consist of two identical spacecraft in circular low Earth orbits (LEO), inclined at 60° to the equator and separated by 10° to 20° in mean local time (MLT). The nominal orbit altitude is 450 km, although the spacecraft are allowed to descend to 400 km before being reboosted. The orbits are depicted in **Figure 2-3.**

The two spacecraft are launched together on a single Taurus launch vehicle on a mission originating from Vandenberg Air Force Base. The

Figure 2-3. Ionosphere-thermosphere science element orbit.

orbit separation is achieved by immediately reducing the altitude of one spacecraft to 400 km. This causes the two orbits to drift with respect to one another. A 10° separation is achieved in slightly more than 3 months. After the desired separation is achieved, the lower spacecraft is returned to a 450 km altitude.

Since one of the key objectives of the Geospace mission is to improve ionosphere-thermosphere modeling and prediction, long-duration observations are highly desirable. The selected orbits are subject to two life-limiting elements, propellant and cost. The 400- to 450-km orbit has relatively high atmospheric density, especially at solar maximum. As a result, the drag is constantly lowering the satellite orbit. The spacecraft carries a propulsion system to periodically return the spacecraft to its target orbit. Cost is also an important factor. Aside from the obvious operations costs, long-duration mission life dictates that the spacecraft be highly reliable. Due to cost constraints, it is expected that the Geospace spacecraft will be largely single-string. Therefore, a design life of 3 years is the best that can be reasonably expected.

Ionosphere-Thermosphere Spacecraft Summary

The design of the two ionosphere-thermosphere science spacecraft is driven by the instrument and mission requirements. The key mission requirements are summarized in **Table 2-8.**

The instrument accommodation requirements are summarized in **Table 2-9.** Instrument performance parameters reflect typical values for the selected instruments based upon similar instruments flown on previous missions.

Attitude Control: The instruments dictate that the spacecraft be flown with a fixed attitude in the local level frame. Since the spacecraft is not required to be agile, a pitch momentum bias is used. A single momentum wheel provides a large momentum to minimize the disturbance torques. Torque rods are used for momentum dumping and attitude adjustments. This control suite easily meets the 3° pointing requirement.

The attitude knowledge requirement of 0.3° is somewhat more challenging. A 2-axis staring Earth sensor provides a continuous assessment of the pitch and roll angles. Yaw knowledge is provided by a set of Sun sensors. A gyro maintains yaw knowledge when the Sun is not in the field of view of the Sun sensors.

Table 2-8. Key ionosphere-thermosphere mission requirements.

Parameter	Value	Driver
Mission Life	3 yr, 5 yr expendables	Propellant, cost
Orbit	450 km circular; 60° inclination; 10° MLT separation	In situ measurements
Orientation	Nadir, fixed yaw	In situ measurements in ram direction
Attitude knowledge	0.3° 3σ	Neutral wind measurements
Attitude control	3°, 3σ	
Cleanliness	Electrically clean ram face	Plasma measurements

Table 2-9. Instrument accommodation requirements for ionosphere-thermosphere spacecraft.

	Mass	Power	Data Rate	
			Burst	Normal
	kg	W	kbps	kbps
Instrument package	18.5	32.8	19.5	10.5
Margin	5.6	16.4		
Total	**24.1**	**49.2**	**19.5**	**10.5**

Mechanical: The mechanical design of the spacecraft is driven by the desire to minimize drag and the need to mount both spacecraft on a single launch vehicle. Also, by keeping the spacecraft center of mass ahead of the center of pressure, the spacecraft is passively stable with respect to the atmospheric disturbances. This simplifies the ACS design and reduces the frequency of momentum dumping. The spacecraft mass budget is presented in **Table 2-10.** The margin embedded in the each subsystem is also provided.

Power: The fixed spacecraft attitude creates a challenging solar array configuration problem. At an inclination of 60°, the Sun beta angle—the angle between the Sun and the orbit plane—can vary from –83.5° to +83.5°. Since the spacecraft is not free to rotate, it must be capable of generating power from a wide range of solar geometries. Based upon the instrument package used for the study, the solution uses deployed panels driven by a one-axis solar array drive. Each of the two panels is approximately 1.5 m^2 in area. During eclipse, the arrays are "feathered" to minimize drag. Since the panels are a significant contributor to spacecraft drag, triple-junction gallium arsenide cells are used to minimize the required area. A fixed-array configuration is feasible, but it will require significantly more array area and/or power management.

Table 2-10. Ionosphere-thermosphere spacecraft mass and power budgets.

	Mass		Power	
	Mass	Margin	Power	Margin
	kg	%	W	%
Instruments	24.1	30	49.2	50
Structure	30.5	22		
Attitude control	32.8	20	63.5	20
Power	34.7	20	20.4	20
Thermal	7.2	22	37.5	50
C&DH	21.6	20	31.2	20
Harness	14.4	22	4.1	31
Propulsion	14.3	20	1.2	20
Subtotal	179.4	21.8	207.0	31.2
Reserve	17.9	10	20.7	10
Total (Dry)	**197.3**	**33.9**	**227.7**	**44.3**
Propellant	16.0			
Total (Wet)	**213.3**			

Command and Data Handling: The C&DH subsystem is driven by the instrument and spacecraft data throughput requirements. The data budget is provided in **Table 2-11.** The spacecraft generates 1.6 Gb per day. The solid-state recorders are sized to hold at least 2 days of science and housekeeping data.

The data are downlinked using an S-band communications link with a data rate of 2 Mbps. At this rate, one day's data can be transmitted in about 13 minutes, suggesting an operations plan consisting of two daily passes about 12 hours apart.

The fixed spacecraft attitude and low orbit altitude permit a straightforward communications subsystem design. The system includes patch antennas on the nadir and zenith spacecraft faces. Together, these provide better than 90% of 4π steradian coverage. Even with the spacecraft transmitting over the full sphere, the downlink has a 5.9 dB margin to a 5-m ground antenna at a 10° elevation angle.

Table 2-11. Ionosphere-thermosphere spacecraft data budget.

	Burst		Normal		Avg. Rate	Compress.	Net Avg.
	Rate	Duty	Rate	Duty			
	kbps	%	kbps	%	kbps	Factor	kbps
Instruments	19.5	10	10.5	90	11.4	1.0	11.4
Spacecraft bus			1.0	100	1.0	1.0	1.0
Data required					12.4	1.0	12.4
Margin						30%	3.7
Subtotal							16.1
Pkt. overhead						15%	2.4
Total Average Rate							**18.5**
Daily Data Volume (Mb)							**1602**

Propulsion: The spacecraft uses a monopropellant hydrazine blowdown system to compensate for launch vehicle injection errors and spacecraft drag. The ΔV budget allocates 17 m/s for the former purpose and 21 m/s per year for the latter. Since the spacecraft must carry 5 years' worth of fuel, the ΔV requirement is 159 m/s.

The hydrazine system consists of a single tank and four thrusters. The four thrusters are mounted at the points of a square encircling the spacecraft center of mass. The thrusters are canted slightly from the spacecraft velocity vector to enable three-axis control.

High-Latitude Imaging Platform

Mission Summary

A proposed circular polar imaging spacecraft is intended to operate in a polar or near-polar circular orbit with a radius of 9 R_E. The spacecraft could be launched to an elliptical orbit by a Delta II 2326 originating from Vandenberg Air Force Base. The spacecraft uses a STAR-24 solid rocket motor to circularize the orbit. The final orbit is shown, to scale, in **Figure 2-4.**

Figure 2-4. Circular polar orbit for high-latitude imaging.

The mission team performed a trade study between a circular and elliptical orbits. The science preference was for a circular orbit due to the better overall viewing time and geographic diversity. The study showed that the elliptical and circular orbiters were approximately the same cost. This somewhat counterintuitive result came from the fact that the higher launch and deployment costs for the circular imager were offset by the higher bus cost for the elliptical imager. The higher bus cost resulted from the harsh radiation environment of the elliptical orbit.

High-Latitude Imaging Spacecraft Summary

The drivers for the circular polar imager are the key mission requirements summarized in **Table 2-12**. The instrument accommodation requirements are summarized in **Table 2-13.** The instrument suite includes a data processing unit that is shared by the imagers.

Attitude Control: The design driver for the attitude control system is the 0.06° attitude knowledge requirement. This pushes the system to use two star trackers and a high-precision gyro. Coarse Sun sensors and a magnetometer are used for contingency operation.

Table 2-12. Key mission requirements for the high-latitude imaging spacecraft.

Parameter	Value	Driver
Mission life	2 yr, 5 yr expendables	Cost
Orbit	9 R_E circular 70-110° inclination	ENA; FUV
Orientation	Nadir	Earth imaging
Attitude knowledge	0.06° 3σ	FUV
Attitude control	1.0°, 3σ	

Table 2-13. Instrument accommodation requirements for the high-latitude imaging spacecraft.

	Mass	Power	Data Rate	
			Burst	Normal
	kg	W	kbps	kbps
Instrument package	25.6	25.1	n/a	31.2
Data proc. unit	7.0	10.0	n/a	n/a
Subtotal	32.6	35.1	n/a	31.2
Margin	9.8	17.6		
Total	**42.4**	**52.7**	**n/a**	**31.2**

The nadir-pointing attitude is maintained by a 3-axis stabilized, pitch momentum bias attitude control system. This approach provides excellent stability and disturbance rejection. A small cold-gas propulsion system is included to provide attitude corrections.

Mechanical: The mission requirements provide few first-order drivers for the spacecraft mechanical systems. An optical bench is used to provide precise control of the instrument pointing. Other mechanical requirements are derived from the instruments and other spacecraft subsystems. The spacecraft mass and power budgets are presented in **Table 2-14**. The margin embedded in the each subsystem is also provided.

Power: The solar array configuration attempts to balance the competing desires of minimal disturbance and minimum cost. The selected approach uses a single-axis array drive. When the Sun vector is less than 36° from the orbit plane, the spacecraft is oriented with the array axis of rotation normal to the orbit plane. The arrays rotate slowly to track the Sun as the spacecraft progresses around the orbit. When the Sun is greater than 36° from the orbit plane, the spacecraft is oriented such that the array axis of rotation is parallel to the velocity vector. In this case, array motion is more limited since in this orientation the Sun stays on one-half of the spacecraft. Although it is not ideal to have moving components on an imaging spacecraft, the impact is very limited. The orbit period is more than 1.5 days, so in the worst case, the arrays must rotate only 10° per hour. In addition, the arrays are quite small—only 1.4 m^2 total panel area.

In such a high orbit, eclipses are very infrequent. A 20 A-hr lithium-ion battery is sufficient to power the spacecraft during the worst-case 80-minute eclipse.

Command and Data Handling: Imaging missions typically require high data throughput. A circular polar imager is no exception. The data budget is provided in **Table 2-15**. The spacecraft generates more than 4 Gb per day. The solid-state recorders are sized to hold at least 2 days of science and housekeeping data.

Since the spacecraft is always nadir pointing, a large antenna can be mounted on the nadir face to compensate for the high orbit altitude. Using a 0.6-m medium-gain antenna and 10-m ground antenna, the spacecraft can support a 2-Mbps S-band downlink with 3.6-dB margin. At this rate, 1 day of data can be downlinked in 35 minutes.

Table 2-14. High-latitude imaging spacecraft mass and power budgets.

	Mass		Power	
	Mass	**Margin**	**Power**	**Margin**
	kg	%	W	%
Instruments	42.4	30.0	52.7	50.0
Structure	48.7	23.1		
Attitude control	22.9	20.0	78.1	20.0
Power	29.1	20.0	18.0	20.0
Thermal	7.1	23.1	30.0	50.0
C&DH	24.4	20.0	31.2	20.0
Harness	14.2	23.1	4.2	30.2
Propulsion	13.9	20.0	1.2	20.0
Subtotal	202.8	23.1	215.4	30.2
Reserve	20.3	10.0	21.5	10.0
Total (Dry)	**223.1**	**35.4**	**236.9**	**43.2**
Propellant	1.8			
Total (Wet)	**224.9**			
Kick motor	218.2			
Total (Launch)	**443.0**			

Table 2-15. High-latitude imaging spacecraft data budget.

	Burst		Normal		Avg. Rate	Compress.	Net Avg.
	Rate	**Duty**	**Rate**	**Duty**			
	kbps	%	kbps	%	kbps	**Factor**	kbps
Instruments	3.5	10	31.2	100	31.2	1.0	31.2
Spacecraft bus			1.0	100	1.0	1.0	1.0
Data required					32.2	1.0	32.2
Margin						30%	9.7
Subtotal							41.9
Pkt. overhead						15%	6.3
Total Average Rate							**48.1**
Daily Data Volume (Mb)							**4159**

The spacecraft uplink and contingency downlink use a pair of patch or quadrifilar helix antennas on the zenith and nadir faces. This provides better than 90% coverage. The contingency downlink rate of 2 kbps provides a link margin in excess of 12 dB to a 10-m ground antenna.

Propulsion: The cold-gas propulsion system consists of a single high-pressure tank and six thrusters. The thrusters are mounted far away from the center of mass, aligned with each of the positive and negative spacecraft axes. The thrusters are used exclusively for attitude control.

(BLANK)

APPENDIX 3.
SELECTED REFERENCES

I. Radiation Belts

Abel, B., and R. M. Thorne, Electron scattering loss in Earth's inner magnetosphere, 1, Dominant physical processes, *J. Geophys. Res., 103*, 2385, 1998.

Baker, D. N., Magnetic reconnection during magnetospheric substorms, in *Substorms 3*, ESA SP-339, 365, 1996.

Brautigam, D. H., and J. M. Albert, Radial diffusion analysis of outer radiation belt electrons during the October 9, 1990, magnetic storm, *J. Geophys. Res., 105*, 291, 2000.

Elkington, S. R., M. K. Hudson, and A. A. Chan, Resonant acceleration and diffusion of outer zone electrons in an asymmetric geomagnetic field, *J. Geophys. Res.*, submitted, 2002

Fujimoto, M., and A. Nishida, Energization and anisotropization of the Earth's radiation belt by the recirculation process, *J. Geophys. Res*., *95*, 4265, 1990.

Hudson, M. K., S. R. Elkington, J. G. Lyon, V. A. Marchenko, I. Roth, M. Temerin, J. B. Blake, M. S. Gussenhoven, and J. R. Wygant, Simulations of radiation belt formation during storm sudden commencements, *J. Geophys. Res.*, *101*, 14,087, 1997.

Kennel, C. F., and H. E. Petschek, Limit on stably trapped particles fluxes, *J. Geophys. Res.*, *71*, 1, 1966.

Kim, H.-J., and A. A. Chan, Fully-adiabatic changes in storm-time relativistic electron fluxes, *J. Geophys. Res.*, *102*, 22,107–22,116, 1997.

Kozyra, J. U., M. W. Liemohn, C. R. Clauer, A. J. Ridley, M. F. Thomsen, J. E. Borovsky, J. L. Roeder, V. K. Jordanova, and W. D. Gonzalez, Multistep Dst development and ring current composition changes during the 4-6 June 1991 magnetic storm, *J. Geophys. Res., 107,* in press, 2002.

Li, X., R. Roth, M. Temerin, J. R. Wygant, M. K. Hudson, and J. B. Blake, Simulation of the prompt energization and transport of radiation belt particles during the March 24, 1991, SSC, *Geophys. Res. Lett., 20*, 2423, 1993.

Li, X., M. Temerin, D. N. Baker, G. D. Reeves, and D. Larson, Quantitative prediction of radiation belt electrons at geostationary orbit on the basis of solar wind measurements, *Geophys. Res. Lett.*, *28*, 1887, 2001.

Lorentzen, K. R., M. P. McCarthy, G. K. Parks, J. E. Foat, R. M. Millan, D. M. Smith, R. P. Lin, and J. P. Treilhou, Precipitation of relativistic electrons by interaction with electromagnetic ion cyclotron waves, *J. Geophys. Res., 105*, 5381, 2000.

Lorentzen, K. R. M. D. Looper, and J. B. Blake, Relativistic electron microbursts during GEM storms, *Geophys. Res., Lett., 28*, 2573, 2001a.

Lorentzen, K. R., J. B. Blake, U. S. Inan, and J. Bortnik, Observations of relativistic electron microbursts in association with VLF wave activity, J. Geophys. Res., 106, 6017-6027, 2001b.

Lorentzen, K. R., J. E. Mazur, M. D. Looper, J. F. Fennell, and J. B. Blake, Multisatellite observations of MeV ion injections during storms, *J. Geophys. Res.*, in press, 2002.

Lyons, L. R., R. M. Thorne, and C. F. Kennel, Pitch angle diffusion of radiation belt electrons within the plasmasphere, *J. Geophys. Res., 77*, 3455, 1972.

Meredith, N. P., R. B. Horne, and R. R. Anderson, Substorm dependence of chorus amplitudes: Implications for the acceleration of electrons to relativistic energies, *J. Geophys. Res., 106*, 13,165, 2001.

Nakamura, R., D. N. Baker, J. B. Blake, S. Kanekal, B. Klecker, and D. Hovestadt, Relativistic electron-precipitation enhancements near the outer edge of the radiation belt, *Geophys. Res. Lett. 22*, 1129–1132, 1995.

Paulikas, G. A., and J. B. Blake, Effects of the solar wind on magnetospheric dynamics: Energetic electrons at the synchronous orbit, in *Quantitative Modeling of Magnetospheric Processes*, *Geophys. Monogr., Amer. Geophys. Un., 21*, 180, 1979.

Reeves, G. D., Relativistic electrons and magnetic storms: 1992–1995, *Geophys. Res. Lett., 25,* 1817, 1998.

Reeves, G. D., D. N. Baker, R. D. Belian, J. B. Blake, T. E. Cayton, J. F. Fennell, R. H. W. Friedel, M. M. Meier, R. S. Selesnick, and H. E. Spence, The global response of relativistic radiation belt electrons to the January 1997 magnetic cloud, *Geophys. Res. Lett.*, *17*, 3265, 1998.

Reeves, G. D., K. L. McAdams, R. H. W. Friedel, and T. P. O'Brien, Acceleration and loss of relativistic electrons during geomagnetic storms, *Geophys. Res. Lett.,* submitted 2002.

Schulz, M., and L. J. Lanzerotti, *Particle Diffusion in the Radiation Belts*, Springer-Verlag, New York., 1974.

Selesnik, R. S., and J. B. Blake, On the source location of radiation belt relativistic electrons, *J. Geophys. Res.*, *105*, 2607, 2000.

Sergeev, V. A., E. M. Sazhina, N. A. Tsyganenko, J. A. Lundblad, and F. Soraas, Pitch-angle scattering of energetic protons in the magnetotail current sheet as the dominant source of their isotropic precipitation into the ionosphere, *Planet. Space. Sci*., *31*, 1147, 1983.

Summers, D., and C. Ma, A model for generating relativistic electrons in the Earth's inner magnetosphere based on gyroresonant wave-particle interactions., *J. Geophys. Res., 105,* 2625, 2000.

Summers, D., R. M. Thorne, and F. Xiao, Relativistic theory of wave-particle resonant diffusion with application to electron acceleration in the magnetosphere, *J. Geophys. Res.*, *103*, 20,487, 1998.

Tverskaya, L. V., N. N. Pavlov, J. B. Blake, R. S. Selesnick, and J. F. Fennell, Predicting the L-position of the storm-injected relativistic electron belt*, Adv. Space Res.,* in press, 2001.

Walt, M., *Introduction to Geomagnetically Trapped Radiation,* Cambridge University Press, 1994.

II. Ionosphere-Thermosphere System

Basu, Su., VHF ionospheric scintillations at L = 2.8 and formation of stable auroral red arcs by magnetospheric heat conduction, *J. Geophys. Res., 79*, 3155, 1974.

Basu, Su., and C. Valladares, Global aspects of plasma structures*, J. Atmos. Solar Terr. Phys., 61*, 127, 1999.

Basu, S., K. M. Groves, J. M. Quinn, and P. Doherty, A comparison of TEC fluctuations and scintillations at Ascension Island, *J. Atmos. Terr. Phys., 61*, 1219, 1999.

Basu, Sunanda, Santimay Basu, C. E. Valladares, H.-C. Yeh, S.-Y. Su, E. MacKenzie, P. J. Sultan, J. Aarons, F. J. Rich, P. Doherty, K. M. Groves, and T. W. Bullett, Ionospheric effects of major magnetic storms during the international space weather period of September and October 1999: GPS observations, VHF/UHF scintillations, and in situ density structures at middle and equatorial latitudes, *J. Geophys. Res., 106*, 30,389, 2001a.

Basu S., Su. Basu, K. M. Groves, H.-C. Yeh, S.-Y. Su, F. J. Rich, P. J. Sultan, and M. J. Keskinen, Response of the equatorial ionosphere in the South Atlantic region to the great magnetic storm of July 15, 2000, *Geophys. Res. Lett., 28*, 3577, 2001b.

Bhattacharyya, A., T. L. Beach, S. Basu, and P. M. Kintner, Nighttime equatorial ionosphere: GPS scintillations and differential carrier phase fluctuations, *Radio Sci., 35*, 209, 2000.

Buonsanto, M., Ionospheric storms: A review, *Space Sci, Rev., 61*, 193, 1999.

Burke, W. J., N. C. Maynard, M. P. Hagan, R. A. Wolf, G. R. Wilson, L. C. Gentile, M. S. Gussenhoven, C. Y. Huang, T. W. Garner, and F. J. Rich, Electrodynamics of the inner magnetosphere observed in the dusk sector by CRRES and DMSP during the magnetic storm of June 4–6, 1991*, J. Geophys. Res., 103*, 29,399, 1998.

Foster, J. C., Storm time plasma transport at middle and high latitudes, *J. Geophys. Res., 98*, 1675, 1983.

Foster, J. C., and F. J. Rich, Prompt midlatitude electric field effects during severe geomagnetic storms, *J. Geophys. Res., 103*, 26,367, 1998.

Hedin, A. E., MSIS-86 Thermosphere model, *J. Geophys. Res.*, *92*, 4649, 1987.

Hedin, A. E., N. W. Spencer, M. A. Biondi, R. G. Burnside, G. Hernandez, and R. M. Johnson, Revised global model of thermosphere winds using satellite and ground-based observations, *J. Geophys. Res*., *96*, 7657, 1991.

Immel, T. J., G. Crowley, J. D. Craven, and R. G. Roble, Dayside enhancements of thermospheric O/N_2 following magnetic storm onset, *J. Geophys. Res., 106*, 15,471, 2001.

Kelley, M. C., *The Earth's Ionosphere: Plasma Physics and Electrodynamics*, p. 126, Academic Press, San Diego, CA, 1989.

Kelley, M. C., F. J. Garcia, J. J. Makela, T. Fan, E. Mak, C. Sia, and D. Alcocer, Highly structured tropical airglow and TEC signatures during strong geomagnetic activity, *Geophys. Res. Lett.*, *27*, 465, 2000.

Kivanc, O., and R. A. Heelis, Structures in ionospheric number density and velocity associated with polar cap ionization patches, *J. Geophys. Res., 102*, 307, 1997.

Lean, J., The Sun's variable radiation and its relevance for Earth, *Annual Review of Astronomy and Astrophysics*, *35*, 33, 1997.

Meier, R. R., J. M. Picone, D. P. Drob, and R. G. Roble, Similarity transformation-based analysis of atmospheric models, data, and inverse remote sensing algorithms, *J. Geophys. Res.*, *106*, 15,510, 2001.

Mendillo, M., M. D. Papagiannis, and J. A. Klobuchar, Ionospheric storms at midlatitudes, *Radio Sci., 5*(6), 895, 1970.

Strickland, D. J., R. E. Daniel, Jr., and J. D. Craven, Negative ionospheric storm coincident with DE 1-observed thermospheric disturbance on October 14, 1981, *J. Geophys. Res., 106*, 21,049, 2001.

Vo, H. B., and J. C. Foster, A quantitative study of ionospheric density gradients at mid-latitudes, *J.Geophys. Res., 106*, 21,555, 2001.

III. Theory and Modeling

Abel, B., and R. M. Thorne, Electron scattering loss in Earth's inner magnetosphere, 1, Dominant physical processes, *J. Geophys. Res.*, *103* (A2), 2385, 1998.

Boscher, D., and S. Bourdarie, Modeling the transport of energetic particles in the magnetosphere with Salammbô, in *Space Weather, Geophysical Monograph Series Volume 125*, edited by P. Song, H. J. Singer, and G. L. Siscoe, p. 297, American Geophysical Union, Washington, DC, 2001.

Elkington, S. R., M. K. Hudson, and A. A. Chan, Acceleration of relativistic electrons via drift-resonant interaction with toroidal-mode Pc5 ULF oscillations, *Geophys. Res. Lett.*, *26* (21), 3273, 1999.

Hudson, M. K., A. D. Kotelnikov, X. Li, J. G. Lyon, I. Roth, M. Temerin, J. R. Wygant, J. B. Blake, M. S. Gussenhoven, K. Yumoto, and K. Shiokawa, Modeling formation of new radiation belts and response to ULF oscillations following March 24, 1991 SSC, in *Workshop on the Earth's Trapped Particle Environment*, *AIP Conf. Proc. 383*, edited by G. D. Reeves, p. 119, AIP Press, Woodbury, New York, 1996.

Hudson, M. K., S. R. Elkington, J. G. Lyon, M. Wiltberger, and M. Lessard, Radiation belt electron acceleration by ULF wave drift resonance: Simulation of 1997 and 1998 storms, in *Space Weather, Geophysical Monograph Series, 125*, edited by P. Song, H. J. Singer, and G. L. Siscoe, p. 289, American Geophysical Union, Washington, DC, 2001.

Rowland, D. E., and J. R. Wygant, Dependence of the large-scale, inner magnetospheric electric field on geomagnetric activity, *J. Geophys. Res.*, *103* (A7), 14,959, 1998.

Schulz, M., and L. J. Lanzerotti, *Particle Diffusion in the Radiation Belts*, Springer Verlag, New York, 1974.

Tsyganenko, N. A., Empirical magnetic field models for the Space Weather Program, in *Space Weather, Geophysical Monograph Series, 125*, edited by P. Song, H. J. Singer, and G. L. Siscoe, p. 273, American Geophysical Union, Washington, DC, 2001.

APPENDIX 4.
LIST OF ACRONYMS AND ABBREVIATIONS

AC	Alternating Current
ACE	Advanced Composition Explorer
ACS	Attitude Control System
AFRL	Air Force Research Laboratory
AGU	American Geophysical Union
AMIE	Assimilation Model of Ionospheric Electrodynamics
AMISR	Advanced Modular Incoherent Scatter Radar
ATS	Applications Technology Satellite
B	Magnetic Field
C&DH	Command and Data Handling
C/NOFS	Communication/Navigation Outage Forecasting System
CCMC	Community Coordinated Modeling Center
CEDAR	Coupling, Energetics and Dynamics of Atmospheric Regions
CIR	Co-rotating Interaction Region
CISM	NSF's Center for Integrated Space Weather Modeling
CME	Coronal Mass Ejection
COSMIC	Constellation Observing System for Meteorology, Ionosphere, & Climate
CRRES	Combined Release and Radiation Effects Satellite
DC	Direct Current
DE-1	Dynamics Explorer-1
DMSP	Defense Meteorological Satellite Program
DoD	Department of Defense
E	Electric Field
ELF	Extremely Low Frequency
EMIC	Electromagnetic Ion Cyclotron
ENA	Energetic Neutral Atoms
EQUARS	Equatorial Atmosphere Research Satellite
ESF	Equatorial Spread F
EUV	Extreme Ultraviolet
FAA	Federal Aviation Administration
FAST	Fast Auroral Snapshot Explorer
FUV	Far Ultraviolet
GAIM	Global Assimilation of Ionospheric Measurements
Gb	Gigabit
GEC	Global Electrodynamic Connections (NASA/STP)
GEM	Geospace Environment Modeling
GEO	Geosynchronous Earth Orbit
GIM	Global Ionospheric Maps
GMDT	Geospace Mission Definition Team
GOES	Geostationary Orbit Environmental Satellite
GPS	Global Positioning System
GTO	Geostationary Transfer Orbit
GUVI	Global Ultraviolet Imager (on TIMED)
HASDM	High Altitude Satellite Drag Model
HCI	Horizon Crossing Indicator
HENA	High-Energy Neutral Atom Imager (on IMAGE)
HEO	High Earth Orbit
HF	High Frequency

HWM	Horizon Wind Model
IGS	International Geodynamic Service for GPS
ILWS	International Living With a Star Program
IMAGE	Imager for Magnetopause-to-Aurora Global Exploration; also Ionospheric Mapping and Geocoronal Experiment, a planned DoD Space Test Program
IMF	Interplanetary Magnetic Field
IRI	International Reference Ionosphere
ISAS	Institute of Space and Astronautical Science, Japan
ISR	Incoherent Scatter Radar
ISTP	International Solar-Terrestrial Physics
I-T	Ionosphere-Thermosphere
ITSP	Ionosphere-Thermosphere Storm Probe
kbps	Kilobits per Second
LANL	Los Alamos National Laboratory
LANL-GEO	Los Alamos National Laboratory Geosynchronous Earth Orbiting Satellites
LEO	Low Earth Orbit
LWS	Living With a Star
m	mass
Mb	Megabit
Mbps	Megabits per Second
MEO	Medium Earth Orbit
MHD	Magnetohydrodynamic
MLT	Mean Local Time
MMS	Magnetospheric Multiscale
MSIS	Mass Spectrometer and Incoherent Scatter
MSM	Magnetospheric Specification Model
MURI	DoD's Multi-University Initiative
NAIC	National Astronomy and Ionosphere Center
NASA	National Aeronautics and Space Administration
NOAA	National Oceanic and Atmospheric Administration
NPOESS	National Polar-Orbiting Operational Environmental Satellite System
NSF	National Science Foundation
NSWP	National Space Weather Program
$p_\perp$	momentum
POES	Polar Operational Environmental Satellite
POLAR	ISTP plasma, energetic particles, fields and imaging mission
PRISM	Parameterized Real-time Ionospheric Specification Model
PSD	Phase Space Density
RBSP	Radiation Belt Storm Probe
R_E	Radius of the Earth
RPA	Retarding Potential Analyzer
SAMPEX	Solar Anomalous and Magnetospheric Particle Explorer
SAT	Science Architecture Team
SBIRS-Low	Space Based Infrared System Low
SDO	Solar Dynamics Observatory
SEC	Sun-Earth Connections

SECAS	Sun-Earth Connections Advisory Committee
SED	Storm Enhanced Density
SEE	Solar Extreme Ultraviolet Experiment (on TIMED)
SEU	Single Event Upset
SHINE	Solar, Heliospheric, and Interplanetary Environment
STEREO	Solar Terrestrial Relations Observatory
STP	Solar-Terrestrial Probe (NASA); Space Test Program (DoD)
SuperDARN	Super Dual Auroral Radar Network
SV	Space Vehicle (generally refers to specific GPS satellite)
TEC	Total Electron Content, the number of electrons in a 1×1 m column between the receiver and the transmitting satellite
TECU	TEC Unit (1 TECU = 10^{16} electrons m^{-2})
TGCM	Thermospheric General Circulation Model
TIMED	Thermosphere, Ionosphere, Mesosphere Energetics, and Dynamics
TWINS	Two Wide-angle Imaging Neutral-atom Spectrometers
UHF	Ultra-High Frequency
ULF	Ultra-Low Frequency
UT	Universal Time
UTC	Universal Coordinated Time
UV	Ultraviolet
VLF	Very Low Frequency
WAAS	Wide Area Augmentation System (FAA program to differentially correct GPS receivers in aircraft)
WG	Working Group
Wind	ISTP Mission to Study the Solar Wind

http://lws.gsfc.nasa.gov